BIOCHEMICAL AND MOLECULAR ANALYSES OF PHYTOALEXIN BIOSYNTHESIS IN APPLE CELL CULTURES

Ph.D THESIS

by

SARKATE AMOL VITTHALRAO

DEPARTMENT OF BIOTECHNOLOGY
INDIAN INSTITUTE OF TECHNOLOGY ROORKEE
ROORKEE-247667, INDIA
FEBRUARY, 2018

BIOCHEMICAL AND MOLECULAR ANALYSES OF PHYTOALEXIN BIOSYNTHESIS IN APPLE CELL CULTURES

A THESIS

Submitted in partial fulfilment of the requirements for the award of the degree

of

DOCTOR OF PHILOSOPHY

in

BIOTECHNOLOGY

by

SARKATE AMOL VITTHALRAO

DEPARTMENT OF BIOTECHNOLOGY
INDIAN INSTITUTE OF TECHNOLOGY ROORKEE
ROORKEE-247667, INDIA
FEBRUARY, 2018

INDIAN INSTITUTE OF TECHNOLOGY ROORKEE

ROORKEE

CANDIDATE'S DECLARATION

I hereby certify that the work which is being presented in the thesis entitled "**BIOCHEMICAL AND MOLECULAR ANALYSES OF PHYTOALEXIN BIOSYNTHESIS IN APPLE CELL CULTURES**", in partial fulfilment of the requirements for the award of the degree of Doctor of Philosophy and submitted in the Department of Biotechnology of the Indian Institute of Technology Roorkee, Roorkee is an authentic record of my own work carried out during a period from July, 2013 to December 2017, under the supervision of Dr. Debabrata Sircar, Assistant Professor, Department of Biotechnolgy, Indian Institute of Technology Roorkee, Roorkee.

The matter presented in the thesis has not been submitted by me for the award of any other degree of this or any other institution.

(**SARKATE AMOL VITTHALRAO**)

This is to certify that the above statement made by the candidate is correct to the best of my knowledge.

(Debabrata Sircar**)**
Supervisor

The Ph. D. Viva-Voce Examination of **Mr. SARKATE AMOL VITTHALRAO,** Research Scholar has been held on **24/02/18**.

Chairman, SRC **Signature of External Examiner**

This is to certify that the student has made all the corrections in the thesis.

Signature of Supervisor **Head of the Department**
Dated: 24/02/18

ABSTRACT

Apple scab disease caused by the fungus *Venturia inaequalis* is the most devastating disease of apple in India and worldwide. Most of the commercial apple cultivars are susceptible to scab disease. Till now, metabolites conferring resistance to scab-disease in apple are largely unknown. Identifying metabolites associated with scab-resistance and their underlying biosynthetic genes may provide novel targets to breed for enhanced scab-resistance.

The first aim of this thesis work is to decipher bioactive anticancer metabolites produced in the cell suspension culture of apple cv. Florina upon elicitor-treatment. Yeast-extract treated apple cell culture showed enhanced accumulation of phenolics acids, which is preceded by the enhancement of the activity of phenylalanine ammonia-lyase (PAL) enzyme. The elicited extract showed significant anticancer activity against human cervical (HeLa cells) and breast (MCF-7 cells) cancer cell lines using MTT assay.

The second aim of this thesis work was to apply metabolomics tool to identify the metabolites responsible for scab-disease resistance in apple and their regulation during host-pathogen interactions. Comparative gas-chromatography-mass spectrometry based metabolomics of *Venturia inaequalis* (VIE)-treated cell cultures showed enhanced accumulation of phenolics with formation of three new biphenyl-dibenzofuran phytoalexins, namely, aucuparin, noraucuparin and eriobofuran.

The third aim of this thesis work was to detect salicylaldehyde synthase (SAS) activity from *Venturia inaequalis* elicitor (VIE)-treated cell suspension cultures of apple (*Malus domestica* 'Florina'). SAS catalyzes non-oxidative C2-side chain cleavage of *2*-coumaric acid to form salicylaldehyde (SALD) in the presence of a reducing agent such as cysteine. Elicitor treatment further resulted in an 8.7-fold increase in the activity of the phenylalanine ammonia-lyase (PAL) enzyme that preceded the peak of SAS activity and total SA accumulation, suggesting the involvement of the phenylpropanoid pathway in SA metabolism. The preferred substrate for SAS was *2*-coumaric acid (*K*m = 0.35 mM), with cysteine being the preferred reducing agent.

The fourth aim of this thesis work was to clone and functionally characterize a biphenyl phytoalexin biosynthetic gene, 3,5-dihydroxybiphenyl *O*-methyltransferase (*MdfOMT*) from elicitor-treated cell suspension culture of apple cv. Florina. *MdfOMT* is involved in biphenyl biosynthesis. The coding sequence of *MdfOMT* was functionally expressed in *E. coli*. *Md*fOMT catalyzed regiospecific *O*-methylation of 3,5-dihydroxybiphenyl at 5´- position. The enzyme showed absolute substrate preference for the 3,5-dihydroxybiphenyl. Although *Md*fOMT product was not detected in the cell cultures the level of noraucuparin, aucuparin and eriobofuran were significantly uplifted upon elicitor-treatment. *Md*fOMT fused with N- and C-terminal yellow fluorescent protein showed cytoplasmic localization in the epidermis of *Nicotiana benthamiana* leaves.

Keywords: Apple, biphenyl, *cell suspension culture*, dibenzofuran, Florina, *Malus domestica*, metabolomics, *O*-methyltransferase (*MdfOMT*), salicylaldehyde synthase, *Venturia inaequalis*.

Acknowledgements

I take immense pleasure in expressing my deep sense of gratitude to my supervisor and mentor **Dr. Debabrata Sircar** for giving me the opportunity to join his research laboratory. His trust in me and constant supervision has been a constant source of positive energy for me. He has patiently listened and accordingly supervised and supported me throughout my Ph.D. His enthusiasm and profound concern for my success has made this journey a joyous one. It has been a great privilege and honour to work and study under his precious guidance. His sincerity, dynamism, vision and motivation deeply inspired me to learn new things.Along with academic support his affectionate behaviour and moral support also helped me through the rough road to finish my thesis. I express my wholehearted indebtedness to him.

I would also like to express my profound gratitude to **Prof. Partha Roy**, Head of Department of Biotechnology for providing the basic infrastructural facilities in the department that allowed me to successfully complete my Ph.D. I'm thankful to him for giving me access to his laboratory instrumentation. His punctuality and sense of duty have been a source of motivation. His expert advices and jovial nature have encouraged me all along the path to success.

Besides, I would like to thank the Department of Biotechnology, and Institute Instrumentation Centre (IIC), IIT Roorkee for instrument facilities to carry out the research work. I am also grateful to my SRC committee members: **Prof. R. Prasad, Dr. Pravindra Kumar and Dr. R.K. Peddinti** DRC chairman: **Prof. Vikas Pruthi** for their continuous advice and kind support.

I also express my sincere gratitude towards **Dr. Harsh Chauhan** and **Dr. Sri Ram Yadav** for their kind and valuable suggestions and other faculty members of Department of Biotechnology during my PhD.

My warmest thanks to my colleagues in my lab and in my department who made this study a successful experience. I was lucky to work with a kind and helpful colleague Mr. Shashank Saini. I especially thank Ms. Deepa Teotia for her timeless support and constructive ideas.

I am thankful to Ms. Kriti Juneja, Mr. Ashwani Kumar, Mr. Mukund Kumar, Ms. Varsha Tomar, Mr. Bhairavnath Waghmode and Ms. Komal Kushwaha for the pleasant working environment and companionship during laboratory works.

I am also thankful to the office staff, Department of Biotechnology for their kind help and support, campus administration and workers team of my hostel, Azad Bhawan, their hard work made my stay comfortable in campus.
A special vote of thanks to my friends in IIT Roorkee namely Mr. Yogesh Sariya, Mr. Vijay Sharma, Mr. Somesh Baneerjee, Mr. Swapneel Jaiswal, Mr. Sunil Sharma, Mr. Ragvendra Singh, Mr. Sandip Nathani and Mr. Harvijay Singh for their encouragement, support and giving unforgettable moments during my stay in IIT and in my life.

Sarkate Amol Vitthalrao

LIST OF ABBREVIATIONS

AOX	Alternate oxidase
B4H	Biphenyl-4-hydroxylase
BIS	Biphenyl synthase
CDS	Coding sequence
cDNA	Complementary DNA
CLSM	Confocal laser scanning microscopy
CoA	Coenzyme A
CYP450	Cytochrome P450
DMSO	Dimethyl sulfoxide
2,4-D	2,4-Dichlorophenoxyacetic acid
DPPH	1,1-diphenyl-2-picrylhydrazyl
DTT	Dithiothreitol
EMBL	European Molecular Biology Laboratory
ESI-MS	Electro-spray-ionization mass spectrometry
EDTA	Ethylenediaminetetraacetic acid
F3H	Flavone-3-hydroxylase
FRAP	Ferric reducing antioxidant power
GC-MS	Gas chromatography- mass spectrometry
GDR	Genome Data Base of Rosaceae
Hpe	Hours post-elicitation
HPLC	High-performance liquid chromatography
IAA	Indole-3-acetic acid
LS	Linsmaier and Skoog
MeOH	Methanol
mRNA	Messenger RNA
MW	Molecular weight
MSTFA	N-methyl-N-(trimethylsilyl) trifluoroacetamide
MTCC	Microbial type culture collection and gene bank
MW	Molecular weight
NCBI	National Center for Biotechnology Information
NAD	Nicotinamide adenine dinucleotide
NADP	Nicotinamide adenine dinucleotide phosphate
NE	Non-elicited
NaOH	Sodium hydroxide
OMT	*O-methyltransferase*
PAL	Phenylalanine ammonia-lyase
PCR	Polymerase chain reaction
PDA	Photodiode array detector

PVPP	Polyvinyl poly pyrolidone
RT	Retention time
RT-PCR	Reverse-transcription PCR
SAS	Salicylic aldehyde synthase
SDS	Sodium dodecyl sulfate
SAM	S-Adenosyl-L-methionine
TIC	Total ion current
TPC	Total phenolics content
TFC	Total flavonoids content
TMS	Tri-methyl-silylation
VIE	*Venturia inaequalis* elicitor
YFP	Yellow fluorescent protein
YE	Yeast-extract

CONTENTS

LIST OF FIGURES

LIST OF TABLES

Chapter 1

Introduction and Literature Review

1.1 Rosaceae

The Rosaceae is moderately large family of the order Rosales which includes approximately 100 genera and 3000 species of herbs, shrubs, and trees (Potter et al., 2007; Lo and Donoghue, 2012). Most of them are deciduous or evergreen and belongs to perennial habitat. Members are distributed worldwide mostly in the region of temperate northern hemisphere (Janick, 2005). This family is well known for producing several commercially important edible fruits, such as apple (*Malus domestica* Borkh.), pear (*Pyrus pyrifolia*), raspberry (*Rubus occidentalis*), strawberry (*Fragaria ananassa*), cherry (*Prunus avium*), peach (*Prunus persica*) etc. The molecular phylogenetic study across Rosaceae family strongly supports for the monophyletic origin (Morgan et al., 1994), which was later used by Takhtajan (1997) to identify twelve (12) sub-families among Rosaceae. The classification proposed by (Kalkman, 2004) includes detailed surveys of vegetative and reproductive morphology, phytochemistry, karyology, ecology, economic uses and conservation strategies. The molecular phylogenetic relationships within Rosaceae is mostly based on sequence information from the chloroplast and the ribosome coding genes (rbcL sequence) (Morgan et al., 1994; Evans and Campbell, 1999; Potter et al., 2002. According to the classification of Angiosperm Phylogeny Group 2003, the order Rosales includes nine families, namely Barbeyaceae, Cannabaceae, Dirachmaceae, Elaeagnaceae, Moraceae, Rhamnaceae, Rosaceae, Ulmaceae, and Urticaceae (Morgan et al., 1994; Potter et al., 2007) (Figure 1.1).

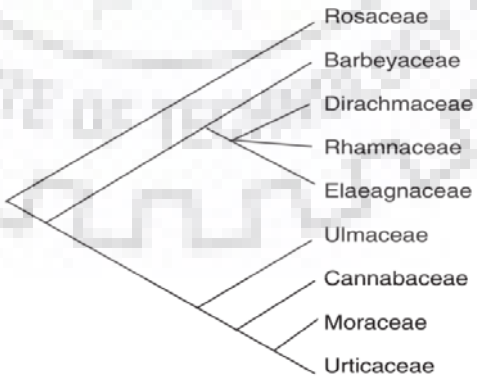

Figure 1.1: Cladogram of Rosales (Morgan et al., 1994)

1.2 Sub-tribe Malinae

The sub-tribe Malinae (previously known as the sub-family Maloideae) of Rosaceae family (Potter et al., 2007) includes many well known and beloved species of economically important pome-bearing fruits, such as apple (*Malus domestica*) and pear (*Pyrus communis*) or cultivated ornamental plants like *Sorbus aucuparia*. Previously members of Malinae were wrongly put into the sub-tribe Pyrinae (Campbell et al., 2007). Nevertheless, the Maloideae sub-family was later re-classified as the sub-tribe Malinae of Amygdaloideae subfamily (Reveal, 2012). The Malinae bears approximately 30 genera with about 1100 species, distributed worldwide, mainly in the temperate and subtropical countries. The sub-tribe Malinae is characterized by presence of accessory fruits called pomes and the basal haploid chromosome count is n =17, while in other members of Rosaceae, basal chromosome number varies (x = 7, 8 or 9) (Velasco et al., 2010). Malinae species are known to be originated as a result of allopolyploidization between Spiraeoideae (x = 9) and Amygdaleoideae (x = 8). The most of the wild species are diploid and other are either triploid or tetraploid (Pereira-Lorenzo et al., 2007). The fruits ingredients are full of vitamins, sugars and acids, which can be used for making preservatives, food products and beverages. The dried fruits and some plants with high vitamin content and essential oils have high commercial value. This sub-tribe Malinae is further characterized by its capability to produce two specialized defense metabolites, the biphenyls and the dibenzofurans, upon pathogen infection. Till date, the biosynthesis of these biphenyls and dibenzofurans are not well understood. The apple (*Malus domestica*) is one of the most important fruit producing plants of the Malinae. Apple fruits are well known for their beautiful texture, high nutrition value and numerous health-protective properties (Boyer and Liu 2004; Gerhauser 2008).

1.3 Origin of Apple

The wild Central Asian apple species (*Malus sieversii*) has previously been identified as the main contributor to the genome of the cultivated apple (*Malus domestica*). The domestication of apples was due to initial introduction of apple in Europe and later hybridization between cultivars and between cultivars and wild species (Harris et al., 2002; Pereira-Lorenzo et al., 2007). The nuclear DNA and chloroplast DNA analysis indicates that domesticated apples are most closely related to wild *Malus* species. The presence of 18-bp duplication in the chloroplast DNA sequence supports the close relationship between wild and cultivated species (Harris et al., 2002).

The wild apples in Almaty (Kazakstan) were the major progenitors of the domesticated apples. The forest of Tian Shan was identified as the area where the apple was domesticated for the first time (Dzhangaliev, 2003; Cornille et al., 2012). Apples are self-incompatible and progeny obtained from their seeds shows high degree of variability with mother apple tree. In Late Neolithic or early Bronze age period farmers frequently collected the fruits of wild relatives of domesticated apple in the middle-east and Europe, seeds carried in saddle bags or horse dropping along the trade routes by caravans or carried by birds through which apples reach the Western Europe from Central Asia (Figure 1.2). Microsatellite markers study of five *Malus* species from Europe indicates that multiple wild species have contributed in domestication of apples. *M. sylvestris*, the wild European crabapple was the major secondary contributor (Cornille et al., 2012).

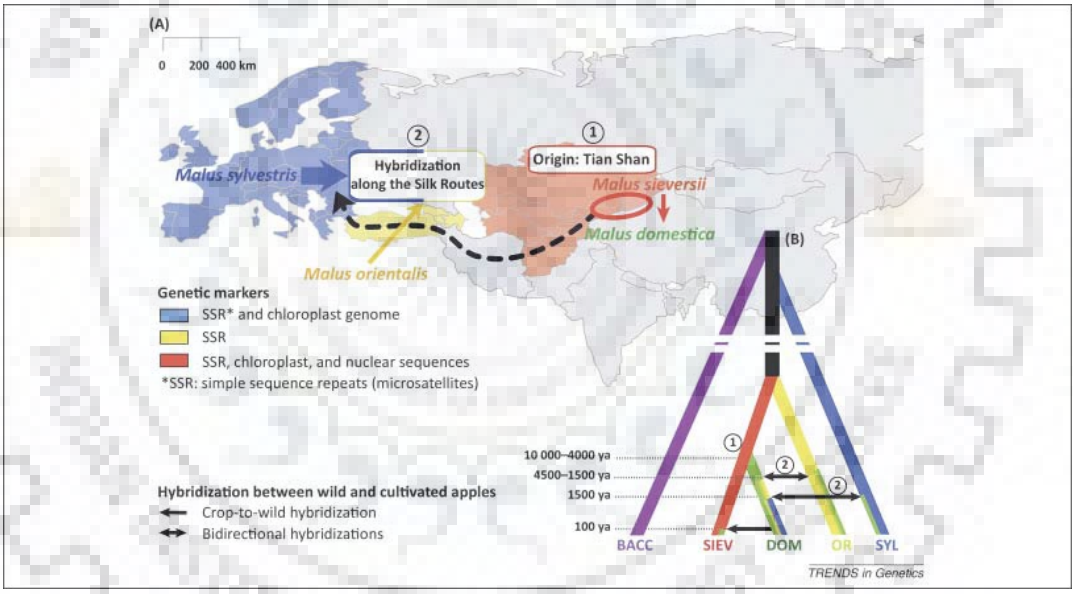

Figure 1.2: Origin and evolutionary history of the cultivated apple (A) based on molecular markers studies. (1) Origin of domesticated apple from the *Malus sieversii* in the mountains of Tian Shan; (2) migration of domesticated apple from Asia to Europe. Arrow thickness indicates proportionality of the genetic contribution of different wild species to the gene pool of domesticated apple, *Malus domestica*. (B) Genealogical relationships between the domesticated and the wild apples. Abbreviations: BACC, *Malus baccata*; SIEV, *M. sieversii;* DOM, *M. domestica*; OR, *Malus orientalis*; SYL, *Malus sylvestris* [Adopted from: Cornille et al., 2014].

1.4 Apple taxonomy and cultivars

Apple is a delicious tree belongs to sub-tribe Malinae of Rosaceae family (Table 1.1). On the basis of observed variations, apple species are divided into smaller and larger groups with particular name. The main problem with *Malus* taxonomy is the similarity between wild and cultivated species and hence identification of distinct categories becomes difficult. Furthermore the scientific names applied to domesticated apple are legion, such as *Malus pumila Miller* and *Malus domestica Borkh*. Recent study indicates that *M. pumila* (*M. sieversii*) is the correct name and major progenitor for domesticated apple (Cornelli et al., 2012). Now the term wild apples is used to *Malus* species other than domesticated apples.

Table 1.1: Taxonomy and classification of apple

Kingdom	Plantae
Phylum	Magnoliophyta
Class	Magnoliopsida
Order	Rosales
Family	Rosaceae
Subfamily	Amygdaloideae
Tribe	Maleae
Subtribe	Malinae
Genus	*Malus*
Species	*Domestica*

There are more than 7500 known cultivars of apple are grown worldwide with range of desired characteristics (Shogo Matsumoto, 2014). Different cultivars are breed to obtain better taste and quality of apple. Wild apples grow directly from seeds while domestic apple are generally propagated by clonal propagation. The most common varieties of apple grown worldwide are Red Delicious, Liberty, Empire, Golden Delicious, Gala, Fuji, McIntosh and Granny smith. In India, based on ripening season apple cultivars are divided into three categories, in early season (from early march to June) Michal, Shlomit, Vista Bella, Anna, Mayan; in mid season (from mid July to mid September) Royal Delicious, Red Delicious, Gala, Red Chief, Starkrimson and Granny smith, while in case of late season (from early September to late December) Firdaus,

Lal ambary, Sunahari, Shireen, Golden Delicious, Red gold Ambri and Fuji cultivars are cultivated. Many of the late-ripening apples tend to have prolonged storage life.

1.5 Indian and worldwide apple production

Apple is considered as one of the most popularly produced fruit around the world, accounts 12% of total global fruit production and stands second after banana in terms of consumption. It is also known as balanced fruit because of rich in most needed nutritious components. Annually over 85 million tons of apples are produced worldwide (FAOSTAT, 2016). Asia shares 62.7 % of total apple production and stands top among the all apple producing continents (Figure 1.3). Recently, China holds the first position with over 43 million tons of apples amongst other producers across the globe and continues to rising because of favorable whether condition and additional apple bearing acreage. United States is the second largest producer with 4.6 million tons and there it is second most commonly consumed fruit. Due to better methods cultivation and storage, Turkey ranks third and produces one of the finest apples in the world. Poland, France and Germany are the major apple producing countries in the Europe. Average yield of apples worldwide are around 4.5 tons/acre while average per capita consumption of apples is over 28.71 billion tons/year. China, US, France and Chile being the most apple exporting countries with over 5.5 million tons of apples export annually, whereas Germany, UK and Russia are the biggest importers, taking 33% of all exports. Over 40% of world apple juice production occurs in China, USA and Poland.

India ranks fifth with 2.8 million tons apple production per year (FAOSTAT, 2016). The top apple producing states of India are Jammu & Kashmir, Himachal Pradesh, Uttarakhand & Arunachal Pradesh with their respective shares of 70%, 21.5%, 6.4% and 1.6%. Further, apple is also produced in Mizoram, Sikkim, Tamil Nadu and Nagaland also. Key apple varieties include; Michal, Mollies Delicious, Maayan, Anna, Chaubattia, Anupam, Rich-e-Red, Gala, Firdous, Lal ambri, Kinnauri Apple etc. As per the information received from there is increase of about 36% in apple production in the country during, 2015-16 as compared to the previous year. The yield of apple during last three years and the production during the current year in major apple producing states of India are given in Table: 1.2.

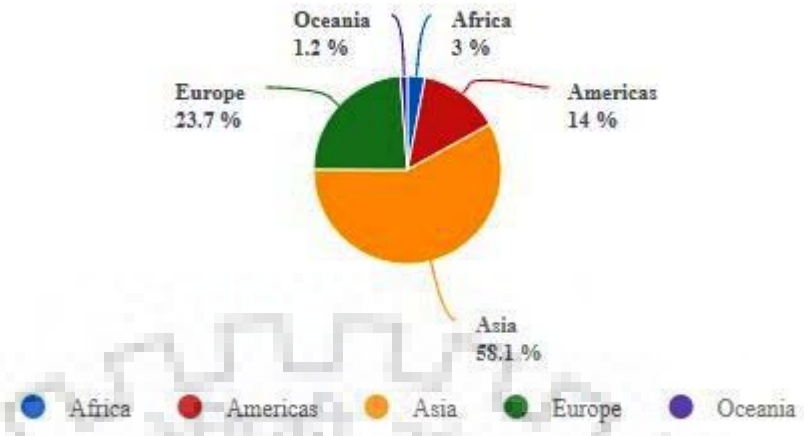

Figure 1.3: Worldwide apple production segregated by production region [FAOSTAT 2016]

Table 1.2: Indian Apple production (data presented in metric tons = MT)

INDIAN STATES	**2014-15**	**2015-16**
JAMMU & KASHMIR	1368.6	2003.0
HIMACHAL PRADESH	625.2	753.3
UTTARAKHAND	106.1	106.1
OTHERS	33.9	34.0
TOTAL (All INDIA)	2133.8	2896.5

Source: Horticulture statistics division, Department of agricultural cooperation and farmers welfares, Govt. of India (http://agricoop.nic.in/).

1.6 Bioactive constituents of apple

Apples and apple products are consumed for their wide range of nutritional and health-protective constituents. Daily consumption of apples reduces risk of cancer, cardiovascular disease and also protects from asthma, pulmonary dysfunction, obesity, and diabetes (Boyer and Liu, 2004; Gerhauser, 2008). Apples are rich source of total soluble and insoluble dietary fiber, minerals, and vitamins, except which other chemical composition of apple is quite similar (Gerhauser, 2008). The free radical scavenging activity of apple was due to the phytochemical content rather than that of vitamin C (Eberhardt et al., 2000). The antiradical activity is analogous with the presence of major amount of polyphenols, phenolic acids and flavonoids in

apple peel as compared to its flesh (Leontowicz et al., 2002). Apples are one of the main sources of dietary flavonoids and phenolics which are associated with lower mortality rate (Vinson et al. 2001; Boyer and Liu 2004). Recent findings suggests that apple fruits have excellent anti-proliferative, antioxidant, gastrointestinal protection from drug injury and cholesterol lowering properties (Eberhardt et al., 2000; Leontowicz et al., 2002; Wolfe et al., 2003; Dianne 2011). Major health-protective antioxidant metabolites present in apples include quercetin-derivatives, catechin, epicatechin, procyanidin, cyanidin-3-galactoside, chlorogenic acid, gallic acid, p-coumaric acid and minor amount of phloridzin (Lee et al., 2003). Cyanidin 3-*O*-galactoside is one of the most common anthocyanin pigment primarily responsible for red colouration in apple skin (Lancaster, 1992; Tsao et al., 2003). Major bioactive metabolites detected from apples are listed in Table 1.3.

Table 1.3: Major bioactive metabolites detected from apple

Metabolite class	**Types of metabolite**	**Reference**
Mono- and Sesquiterpenes	**Mono-terpenes** [(ε)-β-Ocimene, Linalool] **Sesquiterpenes** α-Farnesene, (*ε, ε*)-α-Farnesene, β-Caryophyllene, Germacrene δ, α –Curcumene].	(Rupasinghe et al., 1998; Nieuwenhuizen et al., 2013).
Anthocyanins	**Cyanidine and their glycosides** [(cyanidin 3-*O*-galactoside, Cyanidin 3-O-arabinoside)].	(Lancaster, 1992; Tsao *et al.*, 2003)
Vitamins	Vitamin A, Vitamin B1 (thiamine), Vitamin B2 (riboflavin), Niacin, Folic acid, Pantothenic acid, Vitamin B6, Vitamin C (Ascorbic acid), Vitamin E and Vitamin K.	(Lee and Mattick, 1989).
Phenolics: Free form	Gallic acid, caffeic acid, chlorogenic acid, benzoic acid and syringic acid.	(Francini and Sebastiani, 2013; Boyer and Liu, 2004).
Phenolics: ester-linked	Hydroxybenzoic acid, 4-p-coumaroylquinic acid, 4-caffeoylquinic acid, p-coumaric acid, vanillic acid, vanillin, , *cis*-ferulic acid, *trans*-ferulic acid.	(Rana and Bhushan, 2016 Francini and Sebastiani, 2013)

Flavanoids	**Flavan-3-ols** [(catechin, epicatechin,) and procyanidins (procyanidins B1, B2 and C1)].	(Rana and Bhushan, 2016; Tsao *et al.*, 2003).
	Quericitin and its glycosides [quercetin 3-rutinoside (Rutin), quercetin 3-galactoside, quercetin 3-glucoside, quercetin 3-xyloside, quercetin 3-arabinoside, and quercetin 3-rhamnoside].	(Tsao *et al.*, 2003, Lee et al., 2003)
	Dihydrochalcones and their glycosides (phloretin, Phloridzin and hydroxyphloretin ,phloretin-*O*-glycosides, phloretin-2′-*O*-glucoside and phloretin-2′-*O*-(2″-*O*-xylosyl) glucoside)	(Francini and Sebastiani, 2013; Lee et al., 2003).
Carotenoids	**Carotenes** (α-, β-, γ-, ζ- carotenesand β-zeacarotene), **Xanthophylls** (neoxanthin, violaxanthin, Lutein, antheraxanthin, zeaxanthin, β-Cryptoxanthin, Chrysanthemaxanthin, Flavaxanthin, Auroxanthin and β- cryptoxanthin-5,6-epoxide)	(Delgado-Pelayo et al., 2014, Valadon and Rosemary, 1967)

1.7 Important apple diseases

1.7.1 Apple Scab

Apple scab is the most devastating disease of apple resulting into enormous economic losses to farmers. The apple scab is caused by the ascomyceteous fungus *Venturia inaequalis* (Cooke) G. Wind. Aderh. (Jha et al., 2009). Scab affects almost all apple growing regions of the world (Bus et al., 2011). It was presumed that *V. inaequalis* tracked its host (apple) during domestication in Asia and expands its host province to European wild apples along the Silk route (Gladieux et al., 2008). *V. inaequalis* shows both saprophytic and parasitic life cycle by infecting both leaves and fruits of the host (Becker *et al.,* 1992). The infection starts during winter when ascomycete fungus grows on the fallen leaves and in spring it enters in marsupial stage by forming typical small black fruiting body structures called pseudothelium in which ascospores matures (MacHardy, 1996). The ascospores germinated on the leaves in humid climatic condition, breaking the epithelial surface of young leaves. On contact with the cuticle,

the germ tube differentiates and penetrates through cuticle to form sticky substance rich in proteins and carbohydrates which helps attachment to host surface (Smereka et al., 1987). When a fungal mycelium grows between epithelium and leaf epidermis, it leads to rupture of the epithelium and small conidiophores are formed. The signs and symptoms are detected at this stage, such as leaf appears translucent, oily and greyish, velvety necrotic or chronic lesions appears with greenish brown spores. It infects both young and mature fruits by forming numerous black spots, corky lesions, cracked, deformed fruits which later falls prematurely (Agrois, 2005; Jha et al., 2009). This first life cycle lasts for about two weeks. Depending upon the susceptibility of apple cultivar and weather conditions, several disease cycles can occur throughout the season. These secondary cycles causes tremendous damage in the fruit yield and provide large amount of over-wintering inoculums for next cycle of infection. Scab disease cycle in apple is shown in Figure 1.4

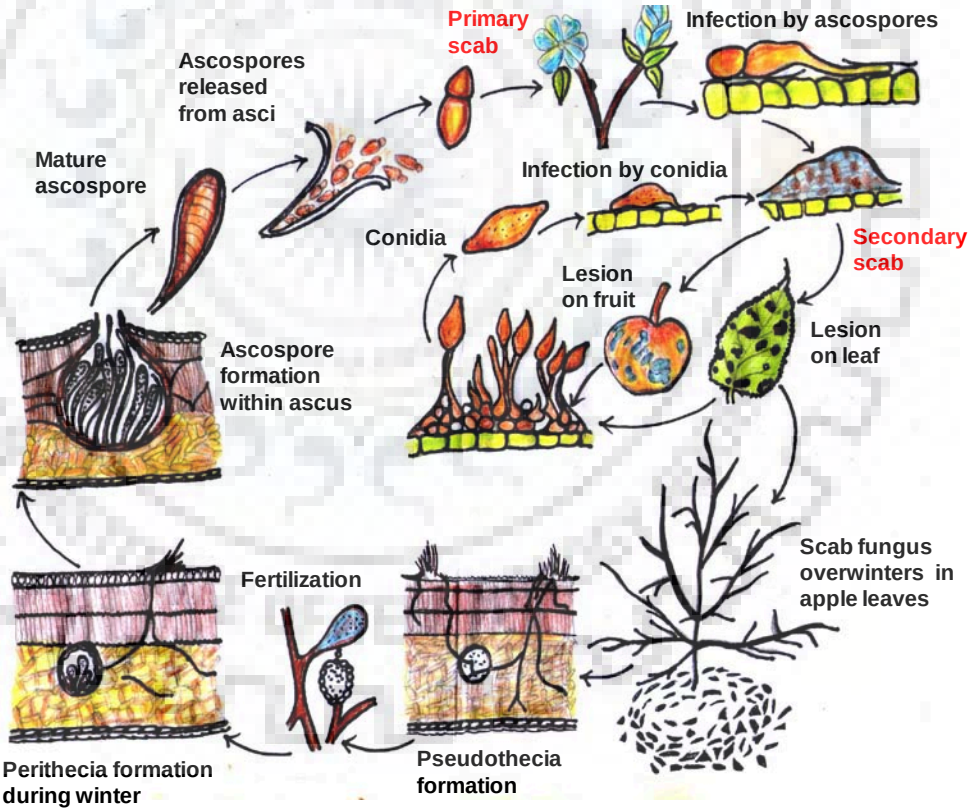

Figure 1.4: Life cycle of apple scab fungus *Venturia inaequalis* [Adopted from: MacHardy et al., 1996]

The current practice of apple scab management uses huge amount of fungicides spay (Way et al., 1989), which causes toxic effect to human health and environment. Furthermore, the use of multiple fungicide spray alone is not sufficient to completely control scab disease. Thereby, breeding of scab-resistant apple plant is considered as the most feasible and economical approach to manage the scab disease and its adverse impacts.

1.7.2 *Alternaria* leaf and fruit blotch

Alternaria is universally distributed fungal genus that includes saprobic, pathogenic and endosymbiont species associated with a wide variety of hosts. On the basis of their morphology, phylogeny and molecular analysis the genus is divided into 22 sections. This pathogen is known to cause leaf spot disease first identified in 1924 in the USA (Roberts, 1924), then expansion occurs through Southeast Asia (Bulajic et al., 1996), South eastern USA, Australia (Harteveld et al., 2013), some part of Europe (Bulajic et al., 1996) and now covers most of the apple growing region globally (Soleimani and Esmailzadeh, 2007). *Alternaria alternata* (*Alternaria mali*) is known to cause alternaria leaf blotch and fruit spot disease in *Malus domestica* (Harteveld et al., 2013). Based on Alternaria allergen a1 and endo-polygalacturonase gene sequences, it was revealed that miscellaneous groups of *Alternaria* species are associated with the cause of the both the diseases (Bessadat et al., 2014). Usually, apple cultivars like Golden Delicious, Pink lady and Gala (Rotondo et al., 2012; Gur et al., 2017) are very susceptible towards *A. mali* attack, however, cultivars like Jonagold exhibit resistance towards *A. mali* due to presence of special kind of phenolic compounds in its fruit peel which inhibits fungal growth on fruit surface (Lattanzio et al., 2006).

The disease cycle of *A. mali* (Figure 1.5) starts from the leaves fallen on the orchard floor where the primary fungal inoculums develops. Initially, small oval brown spots developed on leaf which magnifies into zonate circular or crescent ring shaped. The over-wintering spores on leaves, twigs and buds establish leaf blotch. Germinated spores, blown by wind to different plant parts and other hosts. Leaf blotch symptoms appears at about six weeks after bloom and increases rapidly when conditions are favorable causes premature defoliation (Jung, 2007). The infection, symptoms, spore production occurs optimal at 25 - 30° C. This fungus causes severe losses in apple fruit production in susceptible cultivars. Fruits become corky, light to dark brown spots appears on venticels and usually grows smaller in size. The infected fruit skin get soft when it has damaged by some mechanical wounds, cracks in the calyx or through biological entities (Ginzberg et al., 2014). The trials are under process using many commercial

breeding programs to develop new apple cultivars resistant against fungal pathogens (Kellerhals et al., 2012).

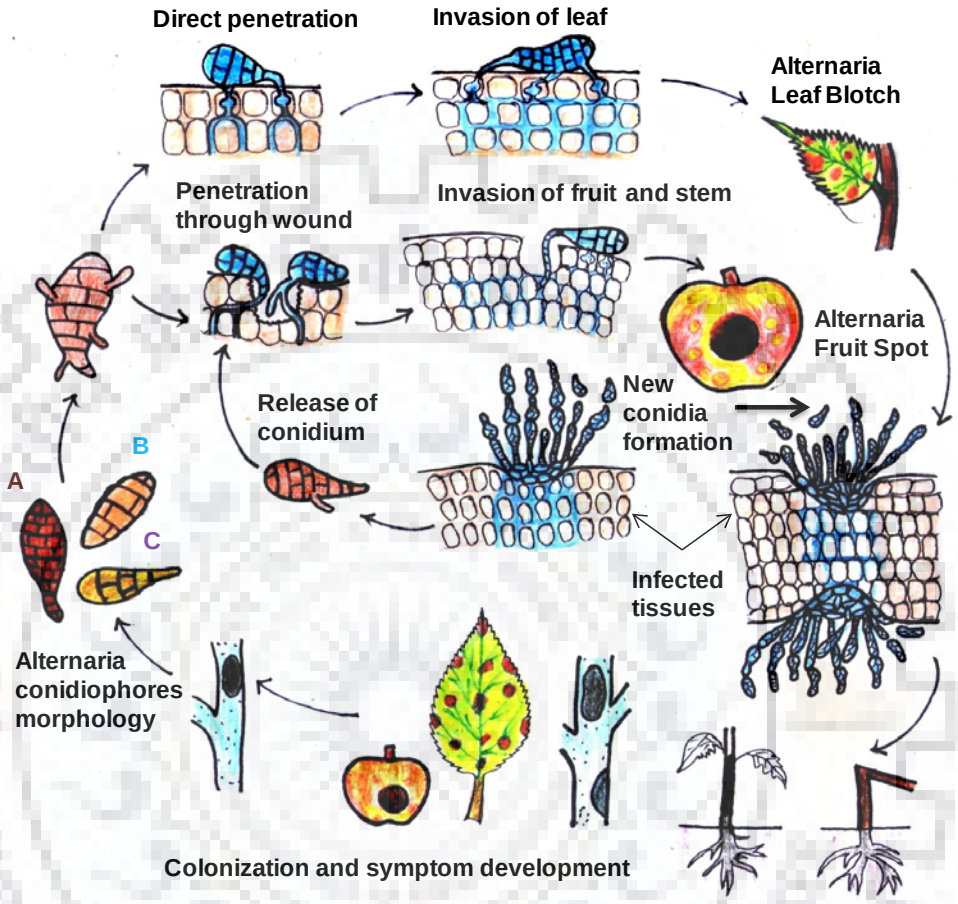

Figure 1.5: Life cycles of leaf and fruit blossom causing fungi of species *Alternaria*. Conidiophore morphology is different for three *Alternaria* species A: *A. aborescens*, B: *A. tenuissima* and C: *A. alternate*.

1.7.3 Fire blight of apple

Fire blight is a destructive and most erratic disease of apples and pears caused by the gram-negative bacterium *Erwinia amylovora*, which infects all aerial parts of the plant (Thomson, 2000). The causative agent of this unpredictable disease can exist in three different forms such as bacterial ooze or exudates, dry tendrils or strands and bacterial cells near infected tissue. In rainy season the bacterial exudates originating from active cankers or blighted blossoms and from shoots during the growing season as shown in Figure 1.6. The polysaccharide exudates

attract pollinating insects, also spread via wind-driven spring. Under low moisture, the dry bacterial tendrils are produced on shoots and fruits which were carried out by wind. The bacterial cells are formed in or near the infected tissues; it may exist epiphytically on the host tissue and on the vascular tissue endophytically (Van der Zwet, 1988). The disease can kill blossoms, fruits, roots, shoots, twigs, branches and entire plant. In blossom blight, floral nectrines are the major site of infection. It spread rapidly to other floral parts and then move down into spur, which became blighted and turning brown and finally dead. In case of shoot blight it starts at the growing shoot tips then spread out other shoots, leaves and branches through stomata and wound infection. The blighted twigs bend, shoots wilt and dried leaves remain attached to the dead branches. From infected twigs it moves into main branches causing distinct stem cankers (Malnoy et al., 2012; Norelli et al., 2003). Blighted and rotten fruit areas turn brown to black and dried out. In rootstock it usually infects near the graft union, causing girdling of rootstock. Young trees can be killed in single season while older trees can survive several years with continuous dieback.

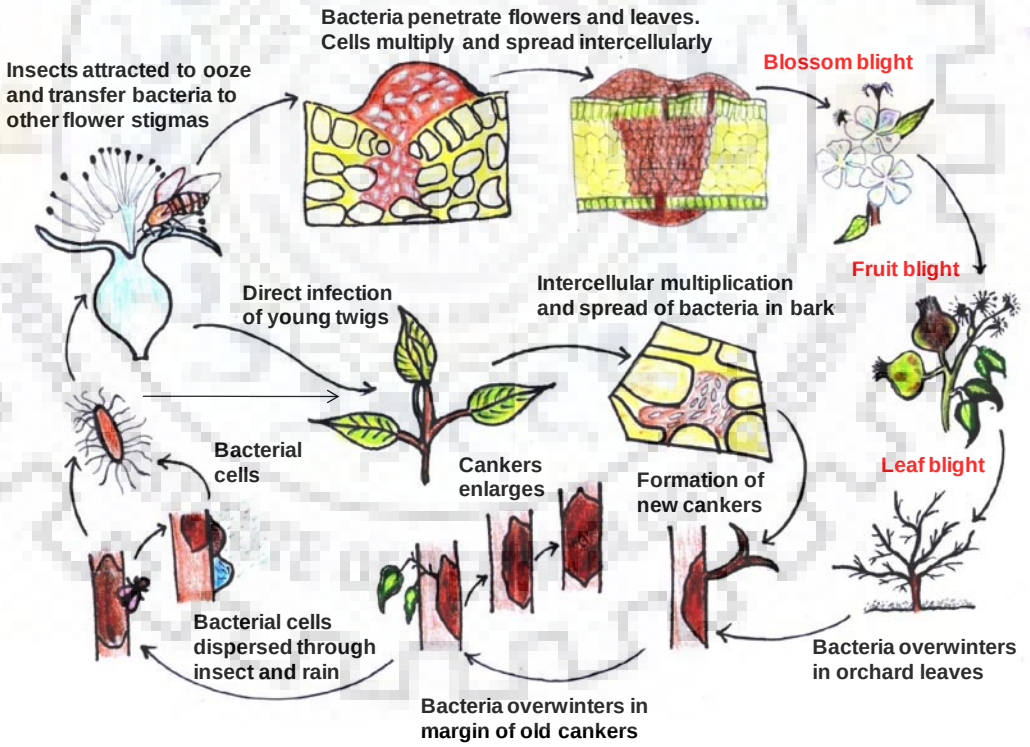

Figure 1.6: Life cycle of *Erwinia amylovora, a* causative agent of Fire blight in apple [Adopted from: Van der Zwet and Beer, 1995].

1.8 Scab resistance in apple

To preserve superior agronomic traits, commercial apple cultivars are mostly selected through clonal propagation of single apple tree. This genetic uniformity of commercial apple orchards seriously affects the disease resistance potential of apple (Gessler and Patocchi, 2007). The apple scab is one of the most devastating diseases of apple in terms of economic damage (Jha et al., 2009). Most of the commercial apple cultivars, generally growing in humid region are susceptible to scab disease, which results into severe loss in apple production every year. However, a number of apple cultivars exhibit scab resistance (Table 1.4). Most of the scab resistant varieties developed primarily from breeding program, but some are also resistant to cedar apple rust, powdery mildew, and fire blight. The transfer of scab-resistant genes by classical breeding method is time consuming (Le Roux et al., 2014) and needs alternative strategy for developing scab-resistant cultivars, such as development of cis-genic apples using genetic enginerring (Vanblaere et al., 2011; Kost et al., 2015; ; Kumar and Jain 2015). The current practice of apple scab management uses huge amount of fungicides spay (Way et al., 1989; Kollar, 1997), which causes toxic effect to human health and environment. Furthermore, the use of multiple fungicide spray alone is not sufficient to completely control scab disease. Thereby, breeding of scab-resistant apple plant is considered as the most feasible and economical approach to manage the scab disease and its adverse impacts. The scab-resistance in apple is controlled by several quantitative trait loci (QTL) (Bus et al., 2011). In order to control scab disease, several apple breeding programs have been conducted before for the introgression of wild apple cultivars (Laurens et al.,2011). In the beginning Rvi6 (*Vf* / *HcrVf2*) gene from scab-resistant parent *Malus floribunda 821* was selected for introgression into scab susceptible cultivars, however it took almost 80 years to introduce *Vf* cultivars in market with a reasonable fruit quality (Bus et al., 2011; Schouten et al., 2014; Wöhner et al., 2017). In the meanwhile new *V. inaequalis* races (race 6 and 7) were detected which overcome *Rvi6* resistance (Parisi et al., 1993; Trapman, 2006). In recent past several other scab-resistance genes like Rvi6 and Rvi15 have been isolated and mapped from various apple cultivars across the globe (Bus et al., 2011). However, only for *Rvi15* gene is available till date to provide complete scab resistance (Schouten et al., 2014). The Rvi15 resistances originate from GMAL2473 accession and until now there is no report of breaking this resistance by any scab race (Gali et al., 2010; Schouten et al., 2014).

Table 1.4: A list of scab resistant and susceptible apple cultivars

Scab-resistant cultivars	Scab-susceptible cultivars
Pristine	Jonathan
William's Pride	Red Delicious
Redfree	Jonamac
Prima	Imperial Gala
Goldrush	McIntosh
Priscilla	Northern spy
Crimson Crisp	Cortland
Jonafree	Campbell Redchief
Florina	Cameo
Scarlet	Empire
Prima	Fuji
Liberty	Northern Spy
Freedom	Granny smith
Firdaus	Crispin
Enterprise	Braeburn

1.9 Metabolomics as tool to identify defense metabolites in apple:

In general, upon pathogen infection, the plant starts synthesizing an array of defense-responsive metabolites, both primary and secondary. Alteration in the metabolic profiles of a plant in response to pathogen infection can be studied with metabolomics approach. This technology provide the opportunity to evaluate pathogen-induced local and systemic alterations in plant metabolite patterns without any prior assumptions Measuring the level of metabolites prior and after pathogen infection may give an exact picture of the physiological status of the plant tissue. Gas chromatography-mass spectrometry (GC-MS) is an emerging technology, routinely used in plant metabolomics (Shuman et al., 2011; Kumar and Nagar, 2015), especially for facilitating the identification and quantification of the primary metabolites such as amino acids, sugars, organic acids (Schauer and Fernie, 2006) and an wide array of secondary metabolites such as phenolics, flavonoids and biphenyls (Chizzali et al., 2012; Nutan et al., 2013; Sil et al., 2015; Misra et al., 2017). Most metabolomics studies on apples published so far were targeted

analyses focusing on specific metabolites and limited to only fruit quality analyses (Aprea et al., 2011; Cuthbertson et al., 2011; Vanzo et al., 2013). Recently, (Sciubba et al., 2015) identified new scab-preventive metabolites from resistant apple cultivar by NMR-based metabolomics. However, untargeted metabolomics analysis provides a more comprehensive view on the differential accumulation of metabolites upon pathogen infection (Eisenmann et al., 2016). Very recently, targeted HPLC-based metabolite profiling of the cell suspension cultures of *M. domestica* cv. 'Florina' showed massive metabolic reprogramming in response to yeast-extract (YE) elicitor-treatment (Sarkate et al., 2017). The authenticity and purity of apple juices has been accessed currently using LC-MS based metabolomics platform (Vaclavic et al., 2012). Attempts have been made to differentiate and correlate the volatiles released after fungal infection from apple fruits (Rowan et al., 2009; Schmarr et al., 2010). The spatial gradients of metabolites accumulated in apple have also been analyzed using metabolomic imaging technique (Zhang et al., 2007). The accomplishment of plant metabolomics predominantly depends on methodologies and instrumentations to comprehensively recognize measure and localize each and every metabolite, which helps in analysis and monitoring of plant metabolome. Nowadays number of integrated techniques and methodologies are accessible for analyses of highly complex samples and broad range of biological targets with the integration of metabolomics with functional genomics and other omics to analyze biochemical and genetic mechanism of cellular function and metabolic regulation. Metabolomics with plant genomics able to provide precious information about gene discoveries, pathways, interaction between small molecules and metabolites or among these metabolite, metabolite fluxes and their concentration in plants through precise and throughput peak annotation via close snapshot of the plant metabolome. The plant metabolome consists of the entire set of metabolites synthesized by these primary and secondary metabolic pathways which gives rise to the biochemical phenotype to that particular plant tissue. The metabolomic analysis helps in qualitative and quantitative profiling of defense related metabolites using direct infusion Orbitrap mass spectrometry (DIMS), gas or liquid chromatography-Mass Spectroscopy (GC-MS/LC-MS) and nuclear magnetic resonance spectroscopy (NMR) used to study global metabolic pattern in plants after pathogen infection at different time-course (Shulaev et al., 2008; Aliferis et al., 2014). The specificity of plant against different pathogen or pest attack synthesize specific chemical defense arsenal. The congregation of chemical compounds not only serves as base in search of novel defense metabolites but also as markers for the nature of plants defensive conditions essential for adaptation and safety of plants. The prime approach in the study of plant metabolomics is to construct the metabolite library which promotes

metabolite identification and biological elucidation of results and bioinformatics tools for visualization and analysis of its metabolome. This approach helps to decipher the plant metabolic regulation under biotic stress (Rajeev Kumar et al., 2014) and also provides identification of potential metabolite biomarker for applications in crop breeding and crop protection (Figure 1.7). Till date, there is no report available on metabolic re-programming of apple plants upon scab-infection, which opens an area of considerable research interest.

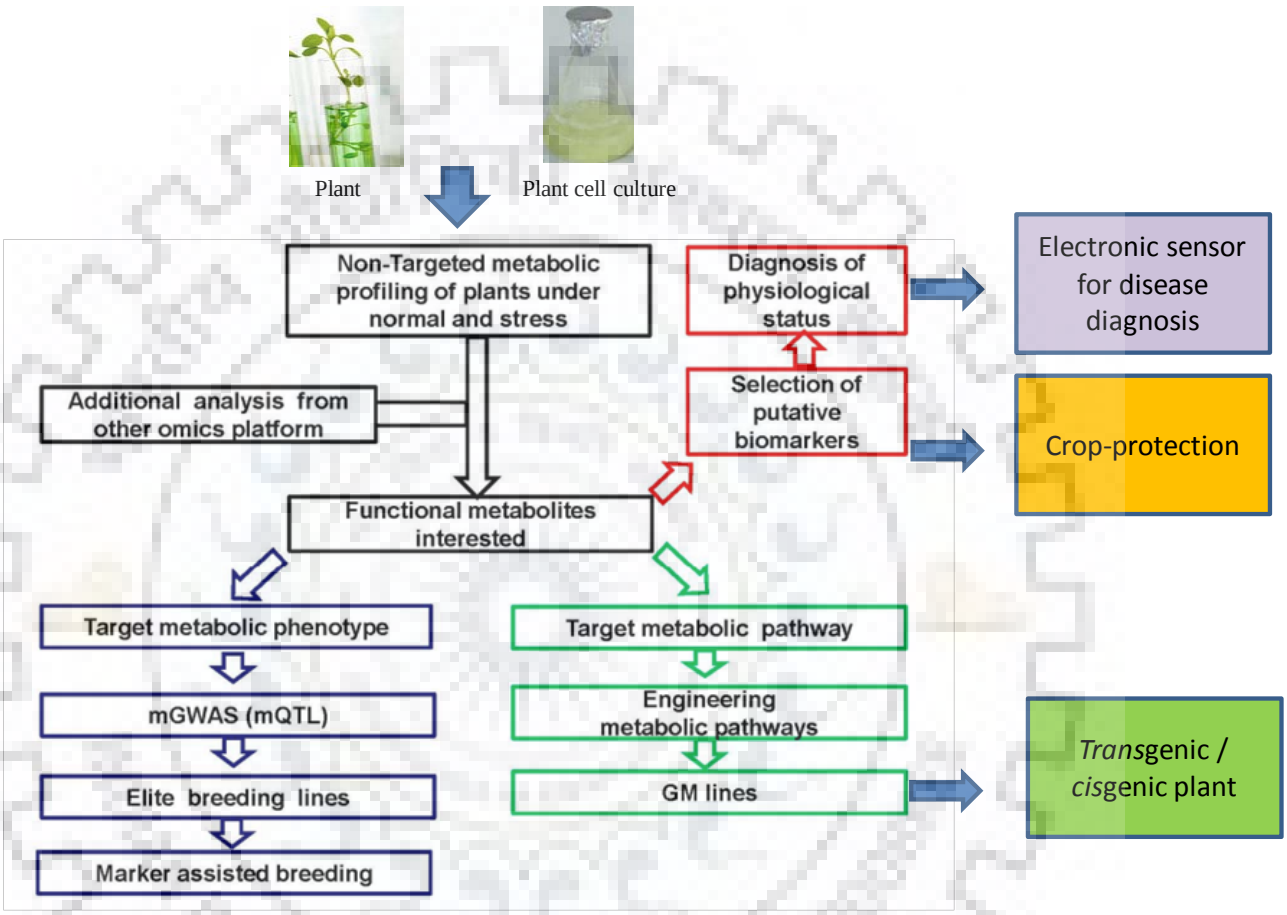

Figure 1.7: Various applications of plant metabolomics. [Adopted from: Hong et al., 2016]

1.10 The apple genome sequence:

The genome sequence of domesticated apple (Malus × domestica Borkh cv. 'Golden Delicious') has been sequenced and made publically available [Genome Data base of Rosaceae (GDR) www.rosaceae.org]. The whole genome sequence of cv. 'Golden Delicious' (Velasco et al., 2010) showed 603.9 Mb total contig size with reconstruction of total 17 chromosome / linkage groups. There are 57,386 putative genes out of which, 42.4% were transposable genetic element, 4021 are transcription factors, 178 miRNA, 992 resistant genes and 1246 biosynthetic

genes. A summary of gene prediction for apple and *Pyrus communis* (European pear) is given in Table 1.5**.** Availability of apple genome sequence will be beneficial for studying fruit and plant characteristics and developing new disease resistant cultivars. Furthermore, apple genome sequence provides the opportunity to perform functional genomics and marker / genome assisted breeding.

Table 1.5: Summary of gene prediction from the apple genome sequence [Adopted from**:** Velasco et al., 2010 and Chagné et al., 2014]**.**

Parameters	*M. domestica*	*P. communis*
Predicted genes	54,921	43,419
Average gene length (including introns)	2,802 nt	3,320 nt
Average CDS length	1,155 nt	1,209 nt
Exons	273,206	221,804
Average exon length	273 nt	237 nt
Single exon genes	10,378	10,909
Introns	218,353	178,385
Average intron length	491 nt	398 nt
Genes per 100 Kb	7.3	7.5

1.11. Defense metabolites / phytoalexins of apple and other members of Malinae:

The members of Malinae, produces an array of pre-formed and inducible defense metabolites to combat with pathogen attack. These metabolites play a crucial role in offering ontogenic and inducible pathogen-resistance to plants.

1.11.1. Pre-formed defense metabolites:

Ontogenic resistance is exhibited by preformed antimicrobial compounds known as phytoanticipins. Phenolic acids and flavon-3-ols, such as quinic acid and its derivatives, epicatechin and catechin play major role as preformed defense metabolites in apple (Mikulic Petkovsek et al., 2009; Schwalb and Feucht, 1999). Phenolic acids like caffeic-, chlorogenic-, benzoic-, and salicylic acids were found to help plant under variable stress condition including pathogen attack (Vasco et al., 2009). It has been found that quercetin-3-O-galactoside, chlorogenic acid present in *Malus* play a crucial role against fungal pathogen, moreover quinic acid also serves as an intermediate of phenylpropanoid pathway (Kanwal et al., 2010). Quercetin-3-O-galactoside found in leaves and fruits show nonspecific and very potent anti-fungal activity (Kanwal et al., 2010) and was shown to reduce the growth of several fungus up to 99 percent. Chlorogenic acid which is found in high concentration in fruits of Malinae reported to help plants in repelling brown rot infection (Villarino et al., 2011). Earlier it has been shown that differential accumulation of flavonols (catechins and proanthocyanidins) was key factors in providing scab resistance in apple cultivars (Treutter and Feucht, 1990). Picinelli et al. (1995) and Mayr et al. (1997) have shown a positive association between procyanidins content and scab resistance in apple. In contrary, Sierotzki and Gessler (1993) have shown that there was no positive correlation between scab-resistance and basal level of flavonols in terms of scab susceptibility of apples. In our study, high basal level of catechin (flavonol) content was also observed in the 'Florina' cell culture. It was also reported that scab-resistant apple cultivars are particularly rich in the content of caffeic, chlorogenic, and ferulic acids and their concentration rapidly increases after scab-infection as compared to susceptible cultivars (Mikulic Petkovsek *et al*., 2003). Furthermore, Liaudanskas et al. (2014) had shown that high pehnolic content of scab-resistant apple is associated with higher nutritional quality and antioxidant properties. Scab resistant apple cultivars bears high amount of phloridzin, which is broken down into phloretin after pathogen infection (Lattanzio et al., 2001). A list of major pre-formed defense metabolites in Malinae is listed in Figure 1.8.

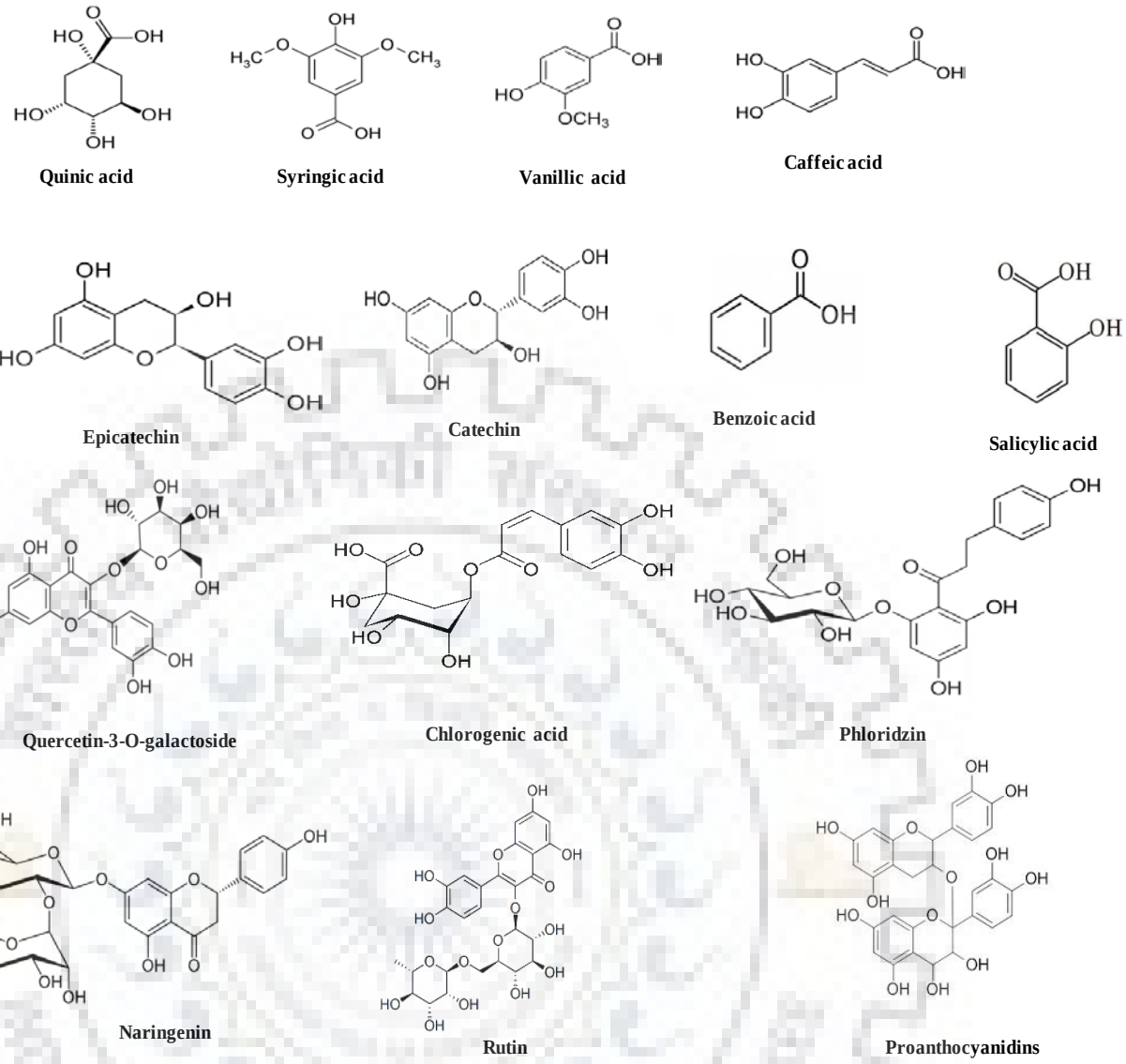

Figure 1.8: Major preformed defense metabolites detected from apples and other members of Malinae.

1.11.2. Salicylic acid: signaling molecule in plants:

Salicylic acid (SA), a C_6-C_1 phenolic metabolite, is considered to be one of the most important endogenous signaling molecules involved in triggering numerous plant defense responses, either locally or systemically (Yalpani et al., 1993). SA-induced local resistance is indicated by the hypersensitive reaction (HR) while in the case of systemic resistance, the signal is transported over long distances where it induces the expression of pathogenesis-related proteins (PR proteins) to trigger systemic acquired resistance (SAR) (Vasyukova and Ozeretskovskaya,

2007). Both HR and SAR are associated with the biosynthesis of SA at the site of infection and in systemic parts of the plant (Gaffney et al., 1993). Considering the economic importance of apple, developing new disease tolerant cultivar is urgently required. It has been recently reported that upon SA application, apple plants showed enhanced resistance towards Glomerella leaf spot disease. However, till date biosynthesis of SA in apple is not well understood (Zhang et al., 2016). In recent past the critical role of SA as signaling molecule in regulation of pathogenesis induced HR and SAR is well established (Vlot et al., 2009). Nevertheless, apart from pathogen-induced SA production, a constitutive level of SA is also detected in many plant species. Constitutive SA level in different plant species is variable, some plants such as *Arabidopsis thaliana* has lower level of endogenous SA whereas plants like *Oryza sativa, Vicia faba* has higher level of endogenous SA (Yu et al., 1997).

Despite important role in triggering plant defense responses, till date the biosynthesis of SA is not well understood (Yang et al., 2015), both at the level of enzymes and genes. Two main pathways of SA biosynthesis in plants are postulated: the chorismate pathway, and the phenylpropanoid pathway (Figure 1.9). The chorismate pathway of SA biosynthesis is well studies in *A. thaliana* (Wildermuth et al., 2001) and *Nicotiana tabbacum* (Catinot et al., 2008). Arabidopsis contains two isochorismate synthase (ICS) genes: ICS1 and ICS2 which catalyze the isomerization of chorismate to isochorismate (Widhalm and Dudareva, 2015). Isochorismate serves as the intermediate for SA biosynthesis. Arabidospsis chorismate mutase (CM1) gene is known to possess isochorismate pyruvate lyase (IPL) activity which converts isochorismate to SA (Strawn et al., 2007). Newly synthesized SA is then exported from the plastids using enhanced disease susceptibility 5 (EDS5) transporter (Serrano et al., 2013).

In the phenylpropanoid pathway, phenylalanine is first converted to *trans*-cinnamic acid in a reaction catalyzed by the phenylalanine ammonia-lyase (PAL) enzyme. From the *trans*-cinnamic acid, two routes have been reported for SA biosynthesis in different plant species. In the first route, *trans*-cinnamic acid undergoes direct C_2-chain cleavage to yield benzoic acid. The mechanism of the C_2-side chain shortening is either *β*-oxidative or non-*β*-oxidative as previously reported. In the *β*-oxidative pathway, *trans*-cinnamic acid is first converted to cinnamoyl-CoA (Gaid et al., 2012; Klempien et al., 2012), followed by the formation of benzoic acid (Widhalm and Dudareva, 2015; Yalpani et al., 1993). Benzoic acid is then hydroxylated at the C_2 position to yield SA. A soluble CYP 450 monooxygenase, benzoate-2-hydroxylase, catalyzing C2-hydroxylation has been reported in tobacco (León et al., 1993). In tobacco,

cucumber and rice, the SA biosynthesis was proposed to proceed exclusively via free benzoic acid (Meuwly et al., 1995; Silverman et al., 1995).

In the non-*β*-oxidative pathway, it was hypothesized that *trans*-cinnamic acid is converted to benzoic acid through the intermediate formation of benzaldehyde, following a mechanism similar to that of 4-hydroxybezoic acid formation in potato tubers (French et al., 1976) and *Daucus carota* (Sircar and Mitra, 2008) and 4-hydroxybenzaldehyde synthesis in the cell cultures of *Vanilla planifolia* (Podstolski et al., 2002). However, it was later demonstrated that application of benzaldehyde to tobacco plants caused many-fold enhancements in the SA level, and upon the application of radio-labeled benzaldehyde, the radioactivity moved to SA via benzoic acid (Ribnicky et al., 1998). In contrast, the application of radiolabeled *trans*-cinnamic acid showed no radioactivity incorporated into benzaldehyde which raised questions about the involvement of benzaldehyde in SA biosynthesis (Jarvis et al., 2000; Malinowski et al., 2007). In the second route, *trans*-cinnamic acid is first hydroxylated to *2*-coumaric acid which then undergoes oxidative or non-oxidative C_2-side chain shortening. In the oxidative mechanism, 2-coumaroyl-CoA undergoes oxidative C_2-side chain cleavage to form SA as reported in *Gaulteria procumbens* (El-Basyouni et al., 1964). In the non-oxidative route, *2*-coumaric acid was proposed to be converted to SA through the intermediate formation of salicylaldehyde. Such conversion of *2*-coumaric acid to salicylaldehyde was reported in *N. tabacum* involving salicylaldehyde synthase activity (Malinowski et al., 2007). The next enzyme involved in the conversion of salicylaldehyde to SA is still elusive. Until now, information on salicylaldehyde synthase activity has been unavailable.

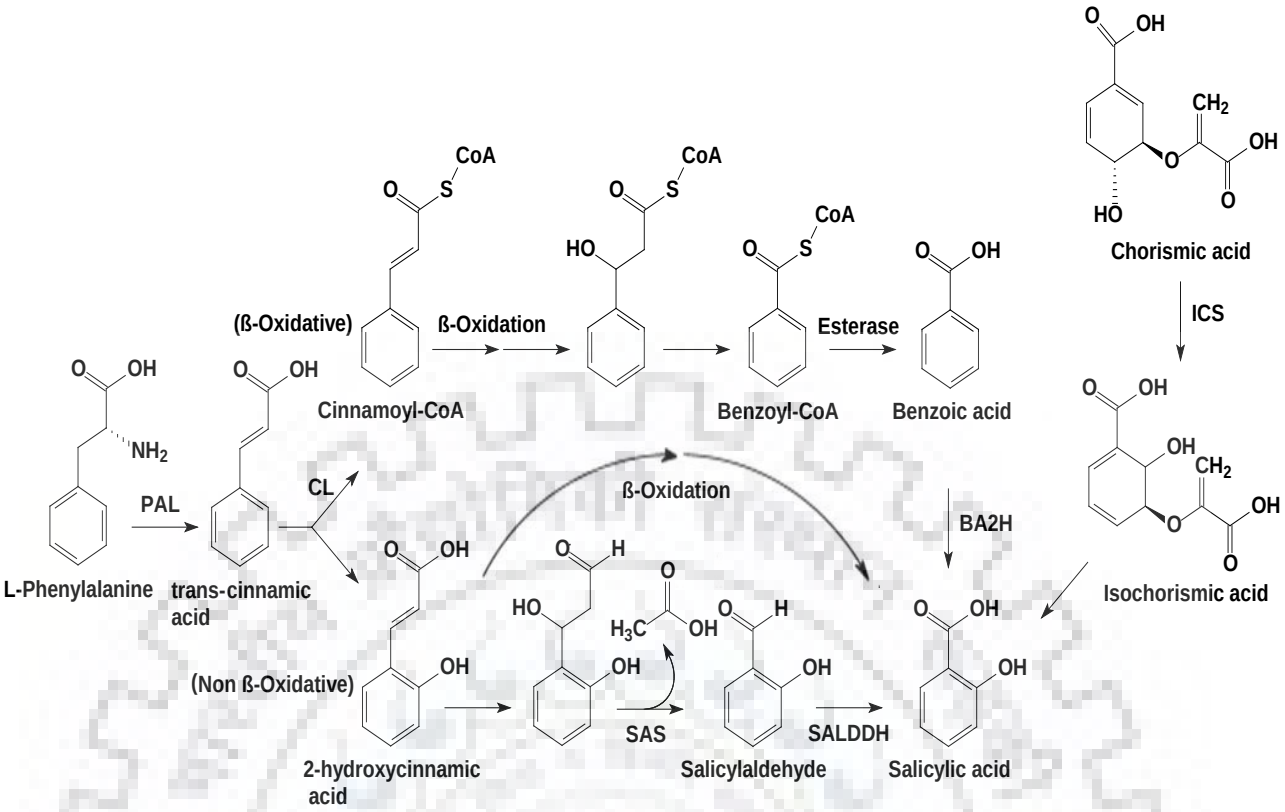

Figure 1.9: Possible biosynthetic route(s) of salicylic acid formation in plants. (*PAL* – phenylammonia lyase, *CL* – cinnamte CoA ligase, *SAS* – Salicylaldehyde synthase, *SALDDH* – Salicylaldehyde dehydrogenase, *ICS* – Isochorismate synthase) [Adopted from: Yalpani et al., 1993; Ribnicky et al., 1998]

1.11.2 Induced defense metabolites of Malinae: the biphenyls and the dibenzofurans:

Plants need to protect themselves from biotic and abiotic stress. Some resistant mechanisms have been developed to overcome the pathogen attack like hypersensitive reaction, monogenic or polygenic traits and generating systemic acquired resistance. The resistance of host plant against parasite attack also depends on the substances produced before and after infection, which inhibits the growth and suppress pathogen infection. Phytoalexins are low molecular weight toxic substances produced and accumulated in plants with response to pathogen infection, physiochemical stresses and confer protection against infecting parasite. Phytoalexin term was derived from a Greek word meaning 'Plant warding off compounds'. These are non-specific toxic chemicals formed only post infectionally, that inhibits growth and development of microbial inducers on hypersensitive tissue formed when host plant cells comes in contact

with these parasites. Phytoalexins tend to fall into several classes including terpenoids, alkaloids and glycosteroid derived mostly from simple phenylropanoid pathway, shikimate pathway and mevalonate pathway (Hammerschmidt et al., 1999).

Upon pathogen attack, the members of the sub-tribe Malinae can produce two special classes of phytoalexins, the biphenyls and the dibenzofurans. The ability to produce these phytoalexins is only confined to this sub-tribe Malinae (Kokubun and Harborne, 1995). The antifungal and antimicrobial activities of biphenyls and dibenzofurans are well demonstrated (Chizzali and Beerhues, 2012; Hrazdina et al., 1997). Both biphenyls and dibenzofurans inhibited the fungal spore germination and fungal mycelial growth under *in vitro* condition. Recently, thirteen biphenyls and four dibenzofurans phytoalexins specific to Malinae were also tested for *in vitro* antibacterial activity against fire blight infection (Chizalli et al., 2012). However their mechanisms of action these defense compounds are still elusive. Earlier, it has been shown that biphenyls and dibenzofurans mainly localized in the sapwood of the plants (Kokubun and Harborne, 1995). These phytoalexins were not found in the leaves (Hrazdina, 2003), with only exception of *Sorbus aucuparia*, which accumulates aucuparin (2,6-dimethoxy-4-phenylphenol), a biphenyl-derivative, in the leaves in response to biotic and abiotic elicitor-treatment (Kokubun and Harborne, 1994). Until Now, any biphenyl- or dibenzofuran-glycosides have not been identified from any intact plants for Malinae. However, scab-resistant apple cell cultures produced these 2'-glucosyloxyaucuparin (biphenyl-glycoside) and dibenzofuran-glycoside, malusfuran in response to elicitor-treatment (Borejsza-Wysocki et al., 1999). It has been reported that biphenyls and dibenzofurans do not occur simultaneously (Kokubun and Harborne, 1995), however, yeast extract-treated cell cultures of the scab-resistant apple cultivar Liberty accumulated both biphenyls and dibenzofurans simultaneously, which suggested a biogenic relationship between the two classes of compounds. Recently, elicitor-treated cell cultures of *S. aucuparia* or /*Pyrus pyrifolia* also showed simultaneous accumulation of both the biphenyls and dibenzofuran (Hüttner et al., 2010; Saini et al., 2017). Till date, ten (10) biphenyls (Fig 1.10a) and seventeen (17) dibenzofurans (Fig 1.10 b) have been detected so far in Malinae (out of 30 genera) (Chizzali and Beerhues, 2012). Out of total 10 biphenyls, aucuparin is the most widely distributed biphenyl whereas γ-cotonefuran is the most abundant dibenzofuran. Among all detected biphenyls, 2'-glucosyloxuaucuparin is unique to *Malus* species, similarly among dibenzofurans, malusfuran is unique to the genus *Malus* (Chizzali and Beerhues, 2012).

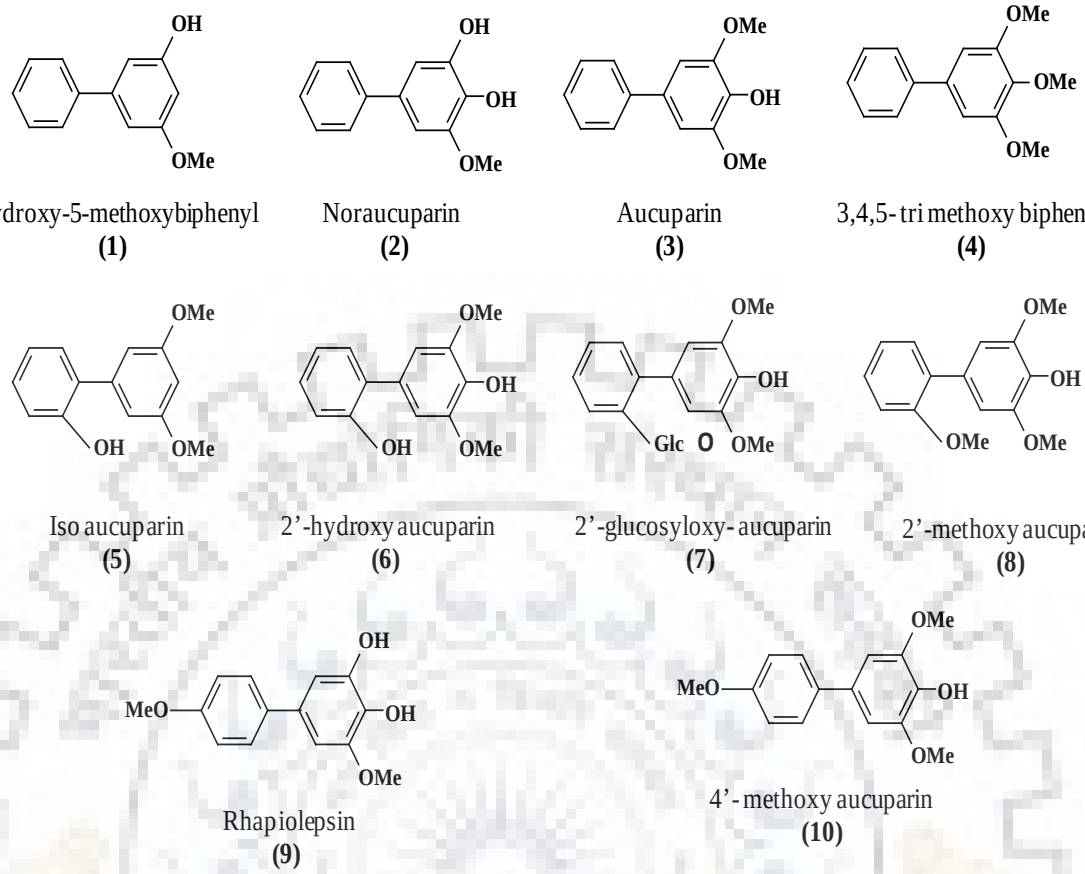

Figure 1.10a: Major biphenyl phytoalexins (1-10) detected from the Malinae.

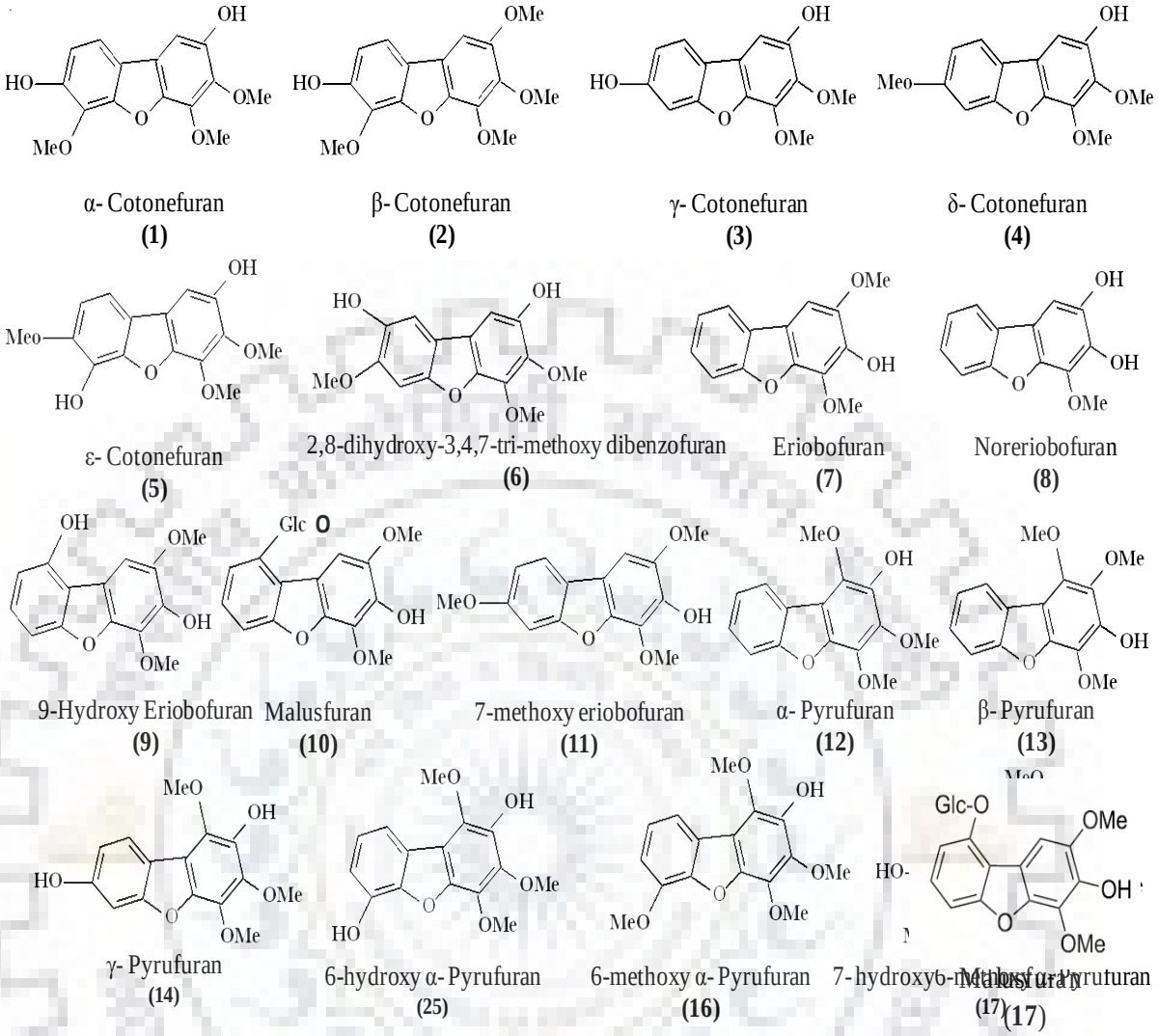

Figure 1.10b: Major dibenzofuran phytoalexins (1-17) detected from the Malinae.

1.12. Biosynthesis of biphenyls and dibenzofurans in Malinae:

The biosynthesis of biphenyls are well elucidated, however dibenzofuran biosynthesis still remains elusive. The biphenyl scaffold is formed by the enzyme biphenyl synthase (BIS) (Liu et al., 2007), which is a type III polyketide synthase. The BIS enzyme catalyzes the condensation of one molecule of benzoyl-CoA with three molecules of malonyl-CoA to produce one molecule of 3,5-dihydroxybiphenyl, the first stable biphenyl (Liu et al., 2004). *BIS* cDNA was cloned and functionally characterized from the *Sorbus aucuparia* cell cultures (Liu et al., 2007). This 3, 5-dihydroxybiphenyl, the starter biphenyl scaffold is further converted into 3-hydroxy-5-methoxybiphenyl in a reaction catalyzed by a *o*-methyltransferase (OMT1) (Khalil et al., 2015). 3-hydroxy-5-methoxybiphenyl is then converted to noraucuparin (3-methoxy-5-phenylbenzene-1,2-diol) by a CYP450 monooxygenase, biphenyl-4-hydroxylase (B4H) (Khalil et al., 2013a). Noraucuparin is then transformed into aucuparin by a second *o*-methyltransferase (OMT2) (Khalil et al., 2015). Recently, a cDNA encoding *OMT1*, *OMT2* has been cloned from cell cultures of *S. aucuparia* (Khalil et al., 2015). However, till date *o*-methyltransferase gene involved in biphenyl biosynthesis has not been cloned from apple system. A *B4H* cDNA has also been cloned from cell cultures of *S. aucuparia* and fire-blight infected *Malus domestica* (Sircar et al., 2015). Till date, enzymes / genes underlying biphenyl to dibenzofurans conversion is not elucidated. However, radio-labeled feeding experiment in cell cultures of *S. aucuparia* demonstrated that dibenzofurans are derived from biphenyl precursors,such as, aucuparin and noraucuparin (Khalil et al., 2015). Two reactions have been postulated for conversion of biphenyl to dibenzofuran, based on detection of various, biphenyl- and dibenzofuran-derivatives at metabolite level. It is likely that noraucuparin or aucuparin first hydroxylated at 2'-position to yield 2'-hydroxy noraucuparin or 2'-hydroxyaucuparin by a CYP450 hydroxylase activity. It is speculated that 2'-hydroxylated noraucuparin or aucuparin undergoes intramolecular cyclization (C-O coupling) by a second CYP450 to yield noreriobofuran or eriobofuran, respectively (Fig 1.11).

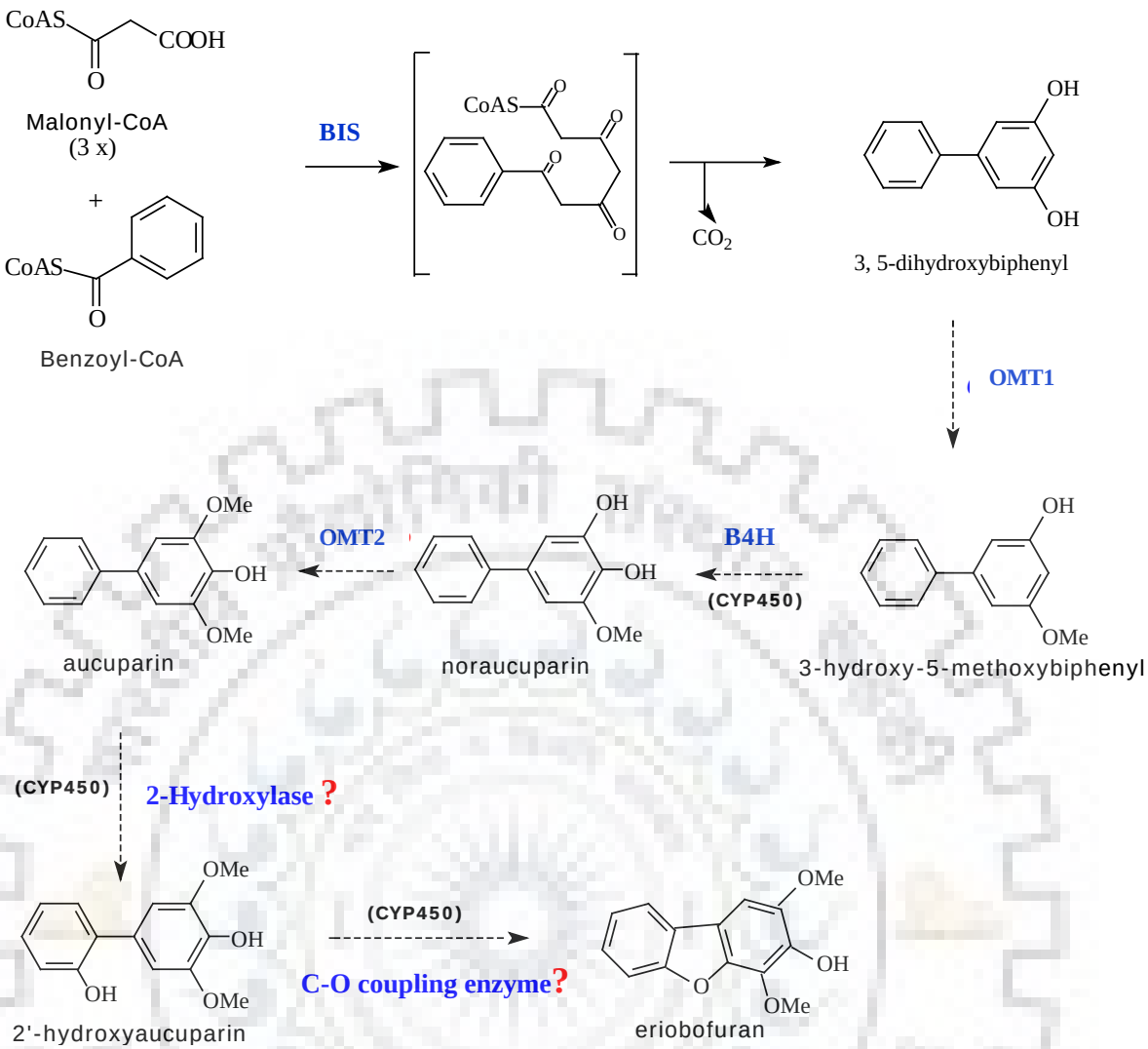

Figure 1.11: Proposed biosynthetic pathway of biphenyl and dibenzofuran formation in apple. Dashed arrow indicates postulated reaction steps in apple. Solid arrow indicates established reaction. [*BIS* = biphenyl synthase; *OMT1*= biphenyl-5-*o*-methyltransferase: *B4H* = biphenyl-4-hydroxylase; *OMT2* = biphenyl-3-*o*-methyltransferase].

1.13. Biphenyl synthase (BIS):

The biphenyl synthase (*BIS*) gene was first isolated, cloned and functionally characterized from yeast extract elicited rowan cell culture (Liu et al., 2004; Liu, ea al., 2007). Benzoyl-CoA was the most efficient substrate for BIS which combines with 3 molecules of malonyl-CoA and forms an tetraketide intermediate which undergoes intermolecular C2→ C7 aldol condensation led to formation of 3, 5-dihydroxybiphenyl after removal of the terminal carboxyl group

(Figure 1.12). The carbon skeleton of two groups of Malinae marker phytoalexins biphenyls and dibenzofurans are formed by these novel BIS (Hrazdina et al., 1997). Biphenyl synthase utilizes benzoyl-CoA and 3 x malonyl-CoA to form identical linear tetraketide intermediate and gives 3,5-dihydroxybiphenyl on the basis of C2→ C7 aldol condensation. There are four gene families of *BIS* has been found n apple based on the alignment of the promoter and coding sequences from cv. Golden Delicious and phylogenetic analysis of nine coding sequences (Chizzali et al., 2012a). When apple cultivar Holsteiner Cox was infected with fire-blight bacterium, only *BIS3* gene was found to be expressed in the transition zone in infected stem. *BIS2* gene was found to be transcribed in leaves but failed to translate into BIS2 protein. BIS3 protein was then localized using immunofluorescence technique in the cortical section of transition zone, specifically associated with the plasmodesmata junctions between adjacent cells (Chizzali et al., 2012a). BIS cDNAs has also been cloned and functionally characterized from *Pyrus communis* (Chizzali et al., 2016).

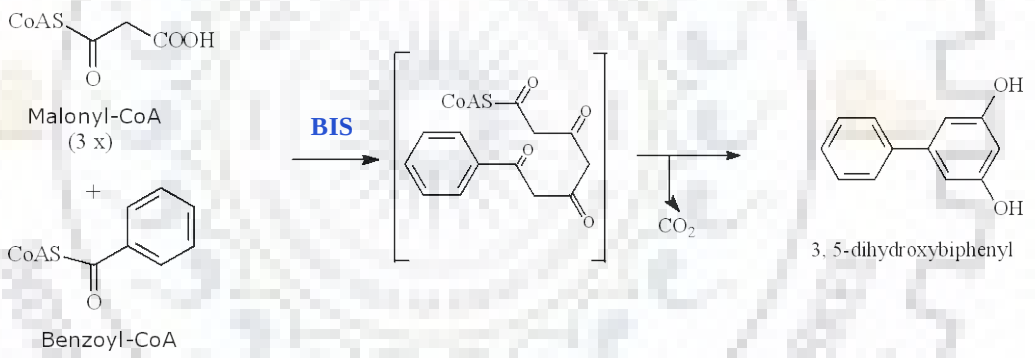

Figure 1.12: BIS catalyzed reaction in biphenyl biosynthesis.

1.14. Biphenyl-4-hydroxylase (B4H):

Cytochrome P450 (CYP) comprises the large, complex and widespread superfamily of structurally diverse and functionally versatile heme monooxygenase class of proteins which engage in variety of endogenous and exogenous reactions of primary and secondary metabolic pathways. Biphenyl-4-hydroxylases is a cytochrome P450 enzyme which catalyzes the intermediary 4-hydroxylation of 3-hydroxy-5-methoxybiphenyl to form noraucuparin. This reaction is catalyzed by the 3-hydroxy-5-methoxybiphenyl-4-hydroxylase enzyme (CYP736A107) which was cloned and functionally characterized from fire-blight infected apple cv. Holsteiner Cox and elicitor-treated cell cultures of *Sorbus aucuparia* (Sircar et al.,

2015). The subcellular localization and transient expression of B4H reporter fusions in *Nicotiana bethamiana* leaf epidermis cells showed ER-localization (Sircar et al., 2015).

1.15. *O*-methyl transferase (OMT):

Plant *O*-methyltransferases (OMTs) constitute a large family of enzymes which catalyze methylation at the oxygen moiety of major secondary metabolites involved in biosynthesis of phenylpropanoids, flavonoids, alkaloids and many other pathways of biotechnological importance. *O*-Methylation plays an important part in lignin biosynthesis, stress response, disease resistance in plants and largely contributes to diversification of natural products. This family of enzymes are generally categorised into class I or class II OMTs on the basis of their structural and enzymatic properties (Joshi and Chiang, 1998; Noel et al., 2003; Lam et al., 2007). Class I OMTs are dependent on Mg^{2+} ions, which catalyses the methylation of hydroxyl groups of caffeoyl-CoA to produce feruloyl-CoA in presence of known enzyme caffeoyl-CoA-OMT (CCoAOMT). This class of enzymes are involved in lignin biosynthesis in plant cells and are characterized by low subunit molecular masses (from 23 to 27 kDa) (Giordano et al., 2016; Zhong et al., 2000). Class II MTs are OMTs that methylate hydroxyl groups of phenylpropanoid and alkalloid derivatives. Class II OMTs do not require Mg^{2+} ions for methylation and separated from CCoAOMTs by presence of higher subunit molecular mass (from 38 to 43 kDa). The evolutionary study suggests that some OMTs may have undergone convergent evolution, while others show divergent evolution.

All S-adenosyl-L-methionine (SAM) dependent methyltransferases which utilizes SAM as methyl group donor have a structurally conserved SAM-binding domain consisting of a central seven-stranded beta-sheet, flanked by three alpha-helices per side of the sheet (Chatterjee et al., 2015). The unique signature sequence for plant O-methyltransferases constitutes of five highly conserved regions, two of which (regions I and IV) are believed to be involved in S-adenosyl-L-methionine and metal binding, respectively. The carboxy terminal glycine-rich signature regions include a 36 amino acid domain located in the mid-terminal section (Ibrahim et al., 1998). *O*-methyltransferases have a common catalytic domain structure that methylate specific substrates and may act as sites for substrate specificity in each enzyme. Comparative evaluation of the predicted amino acid sequences of a number of plants O-methyltransferase cDNA clones shows that they share variable sequence identity, and can be grouped according to the different compounds they utilise as substrates in higher plants (Kota et al., 2004). Members of OMT family usually show a high degree of substrate specificity (Willits et al., 2004).

1.16. Understanding of biphenyl biosynthesis in apple is important: Why?

One defense strategy of plants against pathogens is formation of inducible defence compounds, called phytoalexins. Apple forms biphenyls and dibenzofurans upon pathogen attack. Although this fruit crops have high economic value, biosynthesis of its defence compound is poorly understood. Despite critical role of biphenyl / dibenzofuran phytoalexin in apple to combat pathogen attack, the biphenyls biosynthesis in apple at molecular level is not completely understood. Although *BIS* and *B4H* genes have been characterized in apples, any o-methyltransferase (OMT) genes involved in biphenyl biosynthesis have so far not been cloned and functionally characterized from apples. OMT genes play crucial role in biological diversification of many secondary metabolites. Methylation of hydroxyl-group reduces the solubility of target metabolite, thereby increases the extra-cellular transport of methylated-metabolite resulting into the higher biological activity (Ibrahim et al., 1987).

This incomplete knowledge of biosynthetic pathway is a major reason for designing any metabolic engineering strategy for enhancement of biphenyl phytoalexins. Any successful metabolic engineering of plant natural product requires the following logical steps:

- Metabolomics analyses of pathogen challenged and non-challenged plant system to identify differentially accumulation metabolites.
- Up-regulation of a particular natural product biosynthetic pathway by elicitor treatment (preferably) for enhanced production of metabolite of interest.
- Identification of active enzymes involved in the biosynthetic pathway using cell free extracts, and their characterization.
- Isolation of the corresponding full length cDNA of the target gene(s) usually by homology-based cloning followed by functional characterization of recombinant enzyme.
- Metabolic engineering of target plants using target gene(s).

The complete understanding of biphenyl phytoalexin biosynthesis in apple will provide the basis for future metabolic engineering of biphenyl phytoalexin biosynthesis in economically important apple cultivars.

1.17. Aim of the work:

The biphenyl and dibenzofuran are the specialized phytoalexin in apple and other members of Malinae. However, at molecular level, how biphenyls are formed in apple, are not completely understood. Further, upon pathogen attack, how metabolic re-programming takes place in apple to synthesize an array of defense metabolites is not known. The first aim of my doctoral thesis work is to develop a cell suspension culture of scab-resistant apple cultivar 'Florina'. Cell suspension culture offers an excellent system to understand plant metabolism. Now second aim of my thesis work is to perform a comparative metabolomics of *Venturia inaequalis* elicitor (VIE)-treated cell cultures of apple (*Malus domestica* cv. Florina) to identify differential accumulation of scab-elicitor-induced metabolites in cell culture The third aim of my research is to elucidate the enzymatic steps involved in the biosynthesis of salicylic acid in VIE-treated cell cultures. The fourth and aim of my research is to clone and functionally characterize biphenyl-specific o-methyltransferase gene from elicitor-treated cell cultures of apple. The ultimate aim of this research is to improve our understanding of the defense metabolites / biphenyl phytoalexin biosynthesis in apples, so that metabolic engineering strategies can be successfully applied in the future to enhance pathogen defense potential.

1.18. Objectives:

To fulfill described aim of research following objectives were set for present investigation:

1. To develop cell suspension culture of apple (*Malus domestica* 'Florina')
2. To perform comparative metabolomics of elicitor-treated cell cultures of apple to decipher the bioactive metabolites and the metabolites associated with scab-tolerance.
3. To study the accumulation pattern and biosynthesis of salicylic acid in elicited cell cultures of apple.
4. To clone and functionally characterize *biphenyl-o*-methyltransferase gene from apple cell cultures directing phytoalexin biosynthesis.

Chapter 2

Materials and Methods

2.1. Chemicals and reagents:

The deionized water used for media preparation, buffers, HPLC solvents and aqueous solutions was obtained from Milli-Q water purification system (Millipore). All solutions were sterilized by autoclaving for 20 minutes at 121°C and a pressure of 15 psi. All antibiotics and other thermolabile substances were sterile-filtered with 0.22 µ filter (Sartorius, India) before use. Commonly used glass wares were purchased from Borosil. All authentic standards were procured from following companies:

Aldrich	Genaxy	Ranchem
Alfa Aesar	Himedia	SRL
Duchefa Biochemie	Merck	Sigma

2.1.1. Special chemicals:

2.1.1.1. Chemicals used for Callus induction and maintenance of suspension culture:

Special chemicals used for the development of callus and cell suspension culture are listed in Table 2.1.

Table 2.1: Chemicals used for callus induction and suspension culture

Chemicals	Brand / supplier
2,4- Dichlorophenoxy acetic acid (2,4 D)	Duchefa Biochemie
Kinetin	Himedia
α-Naphthalene acetic acid (NAA)	Himedia

2.1.1.2. Elicitor used:

Yeast extract (YE) and elicitor prepared from *Venturia inaequalis* (VIE) was used to up-regulate metabolite / biphenyl-dibenzofuran biosynthesis in cell suspension culture of apple (*Malus domestica* var. 'Florina') (Table 2.2).

Table 2.2: Elicitors used

Elicitor	Company	Preparation method
Yeast extract (YE)	Himedia, India	YE-elicitor stock solution was prepared by dissolving 1.5 g of yeast extract in 10 ml of distilled water followed by filter sterilization. Seven-day-old cell suspension culture of apple cv. 'Florina' from the linear growth phase were elicited with yeast-extract solution at a final concentration of 3g/L.
Venturia inaequalis elicitor (VIE)	Prepared in laboratory	The strain of *V. inaequalis* (MTCC No.: 1109) was purchased from the Microbial Type Culture Collection and Gene Bank (MTCC), Chandigarh, India. *V. inaequalis* elicitor (VIE) was prepared from fungal cell extracts as described by (Zhang et al., 2016). Briefly, 10 g ground fungal mycelium (Figure 2.1) was added to 1 L acidified water with a final pH of 2. The water extract was then boiled for 1 h, cooled to room temperature and filter sterilized. After filtration, the pH of the fungal extract solution was adjusted to 5.0, and the final volume adjusted to 1 L by adding distilled water. This solution was used as the VIE. For elicitation, 2.5 mL VIE (equivalent to 70 mg fungal polysaccharide) was added to the seven-day-old cell suspension culture (50 mL).

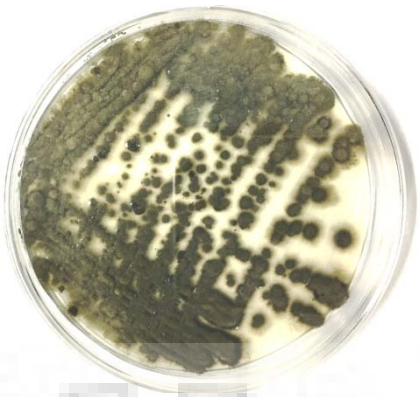

Figure 2.1: *V. inaequalis* mycelium growing on agar plate

2.1.1.3. Solvents & reagents:

Analytical grade chemicals were used in sample preparation and all solvents used for HPLC analyses were of HPLC grade. Solvents and reagents were used for various experimental purposes are as follows (Table 2.3).

Table 2.3: Solvents and reagents

Solvents / reagents	**Brand**
Methanol (HPLC grade)	Merck
Ethanol (Rectified spirit)	Changshu Hyonsung chemicals, China
Ethyl acetate	Merck
Acetonitrile (HPLC grade)	Merck
Dichloromethane (HPLC grade)	Himedia
Sodium hypochlorite	Himedia
Folin-Ciocalteau reagent	Merck
Sodium carbonate	Himedia
DPPH	SRL
Aluminium chloride	Merck

2.1.1.4. Reagents for GC-MS analyses:

Reagents used for GC- MS analyses and sample derivatizations are as follows (Table 2.4).

Table 2.4: Solvents and reagents used for GC-MS analyses

Chemicals	**Brand**
Methanol (HPLC grade)	Merck
Ethyl acetate (HPLC grade)	Merck
Sodium sulphate	Himedia
Dichloromethane (HPLC grade)	Himedia
Phenyl phenol (internal standard)	Himedia
N-methyl-N-(trimethylsilyl)-	Sigma
Methoxy amine hydrochloride	Sigma
Pyridine (MB grade)	SRL

2.1.1.5. Reagents for biochemistry and molecular biology:

Reagents used for biochemistry and molecular biology are as follows (Table 2.5).

Table 2.5: Solvents and reagents used for biochemistry and molecular biology

Chemicals	**Brand**
DMSO	NEB
IPTG	Sigma
dNTPs	NEB
Tris HCl	Sigma
Imidazole	Sigma
DEPC trated water	SRL
Isopropanol	Himedia
Chloroform	Himedia
Phenol	SRL

2.1.1.6. Reagents used for crude protein extraction from cell culture:

Reagents used crude protein extraction from cell culture is as follows (Table 2.6).

Table 2.6: Solvents and reagents used crude protein extraction from cell culture

Chemicals	**Brand**
Polyclar AT	Sigma
HEPES	Himedia
DTT	Sigma
Seasand	Himedia
Polivinylpyrrolidone (PVPP)	Himedia
$NaHPO_4$	Himedia
NaCl	Himedia
Imidazole	Himedia

2.1.1.7. Metabolite standards:

Various metabolite standards used as substrates and products in HPLC / GC-MS analyses are as follows (Table 2.7).

Table 2.7: Metabolite standards

Chemicals	**Brand**
2-Hydroxybenzoic acid	Sigma
2-hydroxycinnamic acid	Sigma
3,5-dihydroxybiphenyl	Synthesized in our research group
3-hydroxy-5-methoxybiphenyl	Synthesized in our research group
Aucuparin	Synthesized in our research group
Benzoic acid	Sigma
Caffeic acid	Sigma
Catechin	Sigma
Chlorogenic acid	Sigma
Eriobofuran	Synthesized in our research group
Ferulic acid	Sigma
L-Phenylalanine	Himedia

Noraucuparin	Synthesized in our research group
o-Coumaric acid	Sigma
p-coumaric acid	Sigma
Pinosylvin	Sigma
Protocatechuic acid	Sigma
Protocatechuic aldehyde	Sigma
Rutin	Sigma
Salicylaldehyde	Sigma
Salicylic acid	Sigma
Sinapic acid	Sigma
Syringaldehyde	Sigma
trans-Cinnamic acid	Sigma
Vanillic acid	Sigma
Vanillin	SRL

2.2. Equipments:

Equipment used for various analyses are listed in Table 2.8.

Table 2.8: Equipments used

Equipment	**Model**	**Brand**
Balance	ME 204 (mg range)	MeltterToledo
Centrifuge 1	1-14 K (cooling)	Sigma
Centrifuge 2	5810-R	Eppendorf
Clean bench	Horizontal laminar flow	Clean air
Digital pH meter	CL54	Toschon
Dry bath	MK-20 (pelltier controlled)	BiochemLifescience
GC-MS	Agilent 6890 gas chromatograph	Agilent
Gel doc	Gel Doc™ XR+ System	Bio-Rad
Hot plate	2MLH	Remi
HPLC	LC- 20 AP	Shimadzu
Incubator shaker	LSI 4018 R	Labtech
Magnetic stirrer	MS 500	Remi

Real time PCR system	Quant studio 3	Applied Biosystem
Rotary vacuum concentrator	Centrivap	Labconco
Sonicator	Q 700	Q SONICA
Spectophotometer	Carry 400	Agilent
Thermocycler	Veriti	Applied Biosystem
Vacuum pump	Millipore	Millipore
Vortex	3003-100	Rivotek
Water bath	Rivotek	Polular Ltd

2.3. Enzyme assay / purification:

Co-factors, buffers and other chemicals used in enzyme assay and partial purification are listed in Table 2.9.

Table 2.9: Chemicals used for enzyme assay / partial purification

Chemicals	**Brand**
DTT (DL-dithiothreitol)	Sigma
HEPES Buffer	Sigma
Tris Buffer	Himedia
Ammonium acetate buffer	Himedia
Cysteine	Himedia
Ascorbic acid	Himedia
β-Mercaptoethanol	Himedia
S-adenosyl-l-methionine (SAM)	Sigma
ATP	Himedia
CoA (Coenzyme A)	Sigma
Polyvinylpyrrolidone (PVPP)	Himedia
NaHPO4	Himedia
NaCl	Himedia
Imidazole	Himedia
Glacial acetic acid	Roth

2.4. Stationary phases used for protein affinity purification, desalting and concentration:

Stationary phases used for protein affinity purification, desalting and concentration are listed in Table 2.10.

Table 2.10: Stationary phases used for protein affinity purification, desalting and concentration

Solvents / reagents	**Brand**
PD_{10} column- cartridge Sepharose G-25 columns	GE Health care
CM/DEAE- Sepharose column	Bio-Rad
Ni-NTA agarose	Qiagen

2.5. Reagents for gel electrophoresis:

Reagents for gel electrophoresis are listed in Table 2.11.

Table 2.11: Reagents for gel electrophoresis

Solvents / reagents	**Brand**
Ultrapure Agarose	Thermofisher Scientific
Ethidium bromide	Hi media
TEMED	SRL
Acrylamibe and Bisacylamide	Merck
SDS	Hi media
EDTA	Hi media
B-mercaptoethanol	Merck
Aluminium persulphate	Hi media
Bromophenol blue	SRL
Coomassie-blue R-250 and G-250	Merck

2.6. DNA and protein Ladders:

DNA and protein Ladders used are listed in Table 2.12.

Table 2.12: DNA and protein ladders

Ladder	**Brand**
1 kb / 100 bp DNA ladder	NEB
Gene ruler DNA ladder Mix	Fermantas
Long range SDS PAGE Standard	Bio-Rad

2.7. Nutrient media for plant tissue culture:

Readymade plant growth media (LS medium) (Linsmaier and Skoog 1965) was used for tissue culture (Table 2.13). 50 mL of media were poured into Erlenmeyer flask (250 mL capacity), then sealed with aluminum foil followed by autoclaving at 121^0C for 20 min.

Table 2.13: Media composition for callus and suspension culture.

Medium	Brand name	Preparation & Storage
A. For callus Linsmaier and Skoog (LS) medium (without sugar and hormone)	Himedia, India	4.2 g media powder was dissolved in 800 mL of deionized water along with 30 g sucrose (3%), 2 µM 2,4-dichlorophenoxyacetic acid (2,4-D), 1 µM kinetin and 1 µM naphthaleneacetic acid (NAA). pH was adjusted to 5.8 with 1 N NaOH, then adjust final volume to 1 L. Sterilize by autoclaving at 121^0C for 20 min. For solid media, 0.7-0.8% agar was added prior to autoclaving.
B. For cell suspension culture Linsmaier and Skoog (LS) medium (without sugar and hormone)	Himedia, India	4.2 g media powder was dissolved in 800 mL of deionized water along with 30 g sucrose (3%), 2 µM 2,4-dichlorophenoxyacetic acid (2,4-D) and 1 µM naphthaleneacetic acid (NAA). pH adjusted to 5.8 with 1 N NaOH, then adjust final volume to 1 L. Sterilize by autoclaving at 121^0C for 20 min. Stored at room temperature.

2.8. Nutrient media for fungal culture (scab-fungus):

Table 2.14: Malt extract peptone medium for *Venturia inaequalis* growth

Medium	**Composition**	**Preparation & Storage**
Malt extract peptone medium For solid media	Malt Extract 30 g/L Peptone 3 g/L Agar 1.5 %	Mix with 800 mL of deionized water; pH adjusted to 7.0 with 1 N HCl, then final volume was adjusted to 1 L. Sterilize by autoclaving at 121^0C for 20 min.

2.9. Bacterial culture medium and reagents:

Table 2.15: Culture medium and reagents for *E. coli* growth

Medium	**Components**
Luria-Bertani (LB) medium	Bacteriological peptone 10g Yeast extract 5g NaCl 10g For solid media, 1.2 % agar was added prior to autoclaving.
Antibiotics	**Ampicillin 100 mg/mL** Prepared in autoclaved water and then filter sterilized. **Chloramphenicol 30 mg/mL** Prepared in pure ethanol and then filter sterilized.
For induction of protein expression	**IPTG (Stock 0.5 M)** Final concentrationin bacterial culture 0.5 mM
For Preservation at -80°C	**Glycerol: LB medium (60:40)** 250 µL Bacterial culture 750 µL

2.10. YMB growth medium for *Agrobacterium tumefaciens* growth:

Table 2.16: Preparation of YMA (or YMB) medium for *A. tumefaciens* growth

Medium	Composition		Preparation & Storage
Yeast mannitol Broth (YMB) / Yeast manitol Agar (YMA)	K_2HPO_4	0.05 g/L	Mix with 800 mL of deionized water; pH adjusted to 7.0 with 1 N HCl, then final volume was adjusted to 1 L. Sterilize by autoclaving at 121^0C for 20 min. For solid media (YMA), 1.5% agar was added prior to autoclaving. Stored at room temperature. Mostly used within 4-5 days.
	$MgSO4.7H_2O$	0.02 g/L	
	NaCl	0.01 g/L	
	Yeast Extract	0.04 g/L	
	Manitol	1.0 g/L	
	Agar (for YMA)	15.0 g/L	

2.11. Activation medium for *A. tumefaciens* transformation

Table 2.17: Activation medium for *A. tumefaciens* growth for transient expression in *Nicotiana benthamiana* leaves.

Medium	Composition		Preparation & Storage
Activation medium	MES/KOH (pH 5.6)	10 mM	Prepared freshly. MES and MgCl2 dissolved in deionized water while Acetosyringone mixed in Ethanol.
	MgCl2	10 mM	
	Acetosyringone	150 mM	

2.12. Antibiotic used in medium for growth of *Agrobacterium tumefaciens*

Different antibiotics used in bacterial culture medium were mentioned in Table 2.18.

Table 2.18: Antibiotics used in bacterial medium

Antibiotic	**Manufacturer**	**Preparation & Storage**
1. Kanamycin	Himedia, India	Stock solution of 30 mg/10 mL was prepared in water and filter sterilized by 0.20 µM filter. From this stock 16.5 µL was added to every 10 mL of YMB media (i.e. 10 µL/mL media) to get a final concentration of 250 mg/L.Stored at 4 ^{0}C. Used freshly or before one week.
2. **Rifampicin**	Himedia, India	10 mg/mL stock solution of rifampicin was prepared in methanol; filter sterilized by 0.20 µM filter. From stock, 50 µL was added to every 10 mL of YMA/YMB media to get a final concentration of 50µg/mL. Stored at 4 ^{0}C.

2.13. Buffers and solutions used for enzyme assay

2.13.1. Buffer for enzyme extraction

Following buffers were used for enzyme extraction of phenyl ammonia-lyase (PAL), Salicylaldehyde synthase (SAS) and O-methyltransferase (MdOMT), as listed in (Table 2.18).

Table 2.19: Buffers used for enzyme extraction

SN	**Name**	**Ingredient**	**Preparation & Storage**
A	For Phenylalanine ammonia-lyase (PAL) (100 mM HEPES, pH 8.0 with 10 mM DTT).	HEPES buffer 2.4 g DTT 154 mg Water to 100 mL	Adjust pH 8.0 by 1 N NaOH, stored at 4^{0}C. DTT was added freshly. Polyclar AT was added before use
B	For salicylaldehyde synthase (SAS) assay	HEPES buffer 2.4 g DTT 77 mg	DTT were freshly prepared and added during

	(100 mM HEPES, pH 8.0 with 5 mM DTT).	Water to 100 mL	extraction. pH 8.0 was adjusted by 1N NaOH.
C	For o-methylatransferase (MdOMT) assay (100mM Tris-HCl, pH 8.5)	Tris buffer 1.41 g Water to 100 mL	pH 8.5 was adjusted by conc HCl, autoclaved and stored at 4 ^{0}C.

2.13.2. Buffer used for enzyme assay:

Following assay buffers were used (Table 2.20) to assay phenyl ammonia-lyase (PAL), Salicylaldehyde acid synthase (SAS), O-methyltransferase (MdOMT) respectively.

Table 2.20: Buffers used for enzyme assay

S.No.	**Name**	**Ingredient**	**Preparation & Storage**
PAL	Assay buffer (100mM Tris-HCl, pH 8.6)	Tris buffer 1.21 g Water to 100 mL	pH 8.6 was adjusted by conc HCl, autoclaved and stored at 4 ^{0}C.
SAS	Assay buffer (200mM Tris-HCl, pH 7.5)	HEPES buffer 2.4 g Water to 100 mL	pH 7.5 was adjusted by conc HCl, autoclaved and stored at 4 ^{0}C.
MdOMT	For o-methylatransferase (MdOMT) assay (100mM Tris-HCl, pH 8.5)	Tris buffer 1.41 g Water to 100 mL	pH 8.5 was adjusted by conc HCl, autoclaved and stored at 4 ^{0}C.

2.13.3. Buffers for affinity purification of His_6-tag fusion protein (Table 2.21)

S.No.	Buffer name	Ingredient	
1	Lysis buffer pH = 8.0	NaH2PO4	3.4 g
		Nacl	0.9 g
		20 mM Imidazole	0.7 g
		dH20	500 mL
2	Washing buffer pH= 8.0	NaH2PO4	3.4 g
		Nacl	0.04 g
		20 mM Imidazole	1.7 g
		dH20	500 mL
3	Elution buffer pH= 8.0	NaH2PO4	3.4 g
		Nacl	8.8 g
		20 mM Imidazole	8.5 g
		dH20	500 mL

2.13.4. Buffers for plasmid isolation (miniprep)

Table 2.22: Buffers for plasmid isolation (miniprep)

S. No.	Buffer	Ingredients	
1	Buffer1	Tris-HCl	3.4 g
		EDTA	0.9 g
		RNase A	0.7 g
		Adjust to pH 8.0 with HCl	
		RNase A was freshly added prior to use.	
2	Buffer 2	NaOH	0.2 M
		SDS	1 % (w/v)
3	Buffer 3	Pottassium acetate	2.55 M
		Adjust to pH 5.5 withglacial acetic acid.	

2.13.5: Buffer for DNA gel electrophoresis:

TAE buffer was used for DNA gel electrophoresis (Table 2.23).

Name of Buffer	Ingredient	Preparation & Storage
50 X TAE Buffer	Tris buffer 242 g EDTA 18.61 g Glacial acetic acid 57.1 ml Water 1L	Adjust pH 8.0 by later addition of Glacial acetic acid, autcoclaved and stored at room temperature.

2.13.6: Buffers and reagents for SDS-PAGE electrophoresis

Table 2.24: Buffers and reagents for SDS-PAGE electrophoresis

Name of Buffer	Ingredient	Preparation & Storage
Stacking Gel (5 %)	Tris buffer (0.5 M) 1.25 mL (pH 6.8) Acrylamide/Bis (30 %) 2.0 mL SDS (10 % w/v) 0.05 mL APS (10 % w/v) 0.05 mL TEMED 5 µL Water 3.0 mL	TEMED added in the last for polymerization and the mixture was poured immediately and gently to avoid bubble formation using pipette. Allowed it to solidify.
Resolving Gel (12 %)	Tris buffer (0.5 M) 1.3 mL (pH 8.8) Acrylamide/Bis (30 %) 0.6 mL SDS (10 % w/v) 0.05 mL APS (10 % w/v) 0.05 mL	TEMED added in the last for polymerization and the mixture was poured immediately and gently to avoid bubble formation using

	TEMED 5 µL Water 1.2 mL	pipette on solidified stacking gel..
Protein loading buffer	Tris buffer (0.5 M) (pH 6.8) 1.0 mL Glycerine 2.0 mL SDS (10 % w/v) 3.3 mL B-mercapoethanol 0.5 mL Bromophenol blue (5% w/v) 0.5 mL	Mixed well and used during staining of protein sample.
Electrophoresis tank buffer	Tris HCl 3.0 g Glycine 14.4 g Na-SDS 1.0 g Water 1000 mL	Mixed well and check pH without adjustment should be 8.3
Staining solution	Ethanol 30 mL Coomassie brilliant blue – 250 200 mg Glacial acetic acid 7 mL Water 43 mL	Mixed well and used for staining the protein bands on gel.
Destaining solution	Ethanol 30 mL Glacial acetic acid 7 mL Water 63 mL	Mixed well used for destaining the gel to get clear protein bands

2.14: Washing solution for regeneration of PD_{10} column and Ni-NTA agarose regeneration

Composition of washing solution used for regenerating PD_{10} column and Ni-NTA agarose regeneration was mentioned in Table 2.25.

Table 2.25: Washing solution for regeneration of PD_{10} column and Ni-NTA agarose regeneration

Name	Ingredient	Washing procedure
NaOH Cleaning solution	NaOH 0.16 M	Wash PD10 column with five column volumes of NaOH cleaning solution followed by five volume of distilled water. After washing pH was checked pH (should be neutral) to confirm cleaning.
Ni-NTA agarose washing and regeneration solution	Acetic acid 0.2 M Glycerol 30 % Deionized water	Wash with the following solutions in the same order.

2.15: Reagents used for protein estimation:

Bradford reagent was used for protein estimation (Table 2.26).

Table 2.26: Composition of Bradford reagent used for protein estimations

Name	Ingredient	Preparation & Storage
Bradford dye solution	Coomassie®-Brilliant Blue G 250 100 mg Ethanol (96%) 50 mL Orthophosphoric Acid (85%) 100 mL Water to 1000 mL	Dissolve well Coomassie®-Brilliant G 250 in ethanol, add Orthophosphoric acid and make up volume to 1 L with water. Filter the solution with filter paper (Whatman No. 1) and keep in refrigerator in dark bottle.

2.16. Materials used for molecular biology experiments

2.16.1. mRNA extraction, cDNA synthesis and real time PCR reagents:

Various reagents and enzymes used for mRNA extraction, cDNA synthesis and for real time PCR analyses are listed in Table 2.27.

Table 2.27: Kits, enzyme and reagents used in molecular biology

Enzyme	**Brand**
DNeasy Plant Mini kit	Qiagen
RNeasy Plant Mini kit	Qiagen
M-MuLV reverse transcriptase	NEB
Taq. DNA polymerase	NEB
Phusion® HF DNA polymerase	NEB
dNTPs	NEB
Fast Alkaline phosphatase (FastAP)	Thermofisher Scientific
Restriction endonuclease	NEB
RiboLock RNase inhibitor	Thermofisher Scientific
T4 DNA ligase	NEB
Minelute Gel extraction kit	Qiagen
Genelute PCR Clean-up kit	Sigma
Power Up ™ SYBR ™ Green Master Mix	Applied Biosystems

2.16.2. Host cells (Competent *E. coli*)

Table 2.28: Host cells.

E. coli	**Purpose**	**Genotype**
DH5α	This strain was used for the initial cloning and plasmid amplification into various vectors	F' φ80δlacZ9M15 end A1 hsdR17(rk-mk+)supE44thi-1 λ-gyrA96 relA1 9(lacZYA-argFV169) deoR
BL21(DE3)pLysS – For overexpression of protein	Used for protein expression of target gene cloned in pRSET B vector	F- *ompT hsdS*B (rB-mB-) *gal dcm* (DE3) pLysS (CamR)

2.16.3. Vectors

Table 2.29: Cloning and expression vectors used

Vectors	**Characters/purpose**	**Supplier**
A-Cloning vector		
pGEM-T easy	3kb T-overhanged vector with *lacZ* and ampicillin resistance genes for subcloning of *Taq* DNA polymerase-amplified PCR products.	Invitrogen
B-Expression vectors		
pRSET B	2,9 kb expression vector with N-terminal His_6-tag and ampicillin resistance gene	Invitrogen

2.16.4. Primers used

All primers used in various PCR amplifications were obtained from Eurofin genomics (Bangalore, India).

Table 2.30a: Primers used for gene expression analyses by qPCR (for metabolomics samples)

Gene name	Primer No.	Primer sequence (5' - 3')	GDR Accession No
PAL	Q1	TGGCGAGTGAGAAGAATGC	MDP0000191304
	Q2	TCTTCCTCGAAAGCTCCAATCT	
F3H	Q3	GCTCTCCCTGCCTCGAATG	MDP0000190489
	Q4	GGATGTGGAACCGTTGATT	
AOX	Q5	GGAGCGGCGACGGTTT	MDP0000643331
	Q6	GCGCGCTGCTCATCATC	
BIS3	Q7	CCATCAAATGTCTACTACCAAGAG	MDP0000287919
	Q8	AGCTTTGCCTTCTTCAATCGACTTC	
Actin	Q9	GTGAGGCTCTATTCCAACCATC	MDP0000921834
	Q10	GGAACACAAATTGGGCAAGTAT	

Table 2.30b: Primers used for the cloning and localization and expression analyses of *MdOMT*

Primer	Sequence (5' - 3')*
1	GATGCTAGCATGGCTTCTCTAGAGGAACC [a]
2	GATGGTACCCTACTTGTAGAATTCCATGATCC [b]
3	GAAGAGAATTCTCAAGCTCTACA [a]
4	TGCCCGCAGACAACTTTGTTTAAT [a]
5	TGAGCTC TGTCAAAGGC AATTCC [b]
6	CACTGCAGCTGGTGGTTTCTT
7	CAAGCTCAATTGCTGACTGCAT
8	GTGAGGCTCTATTCCAACCATC
9	GGAACACAAATTGGGCAAGTAT
10	TGGCGAGTGAGAAGAATGC
11	TCTTCCTCGAAAGCTCCAATCT
12	CCATCAAATGTCTACTACCAAGAG
13	AGCTTTGCCTTCTTCAATCGACTTC
14	GGGGACAAGTTTGTACAAAAAAGCAGGCTTAACCATGGCTTCTCTAGAG GAACCA
15	GGGGACCACTTTGTACAAGAAAGCTGGGTCCTACTTGTAGAATTCCATGAT CCA
16	GGGGACCACTTTGTACAAGAAAGCTGGGTCCTTGTAGAATTCCATGATCCA

*Restriction sites underlined; a, *Nhe*I; b, *Kpn*I

2.17. Antioxidant and cytotoxic activity of bioactive phenolic metabolites isolated from the yeast-extract treated cell culture of apple

2.17.1. Plant materials

Apple cultivar 'Florina' (Malus domestica cv. 'Florina') was obtained from Central Institute of Temperate Horticulture (CITH), Srinagar, India. Apple plants were maintained under temperate condition in a micro-climate control green house (temperature 20 -22 ^{0}C and relative humidity of 65-70 %). Analytical grade chemicals were used in sample preparation and all solvents used for HPLC analyses were of HPLC grade. All authentic standards were procured from Sigma-Aldrich Chemical Co. Ltd (India). Growth regulators and plant growth media were purchased from Himedia (India). MCF-7, HeLa and HEK-293 cell lines were obtained from National Center for Cell Science (NCCS), Pune, India. DMSO (cell culture grade), MTT (3-(4,5-dimethyl-2-thia-zolyl) 2,5diphenyl-2H-tetrazoliumbromide), 5-Fluorouracil (5-FU), plant growth media, plant growth regulators were obtained from Himedia (India).

2.17.2. Induction and maintenance of cell suspension cultures

Primary callus culture was derived from the young leaves. Three to four top young leaves (8-10 days old) were collected and surface sterilized. After surface sterilization, leaf segments were cut into 10 mm sections and put on basal LS medium (Linsmaier and Skoog, 1965) supplemented with 30 g l^{-1} sucrose, 7 g l^{-1} agar and various concentrations and combinations of 2,4-D (0.5, 1.0, 2.0, 2.5 µM); NAA (0.5, 1.0, µM) and kinetin (0.5, 1.0, µM) in dark condition for callus induction. Optimum growth regulator combination was selected based on highest callus growth. The pH of the medium was adjusted to 5.8. Aseptic cultures were maintained at 26˚C in dark. Calli were propagated by regular sub-culturing at 4-weeks interval. Medium without plant growth regulators served as control. Friable soft calli were selected for the initiation of cell suspension culture. Cell suspension was initiated in dark by shaking 3 g of calli at 120 rpm in 50 ml of the liquid LS-medium (in 250 ml Erlenmeyer flasks) containing 2 µM 2,4-D and 1 µM NAA. Cells were harvested at 7- to 9 -day intervals by vacuum filtration.

2.17.3. Elicitor Preparation and treatment

Elicitor stock solution was prepared by dissolving 1.5 g of yeast extract in 10 ml of distilled water followed by filter sterilization. Seven-day-old cell suspension culture from the linear growth phase were elicited with yeast-extract solution at a final concentration of 3g/l. Flasks were kept at 26^0 in dark in an orbital shaker at 100 rpm. After onset of elicitation, cell cultures were harvested at defined post-elicitation time points: 0, 12, 24, 48 and 72 hours post elicitation (hpe). In the control treatment, similar volume of sterile distilled water was added in lieu of the yeast extract. Three replicates were used for each treatment, and the experiment was repeated two times.

2.17.4. Sample preparation

The cells were harvested at defined post-elicitation time points by vacuum filtration and kept in hot air oven at 60^0 C for 4h. Dried cell mass (2g) was crushed in liquid nitrogen and subsequently extracted with 5 ml methanol (50%; v/v) at room temperature. The suspension was homogenized for 5 min and then centrifuged at 5000 rpm for 15 min. The resulting supernatant was filtered using a 0.45 µ syringe filter and directly used for HPLC analysis of phenolic metabolites as well as for the evaluation of total soluble phenolics, total flavonoids and antioxidant potential. A separate sample preparation procedure was followed for cytotoxicity assays. Methanolic extract was evaporated in a rotary evaporator to remove methanol and remaining aqueous phase was lyophilized and re-dissolved in 500 µl of dimethyl sulphoxide (DMSO). DMSO extract at various dilutions were used for cytotoxicity assays.

2.17.5. HPLC analysis of phenolic acid:

HPLC analysis of metabolites was performed on a Phenomenex™ (Torrance, USA) C_{18} column (RP-Hydro, 4µm, 250 x 4.6 mm) using a Shimadzu-HPLC system (Shimadzu Corporation, Kyoto, Japan) equipped with a CBM-20A controller, LC-20AP pump, SPD-M20A PDA detector. Peaks were identified by comparing their retention time and UV-spectra with those of authentic standards. Data was acquired and processed with LC-Solution software (Shimadzu Corporation, Kyoto, Japan) on Windows 7 ™ platform. Chromatograms were monitored with a PDA detector on a Windows 7 Professional platform with a Lab Solutions Multi LC-PDA software (Shimadzu). An isocratic solvent system 1mM TFA in water: methanol [70:30; (v/v)] with a flow rate of 1.0 ml/min for 60 min was used to elute the phenolic acids and flavonoids.

2.17.6. Determination of total phenolic content (TPC)

Total phenolic content was determined using Folin-Ciocalteau method (Singleton et al., 1999). Briefly, 0.2 ml of 50% methanolic extract was mixed with 0.5 ml Folin-Ciocalteau reagent (dilution 1:9 with water) and incubated at room temperature for 5 min to initiate the reaction. Thereafter, 0.3 ml of 5% sodium carbonate was added to the mixture followed by 20 min incubation in dark at room temperature. The absorbance was measured at 765 nm. Total phenolic content was expressed as micrograms of gallic acid equivalents per gram dry mass.

2.17.7. Determination of total flavonoid content (TFC)

Total flavonoids content was measured as essentially described by (Wang et al., 2008). Methanolic extract (0.5 ml) was added to, 0.5 ml of 2% $AlCl_3$ solution in ethanol and incubated at room temperature. After 1 h incubation, absorbance was measured at 420 nm. Total flavonoid content was expressed as micrograms of quercetin equivalent per gram dry mass.

2.17.8. Estimation of antioxidant activity

2.17.8.1. DPPH radical scavenging activity assay

DPPH (1, 1-diphenyl-2-picrylhydrazyl) assay was performed as essentially described by (Turkoglu et al., 2007). 200 µl of various concentration of methanolic extract was added to 800 µl of 0.004% methanol solution of DPPH. After a 30 min incubation period at room temperature, the absorbance was measured at 517 nm using a blank. Blank reaction consisted of all reagents except the callus extract. Percent (%) inhibition of free radical by DPPH was calculated using following formula.

Inhibition (%) = $(A_{blank} - A_{sample}/A_{blank}) \times 100$

The results were expresses as IC_{50} values. The EC50 value is the concentration of an antioxidant required to lower the initial concentration of DPPH by 50%. Ascorbic acid was used as standard antioxidant. All experiments were performed in triplicates.

2.17.8.2. Ferric reducing antioxidant power (FRAP) assay

Ferric reducing antioxidant power (FRAP) antioxidant potential was determined according to the method described by (Benzie and Strain, 1996) with minor modification. FRAP reagent was prepared fresh mixing 1 ml of 10 mM 2,4,6-tripyridyl-s-triazine (TPTZ) solution with 10 ml of 300 mM acetate buffer in 40 mM hydrochloric acid and 1 ml of 20 mM $FeCl_3 \cdot 6H_2O$. Briefly,

30 µl of methanolic extract, 70 µl of water was added to 1 ml of freshly prepared FRAP reagent and the mixture was incubated at 37°C for 15 min. Thereafter, the absorbance was measured at 593 nm against a blank. In blank reaction, methanolic extract was replaced by water. A calibration curve was prepared using different concentrations of ascorbic acid. Results were expressed as micromoles of ascorbic acid equivalents per milligram of extract (µmol of AAEs/mg).

2.17.9 Preparation of cell-free extract

Cell-free extract was prepared according to (Sircar and Mitra, 2008) at defined post elicitation time points (0h, 12 h, 24 h, 48 h and 72 h) to determine phenylalanine amonia-lyase (PAL) activity. All steps were carried out at 4 ^{0}C. Cells (4 g) were collected by filtration, mixed with 5% (w/w) Polyclar AT (Himedia, India) and homogenized in 5 ml of HEPES buffer (100 mM , pH 8.0) containing 10 mM dithiothreitol (DTT). The homogenate was centrifuged at 10,000 rpm for 25 min at 4°C. An aliquot of the supernatant (2.5 ml) was passed through PD10 column (GE Healthcare) equilibrated with Tris-HCl buffer (200 mM, pH 7.0). The soluble protein content was determined according to the Bradford method (Bradford, 1976) using bovine serum albumin as the standard.

2.17.10. Assay of phenylalanine ammonia-lyase (PAL)

PAL activity was determined according to Sircar and Mitra, 2008. Cinnamic acid, the product of PAL-catalyzed reaction was determined by HPLC using Waters Symmetry^{TM} C_{18} reversed-phase column (3.5µm, 75 x 4.6 mm). An isocratic linear solvent system comprising 1mM TFA in water: methanol (55:45; v/v) with a flow rate of 1 ml/min for 10 min was used to separate cinnamic acid. Cinnamic acid was monitored at 280 nm.

2.17.11. Cytotoxicity assay

Elicited cell culture extract (48 hpe) was used to measure the cytotoxicity against human cervical cancer cell line (HeLa cells) and human breast cancer cell line (MCF-7 cells). CHO-cells were used as non-cancer cell line. Cytotoxicity assay was performed as described before (Mosmann et al., 1983). Briefly, 5 x 10^3 cells in 100 µl of Dulbecco's Modified Eagle Medium were seeded in 96-well plates. Then the serial dilutions of the cell culture extracts (0, 6.25,

12.5, 25, 50, and 100 µg/ml) dissolved in DMSO were added to the monolayer. In all the treatments, the final DMSO concentration was 1% which was also used as negative control. After incubation for 24 hours the cultures were analyzed by MTT assay by the addition of 10 µl of 5 mg/ ml MTT and further incubating at 37^0 C for 4 hours. The MTT-containing medium was then removed and precipitated formazone crystals were dissolved in 100 µl of DMSO. The absorbance was measured on a Fluostar optima (BMG Labtech, Germany) microplate reader at 570 nm. The percentage inhibition and IC_{50} values were calculated as essentially described (Kumar et al., 2004). 5-Fluorouracil (5-FU) was used as positive control.

2.22.12. Acridine orange staining to detect apoptosis

Cell apoptosis was checked by monitoring the plasma-membrane permeability, nuclear morphology and the chro-matin condensation of MCF-7 and HeLa cells, through Acridine orange (AO)/Ethidium-bromide (EB) dual stain-ing method as essentially described by (Chakraborty et al. 2010). Briefly, 0.5 × 106 cells were seeded for the assay in a 12-well plate and incubated with concentrations equivalent to the IC 50 value of elicited extract from 'Florina' cell culture and 5-FU (positive control), respectively, for 24 h and then washed properly with PBS (phosphate buffered saline). Thereafter, 500 µg/ml of AO/EB dye mixture (500 µl) was added in each well and cells were observed under fluores-cent microscope. (Zeiss, Axiovert 25, Germany).

2.17.13. Sampling and statistical analyses

All the experiments were conducted in a completely randomized design with three biological replicates and three technical repeats. The data was subjected to statistical analyses following standard procedures. The data are expressed as mean ± SD.

2.18. GC-MS based untargeted metabolomics of apple cell cultures treated with *Venturia inaequalis* elicitor

2.18.1. Plant material and elicitor-treatment

Apple (*Malus domestica* cv. 'Florina') cell cultures were developed as described before (Sarkate et al, 2017). Cell cultures were grown in liquid LS medium containing 2 µM 2,4-D and 1 µM NAA at 26 ^{0}C in the dark on an orbital shaker at 120 rpm. An elicitor prepared from apple scab fungus, *Venturia inaequalis* was used in this study. *V. inaequalis* strain (MTCC No.: 1109) was purchased from microbial type culture collection and gene bank (MTCC), Chandigarh, India. *V. inaequalis* elicitor (VIE) was prepared by homogenizing the fungal hyphae as described before (Zhang et al., 2016). Briefly, VIE was prepared by adding ground fungal mycelium (*ca.* 10 g) into 1 L of acidified water (pH 2.0). Water extract was then boiled for 1 h on a hot plate, cool down to room temperature and filter sterilized. After filtration, the pH of the fungal extract solution was adjusted to 5.0 and the final volume was adjusted to 1L by adding distilled water. This solution was used as the VIE. Elicitor-treatment was performed by adding 2.5 mL of the VIE (~ 70 mg of fungal polysaccharide) to the seven-day-old cell apple suspension culture (50 mL). Upon elicitor-treatment, cells were harvested at defined time points: 0, 6, 9, 12, 24 and 48 hours post elicitation (hpe). In the control treatment, similar volume of sterile distilled water was added in lieu of the VIE. All experiments were performed with at least three biological repeats.

2.18.2. Elicitor preparation and treatment

Venturia inaequalis elicitor was used in this study. The strain of *V. inaequalis* (MTCC No. 1109) was purchased from microbial type culture collection and gene bank (MTCC), Chandigarh, India. *V. inaequalis* elicitor (VIE) was prepared from fungal cell extract as described by (Zhang et al., 2000). Briefly, 10 g of ground fungal mycelium was added to 1 L of acidified water with final pH of 2. Water extract was then boiled for 1 h, cool down to room temperature and filter sterilized. After filtration, the pH of the fungal extract solution was adjusted to 5.0 and the final volume was adjusted to 1L by adding distilled water. This solution was used as the VE. For elicitation, 2.5 ml of the VIE (equivalent to 70 mg of fungal polysaccharide) was added to in the seven-day-old cell suspension culture (50 mL). After onset of elicitation, cell cultures were harvested at defined post-elicitation time points: 0, 6, 12, 24, 36, 48 and 72 hours post elicitation (hpe). In the control treatment, similar volume of sterile

distilled water was added in lieu of the VIE. At least three replicates were used for each treatment, and the experiment was repeated two times.

2.18.3. Extraction of polar metabolites

The VIE-treated apple cell cultures were harvested by vacuum filtration at defined time points (0-72h) and kept in hot air oven at 60^0 C for 4h. Dried cell mass (2g) was crushed in liquid nitrogen and fine powdered samples were used for metabolite extraction. The extraction of polar metabolites for GC-MS analyses was performed according to the protocol described by Kim et al (2013) with suitable modifications. An extraction mixture was prepared by adding methanol/water/chloroform in the ratio of 2.5:1:1 (v/v/v) and stored at -20 ^{0}C. Pre-cooled extraction mixture (1 mL) was then added to 200 mg powdered samples in a 1.5 ml micro centrifuge tube and vortexed vigorously at room temperature for 2 min. In order to identify extraction efficiency, 50 µL of 2-phenylphenol (from 2 mg/mL methanol stock) was spiked in the extraction mixture as the internal standard (IS) and vortexed again for 1 min. The extracts were then centrifuged at 14000 g for 5 min. The resulting supernatant (0.8 mL) was transferred into a new 1.5 mL tube and then 0.4 mL of water (0.4 ml) was added to the supernatant, whole mixture was vortexed for 10 s and subsequently centrifuged at 14000g for 5 min. The polar upper phase (methanol/water) was transferred to a new micro-centrifuge tube and then dried out in a vacuum concentrator (Labconco, Centrivap; USA) at 20^0 C for 2 h followed by 12 h freeze drying in a lyophilizer. Finally dried material was subjected to double derivatization for GC-MS analyses as described by (Lisec et al., 2006). Briefly, the first, derivatization was performed by adding 40 µL of methoxyamine hydrochloride (stock solution: 20 mg/ml in pyridine) to the dried sample and incubating the solutions at 37 °C for 2h. Then second derivatization was performed by adding 80 µL of N-methyl-N-(trimethylsilyl)-trifluoroacetamide (MSTFA) at 37 °C for 30 min. Dderivatization reaction prepared with empty tube served as control.

2.18.4. GC-MS analysis

GC- MS analysis was performed on Agilent 7890A gas chromatograph (Agilent technologies, CA, USA) coupled with an Agilent 5975C mass detector (Agilent technologies, CA, USA). Double-derivatized sample (2 µl) was injected into GC-MS by automatic sampler (7683 B series, Agilent Technologies) with a split ratio of 1:5. DB-5 MS column (5 % phenyl methyl

polysiloxane: 30m x 0.25mm i.d. x 0.25 µm, Agilent technologies) was used for metabolite separation. The temperature program was as follows: Initial temperature of 80 ^{0}C for 1 min, followed by temperature increase to 220 ^{0} C at the ramp rate of 10 ^{0}C/min, followed by temperature increase to 310^0 at the ramp rate of 20 ^{0}C /min and finally a 10 min hold at 320^0 C. Total run time calculated was 39 min. Helium was used as carrier gas at a flow rate of 1mL/min. The inlet temperature and interface temp was set 280^{0}C. The MS unit was tuned to its maximum sensitivity and the mass range for total ion current was m/z 80−600, and the detector voltage was set at 170 V. Each sample was replicated three times. Scan was started after solvent delay of 7 min with scan frequency 4 S^{-1} (2.0 HZ).

2.18.5. Metabolite identification

Metabolites were identified by matching the mass spectra of target metabolite (3:1 signal to noise ratio) with the NIST-11 mass spectral library (National Institute of Standards and Technology), and our in-house mass spectral database that include several secondary metabolites, amino acids, organic acids, and sugar standards. Metabolite identity was reported only when the matching value of the mass spectra comparison was more than 80 percent, and an increase in the area of the corresponding peak was observed when spiking the sample with the corresponding pure standard. Each mass spectrum was carefully analyzed for co-elution detection. Co-elution was not detected in any of the identified peaks.

2.18.6. Metabolite data pre-processing and statistical analysis

Raw GC-MS data files obtained from Agilent ChemStation™ software were deconvoluted by Automated Mass Spectral Deconvolution and Identification System (AMDIS) using tools available with WsearchPro (www.wsearch.com.au). Metabolite data obtained were further converted into .csv (comma separated values) format before uploading in Metaboanalyst 3.0 (http://www.metaboanalyst.ca). TIC values were normalized using internal standard. After that, the data were, log transformed with Pareto scaling (mean-centered and divided by the square root of standard deviation of each variable) followed by normalization before statistical analyses. Multivariate statistical analysis like ANOVA (using Fisher's LSD method; p value < 0.05), principal component analysis (PCA) were performed by using interactive online tool Metaboanalyst 3.0. The output for PCA data consisted of score plots for visualizing the contrast between various time points of VIE-treated samples and loading plots to explain the cluster

separation. A heat map was created using interactive heat map tool of Metaboanalyst 3.0. A simplified metabolic pathway was manually constructed using information from the Kyoto Encyclopedia of Genes and Genomes (KEGG) database via pathway analysis in Metaboanalyst 3.0.

2.18.7. Quantitative Real-Time PCR

Total RNA was isolated from the VIE-treated apple cell cultures at defined time points (0-48 h) using RNeasy Plant Mini Kit from Qiagen (www.quiagen.com). Total RNA (1 µg) was reverse transcribed at 42°C using Oligo (dT) primers and RevertAid H Minus reverse transcriptase (Fermentas; www.thermoscientificbio.com) to form cDNA. Quantitative RT-PCR was performed with the QuantStudio 3 Real-Time PCR System (Thermo Fisher Scientific) using Power Up™ SYBR Green Master Mix (Thermo Fisher Scientific) following the manufacturer's instruction. PCR program: 40 cycles at 90° C for 15 sec followed by 55° C for 1 min and final extension at 72° C for 1 min. Melt-curve analysis was performed to evaluate gene-specific amplification. Amplification and correlation efficiencies of each PCR were determined using six serial dilutions of cDNA from all samples. To derive relative quantification, the PCR efficiency was used to transform the cycle threshold values into raw data. Expression of the apple genes cv. 'Florina' viz, phenylalanine ammonia-lyase *(MdPAL)*, flavanone 3-hydroxylase *(MdF3H)*, alternative oxidase (*MdAOX*), and biphenyl synthase isoform 3 (*MdBIS*3) were evaluated using the gene-specific primers listed in table 2.30a [PAL: primers Q1 forward and Q2 reverse; F3H: primers Q3 forward and Q4 reverse; AOX: primers Q5 forward and Q6 reverse; BIS3: primers Q7 forward and Q8 reverse]. Primers were designed based on the sequence of corresponding apple unigene present in GDR (Genome database of Rosaceae; www.rosaceae.org). All samples were normalized using mRNA of the reference gene, apple *actin*, as an internal control sample for each line (primers Q9 forward and Q10 reverse). Scaling of expression level was performed in relation to the respective mRNA expression levels in the control (0h) cells, which were set to 1. Three technical repeats were performed. Pfaffl, 2001, mathematical model was used for the estimations of efficiency and gene expression levels.

$$\text{Ratio} = (E_{\text{target}})^{\Delta Ct_{\text{target}}(\text{control} - \text{sample})} / (E_{\text{ref}})^{\Delta Ct_{\text{ref}}(\text{control - sample})}$$

Table 2.31a: Composition of qPCR reaction.

Component	**Volume**	**Remarks**
Power Up ™ SYBR™ Green Master Mix (2X)	5 µl	SYBR®Green I Dye, AmpliTaq Gold® DNA Polymerase, dNTPs with dUTP and buffer components.
Forward primer (10 pmole)	0.5 µl	Final concentration 0.125 µM
Reverse primer(10 pmole)	0.5 µl	Final concentration 0.125 µM
Template DNA	1 µl	Final concentration 1 ng
Water nuclease free	3 µl	Final volume to 10 µl

Table 2.31b: qPCR reaction program

Steps	**Temperature ^{0}C**	**Time**	**Remarks**
Intial denaturation	95	2 min	Denaturation and activation of the hot start Taq polymerase
Denaturation	95	15 s	
Annealing	52 (*PAL, F3H)* 54 *(AOX, Actin*) 48 (*BIS 3*)	1 min	Veriflex step
Extension	72	1 min	Data acquisition
The last three steps are repeated for 40 cycles before the melt curve step			

2.19. Salicylaldehyde synthase activity from *Venturia inaequalis* elicitor-treated cell culture of apple:

2.19.1. Induction and maintenance of cell suspension cultures

Apple cell suspension cultures were derived from the young leaves (8-10 days old) of greenhouse grown plants as described before (Sarkate et al., 2017). Cultures were grown at 26 ˚C in the dark under continuous shaking at 120 rpm. The cells were harvested by vacuum filtration on the 7th day.

2.19.2. Elicitor preparation and treatment

Venturia inaequalis elicitor (VIE) was used in this study. VIE was prepared as described in table 2.2. For elicitation, 2.5 mL VIE (equivalent to 70 mg fungal polysaccharide) was added to the seven-day-old cell suspension culture (50 mL). After the onset of elicitation, the cell cultures were harvested at defined time intervals: 0, 6, 9, 12, 24 and 48 hours post elicitation (hpe). In the control treatment, a similar volume of sterile distilled water was added in place of the VIE. At least three replicates were used for each treatment.

2.19.3. Extraction and quantification of salicylic acid

Frozen cells (approximately 2 g) were used to extract and detect the total (free and conjugated) salicylic acid (SA) precisely as described previously (Fragnire et al., 2011). SA was detected by HPLC using a YMC-Triart (Kyoto, Japan) C_{18} analytical column (reverse phase, 250 x 4.6 mm, 5 µm, 12 nm). A binary gradient solvent system consisting of 1 mM TFA in water (A) and methanol (B) with a flow rate of 1.0 mL/min for 80 min was used to eluate the SA and other phenolics. The two mobile phases were used in the gradient mode under the following concentration times (%/min) of B: 0-10% B in 27 min, 10 - 40% B over a 28 min period, 40% B for 5 min, 40 - 44% B for 2 min, 44% B for 8 min, from 44 to 10% B in 3 min and 7 min at 10% B to re-establish the initial conditions before the injection of another sample. SA was identified by comparing the retention time and UV-spectra with authentic standards (Sigma-Aldrich).

2.19.4. Precursor feeding experiments

To ascertain the 2-coumaric acid-derived formation of salicylaldehyde, feeding experiments were performed. 2-Coumaric acid was dissolved in DMSO (50% v/v with water), filter sterilized, and 2 mM final concentration was fed to the VIE-treated cell culture after 6 h of elicitation. Culture treated with an equal amount of DMSO served as the control. After 24 h, the cells were harvested, extracted and analyzed by HPLC for salicylic acid content.

2.19.5. Preparation of cell-free extracts and partially purified protein

The cell-free extract was prepared by homogenizing cell suspension culture (approximately 3 g) in 6 mL 100 mM HEPES buffer, pH 8.0, supplemented with 5 mM cysteine and 1% (w/w) polyvinylpyrrolidone (PVPP). All of the steps for the preparation of the cell-free extracts were carried out at 4 °C. The homogenate was centrifuged at 14,000 x g for 30 min, and the supernatant was collected. An aliquot of the supernatant (2.5 mL) was desalted using a PD_{10} column (GE Healthcare) pre-equilibrated with 200 mM Tris-HCl buffer, pH 7.5, containing 5 mM cysteine. Protein concentrations were determined according to (Bradford., 1976) using bovine serum albumin (BSA) as the standard. To prepare the partially purified protein, 10 g cell biomass was slowly homogenized in 20 mL 100 mM HEPES buffer, pH 8.0, containing 10 mM DTT, followed by centrifugation at 12,000 x g for 60 min. The supernatant was collected and filtered. Ammonium sulfate was added to the crude extract to 40% saturation, mixed properly and centrifuged at 10,000 x g for 10 min. The transparent supernatant was applied to a CM-Sepharose column (1.5 × 8 cm, Bio-Rad) pre-equilibrated with 100 mM HEPES buffer, pH 8.0. The flow through of the CM column was collected and passed through a DEAE-Sepharose column (1.5 × 10 cm, Bio-Rad), pre-equilibrated with 100 mM HEPES buffer, pH 8.0. The bound proteins on the DEAE column were eluted with a step gradient of NaCl in the same buffer (50, 100, and 200, 500 and 1000 mM). Fractions showing SAS activities were pooled, concentrated using Amicon^{R} Ultra-4CFU membrane (Millipore, Bedford, USA) concentrators with a 10 KDa cut off range followed by desalting using a PD_{10} column (GE Healthcare) pre-equilibrated with 200 mM Tris-HCl buffer, pH 7.5, containing 10 mM cysteine. The purity of the protein was monitored on 12% SDS–PAGE, and the relative molecular weight was determined using molecular weight markers (Bio-Rad). The protein concentration was determined using the Bradford method with bovine serum albumin (BSA) as the standard.

2.19.6. Assay of phenylalanine ammonia-lyase (PAL)

PAL assay was performed according to (Sircar and Mitra, 2008). The assay contained 400 µL Tris-HCl buffer (100 mM; pH 8.0), 500 µL L-phenylalanine (20 mM) and 100 µg protein. The

assay mixture was incubated for 30 min at 37 ^{0}C. The reaction was terminated by 500 µL 5 M HCl. The acidified mixture was centrifuged at 10,000 x g for 10 min, and the supernatant was directly analyzed by HPLC for product formation (Sircar and Mitra, 2008). The results were expressed as the mean values of triplicate assay.

2.19.7. Assay of salicylaldehyde synthase (SAS)

SAS activity was determined by monitoring the salicylaldehyde formation from 2-coumaric acid using HPLC. For the time course analyses, the composition of enzymatic assay consisted of 100 µg protein (cell-free extract), 5 mM *2*-coumaric acid and 10 mM cysteine. The final enzyme assay reaction volume was adjusted to 200 µL with Tris-HCl buffer (200 mM; pH 7.5). The assay was incubated at 35 °C for 30 min, and then reaction was stopped by adding ice cold acetic acid and methanol (1:9 ratio; v/v) in a 1:1 ratio followed by centrifugation at 12,000 x g for 10 min. The supernatant containing the SAS reaction product (salicylaldehyde) was analyzed by HPLC and GC-MS. For the biochemical characterization of SAS, partially purified protein (10 µg per assay) was used instead of crude extract. For enzyme characterization, the pH values were tested in the range from 5.5 to 11.5, temperature optima were tested from 15 °C to 55 °C, incubation times were tested from 1 to 120 min and protein concentrations in the range of 1 to 200 µg per assay. The enzyme stability was tested at room temperature, 4 °C, and -20 ºC for 24 h. In order to test the substrate requirement and specificity of SAS, a set of potential substrates such as *trans*-cinnamic acid, 4-coumaric, ferulic, caffeic and sinapic acids were tested at 5 mM concentrations using 10 µg partially purified protein. The reducing agent requirement was tested by adding cysteine (2-20 mM), dithiothreitol (2-20 mM) or *β*-mercaptoethanol (2-20 mM) in separate assays. Assays without any cofactor and with boiled enzyme extract were performed to see if there was any non-enzymatic (spontaneous) conversion of 2-coumaric acid to salicylaldehyde. Three independent assays were performed, and results were expressed as the mean values ± SD.

2.19.8. Analysis of SAS reaction products by HPLC and GC-MS

The product of SAS reaction was analyzed on a HPLC system from Shimadzu (Shimadzu, Japan). HPLC as equipped with a controller (CBM-20A), a pump (LC-20 AP) and a photo-diode array detector (SPD-M20A). A Lab Solutions Multi LC-PDA software from Shimadzu was used for data acquisition using Windows 7 Professional operating system. Separation was attained on a YMC-Triart (Kyoto, Japan) C_{18} reverse phase column (dimension: 250 x 4.6 mm, 5 µm particle size) attached with a C_{18} guard column (Phenomenex Security Guard™; 4 × 3 mm). An isocratic solvent system consisting of 1 mM TFA in water and methanol [40:60; (v/v)] with a flow rate of 1.0 mL/min for 60 min was used to detect the product of the SAS reaction. The detection wavelengths were 256 nm for salicylaldehyde (product of 2-coumaric acid), 249 nm for benzaldehyde (product of trans-cinnamic acid), 280 nm for 4-hydroxybenzaldehyde (product of 4-coumaric acid), 280 nm for 3,4-dihydroxybenzaldehyde (product of caffeic acid) and vanillin (product of ferulic acid) and 310 nm for syringaldehyde (product of sinapic acid). The identity of the enzymatic product was confirmed by co-chromatography (HPLC) using authentic reference compounds. The chemical identity of the SAS reaction product was further confirmed by GC-MS analyses. For GC-MS analyses, the reaction volume was increased to 1 mL. After 30 min incubation, the assay was stopped by adding trichloroacetic acid (100 µL, 3 M) and immediately extracted twice with a double volume of dichloromethane. Dichloromethane was evaporated, and the dried residue was derivatized by adding 60 µL MSTFA [N-methyl-N-(trimethylsilyl)-trifluoroacetamide] at 60 °C for 30 min. One derivatization reaction was also prepared using a control assay containing denatured protein. GC-MS was performed on an GC-MS system comprised of an Agilent 7890A gas chromatograph (Agilent, USA) and an Agilent 5975C mass detector (Agilent, USA). Derivatized sample (2 µL) was injected in GC-MS using an automatic sampler (7683 B series, Agilent Technologies) with a split ratio of 1:5. Samples were separated on fused silica capillary column DB-5 (5% phenyl methyl polysiloxane: 30 m x 0.25 mm i.d. x 0.25 µm, Agilent Technologies). The temperature program was as follows: initial temperature 80 ^{0}C for 2 min, then temperature was increased to 220 ^{0} C at the ramp rate of 10 ^{0}C/min, followed by a temperature increase to 310 ^{0} C at the ramp rate of 20 ^{0}C/min and finally a 10 min hold at 320 ^{0}C. The total run time calculated was 39 min. Helium was used as carrier gas at a flow rate of 1 mL/min. The inlet and interface temperatures were set to 280 ^{0}C.

2.19.9. Determination of kinetic parameters

The kinetic properties of SAS were calculated by using Hyper 32 program (Sircar et al., 2011). For kinetic parameter determination, different concentrations (0.005-20 mM) of 2-coumaric acid and 4-coumaric acid were used keeping the cysteine concentration fixed (10 mM). The experiments were repeated three times with independent enzyme preparations, and the mean data values were used to calculate the apparent K_m values using the Hanes plot of the Hyper 32 program.

2.20. Molecular cloning and functional analyses of a biphenyl phytoalexin-specific *O-methyltransferase* (*MdOMT*) from cell suspension culture of apple cv. 'Florina'

2.20.1. Plant material and chemicals

Apple cell suspension cultures were derived from the young leaves (8-10 days old) of greenhouse grown plants as described before Aucuparin and noraucuparin were synthesized following the protocols of Hüttner et al.(2010). Chemical synthesis of eriobofuran was performed as described by Oliveira et al. (2003; 2004) and Zhao and Larock (2006).

2.20.1.1. Chemical synthesis of aucuparin, noraucuparin and eriobofuran

Aucuparin and noraucuparin were synthesized from 3,4,5-trimethoxybiphenyl by following the protocols of Hüttner et al. (2010). First, 3,4,5-trimethoxybiphenyl was synthesized as described by Hüttner et al. (2010). Aucuparin was synthesized from 3,4,5-trimethoxybiphenyl by position selective single demethylation (removal of methoxy group at carbon no 4) using MgI_2 reagent (Bao et al., 2009). The second demethylation reaction was done by using BBr_3 to produce noraucuparin (Figure 2.2). Eriobofuran was synthesized following the protocols of Oliveira et al., 2004. Briefly, eriobofuran was synthesized from 2,3,4-trimethoxydibenzofuran. 1.5 mmol of 2,3,4-trimethoxydibenzofuran was dissolved in dry ether, followed by evaporation. The residue was heated at 80 ^{o}C and then reaction was stopped by adding water: Na2S2O3:HCl (5%) (1:1:1). The aqueous phase was chloroform extracted and organic layer dried over anhydrous Na2SO4. Crude yield was fractionated over silica gel CC (4% MeOH in CH2Cl2) and the resulting fraction 1 was further purified using silica gel column wit chlorofom as eluent to yield eriobofuran 0.4 mmol, 30% yield). Chemically synthesized aucuparin, noraucuparin and eriobofuran were subjected to GC-MS analyses of their silylated-derivatives. In GC-MS, the temperature program was set as: 70 ^{0}C initial temperature for 3 min, then temperature

increased to 300 ^{0} C at the ramp rate of 10 ^{0}C/min, and finally a 3 min hold at 300^{0} C. Total run time calculated was 29 min. Helium gas of ultra-high purity was used as carrier gas at a flow rate of 1ml/min. Split eration was 1/10. The MS scan range was set at m/z 80−600, and the detector voltage was set at 1700 V. The purity and correctness of structure of noraucuparin, aucuparin and eriobofuran were confirmed by comparing the mass-spectrum of silylated-derivative of newly synthesized aucuparin and noraucuparin with the previously published data (Hüttner et al., 2010). Chemical synthesis of aucuparin and noraucuparin was shown below in figure 2.2.

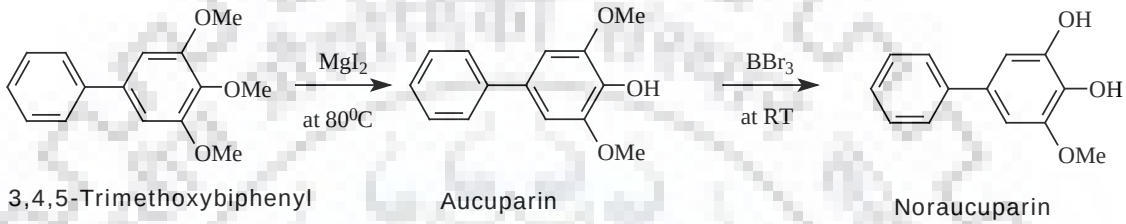

Figure 2.2: Chemical synthesis of aucuparin and noraucuparin

2.20.2. Experimental materials and treatments

Cell cultures and green house grown plants of apple (*Malus domestica* cv. 'Florina') were used as experimental tools in the current study. Seven-day-old cell cultures, growing in log-phase were treated with the elicitor prepared from the scab-fungus *Venturia inaequalis* [strain no.: MTCC No.: 1109; procured from microbial type culture collection and gene bank (MTCC), Chandigarh, India]. *V. inaequalis* elicitor (VIE) was prepared from the fungal mycelium extracts, as described in Table 2.2. Elicitation was performed with 2.5 mL of VIE (equivalent to 70 mg of fungal polysaccharide), added to the 50 mL of cell culture. Cell cultures were harvested at defined post-elicitation time points: 0, 0.5, 1, 3, 6, 9, 12, 24, 36, 48 and 72 hours post elicitation to measure the levels of biphenyl-derived phytoalexins and gene expression level. Equal volume of distilled water in lieu of VIE was added to the control treatment. A minimum of three replicates were used for each treatment. Immature leaves of greenhouse-grown apple shoots (*Malus x domestica cv.* 'Florina') were inoculated with conidial suspension (5 x 10^{6} conidia/mL) of *V. inaequalis*. Infected leaves and stems were used for the RNA isolation and phytoalexin analyses. Leaves and stems were routinely photographed till 20 day post infection to capture disease symptoms.

2.20.3. Extraction and analyses of phytoalexins

Freeze-dried cell culture (ca. 2g) and apple shoot intermodal segments were extracted for phytoalexins isolation. Cell mass (1 g) was extracted in methanol and then methanolic extracts were examined by HPLC for the separation and quantification of phytoalexins. HPLC separation was performed on a Phenomenex™ Synergi Hydro RP (Torrance, USA) C_{18} column (250 × 4 mm, 4µm). A Shimadzu -HPLC system equipped with an SPD-M20A Photo Diode Array (PDA) detector was used. Solvent system comprising of an isocratic mixture of 1 mM TFA in water: methanol [60:40; (v/v)] with 1.0 ml/min flow rate for 60 min was. The phytoalexins were identified by comparing the retention time and UV-spectrum with those of authentic standards (chemically prepared). Detection wavelength was at 269 nm.

2.20.4. Isolation and cloning of apple cDNA encoding *Md*OMT

Genome sequence of apple cv Golden Delicious (apple genome version 0.1 cDNA) (Velasco et al. 2010) was searched for putative *O-methyltransferase (MdOMT)* gene involved in the conversion of 3,5-dihydroxybiphenyl to 3-hydroxy-5-methoxy-biphenyl *via* the BLASTN server of the GDR (Genome Data Base of Rosaceae: www.rosaceae.org), using available published plant secondary metabolism specific OMT sequences as queries (Table 2.32) and resulting sequences were filtered against OMT sequences related to the plant secondary metabolism. Based on bioinformatics processing, apple unigenes MDP0000745475 and MDP0000770800 served as the most promising candidates to derive 5' and 3' flanking primers for the cds amplification of the putative *Md*OMT cDNA from the elicited apple cell cultures (Table 2.30b). *Md*OMT coding sequence was PCR amplified from the elicited (6 hpe) apple cDNA pool (cDNA synthesis protocol in Table 2.33) using Phusion® High-Fidelity DNA polymerase (NEB®, www.neb.com). The forward primer 1 (with a *Nhe*I restriction site) and reverse primer 2 (with a *Kpn*I restriction site) (Supplementary Table S2) was used to PCR amplify *Md*OMT. The PCR programs were set as: 98˚C for 30 s, followed by 30 cycles of 98˚C for 10 s, 58˚C for 30 s and 72˚C for 60 s, and 10 min final extension a t 72˚C. 3' UTR was PCR amplified via 3' race protocol using gene specific forward primer 3 designed 525 upstream the stop codon (Table 2.30b) (derived from a 300-bp downstream segment of MDP0000770800; GDR) using SMART RACE cDNA Amplification Kit (Clontech) The 5' UTR sequence was confirmed by amplifying a genomic DNA fragment (genomic DNA was isolated using DNeasy Mini Kit from Qiagen; www.qiagen.com) with gene specific forward primer 4 (derived from 199-bp upstream segment of MDP0000770800) and

reverse primer 5 (Table 2.30b). The PCR product of expected size was purified using GenElute™ PCR clean-up kit (Sigma-Aldrich Chemical Co. Ltd. India).

*Md*OMT nucleotide sequence submitted GenBank (NCBI) data libraries and available under accession number of **MF740747**

Table 2.32: Homology of apple unigenes present in GDR with other plant secondary metabolite specific *O*-methyltransferase (OMT) sequences.

Candidate OMT sequence	**Source plant**	**Accession No.**	***M. domestica* unigenes sharing highest identity (% amino acid sequence identity)**
Nor-aucuparin *O*-methyltransferase	*Sorbus aucuparia* [Khalil et al., 2015]	AHM25236.1	MDP0000770800 (97.3%) MDP0000745475 (96.4%)
		AHM25237.1	MDP0000208322 (94.7%) MDP0000656929 (94.7%)
Pinosylvin *O*-methyltransferase 1	*Pinus sylvestris* [Paasela et al., 2017]	AQX17825.1	MDP0000656929 (57.14%) MDP0000479113 (57.14%)
Pinosylvin *O*-methyltransferase 2	*Pinus sylvestris* [Paasela et al., 2017]	AQX17823.1	MDP0000642867 (33.6%) MDP0000703981 (36.1%)
Resveratrol di-O-methyltransferase	*Vitis vinifera* [Schmidlin et al., 2008]	B6VJS4.2	MDP0000182342 (55.3%) MDP0000391248 (55.5%)
Orcinol *O*-methyltransferase	*Rosa hybrid* [Lavid et al., 2002]	AAM23005.1	MDP0000283649 (55.8%)

Table 2.33. Reverse transcription (RT) reaction mixture for cDNA synthesis

Mixture 1	**Volume**	**Mixture 2**	**Volume**
RNA 1 µg	1 µl	10 X RT buffer	2 µl
Oligo dT primer (3´CDS) 10 pmol	1 µl	dNTPs (1 mM each)	2 µl
		RNase inhibitor (10 u)	0.5 µl
Water	10.5 µl	Reverse transcriptase (200u)	1 µl
		Water	2 µl

Mix 1 was added in PCR tube and centrifuged briefly, incubated in PCR for 5 min at 65 °C, thereafter kept on ice for 5 min. Then mix 2 was added and mixed well by providing short spin. This mixture was incubated in PCR for 90 min at 42 °C and reaction terminated at 70 °C for 10 min. cDNA was ready for use and divided in aliquots to avoid multiple freeze/thaw cycles and stored at -80 °C.

2.20.5. Agarose gel electrophoresis

PCR amplified DNA was separated on agarose gel. This is based on the principle that small DNA molecules migrate faster than larger molecules through the agarose matrix under effect of electric current. In this study, 2% agarose gel was used to analyze samples shorter than 500 bp length. For larger sizes, 1% agarose gel is used. Ethidium bromide is used for visualization of bands. It intercalates in nucleic acid molecules and its fluorescence increases 20 fold after binding to nucleic acid molecules.

2.20.6. DNA purification from agarose gel or after digestion reactions

DNA fragments of the right size were extracted from gel using a kit. First, the gel matrix was solubilized in a buffer by 50C. The solution was transferred to Nucleospin column (Qiagen) where DNA binds to the silica membrane, but other components were washed away using wash buffer. Finally, DNA was eluted by water or elution buffer. In case of purification of DNA fragments after digestion reactions, the reaction product was mixed with wash buffer instead of gel solubilizer buffer. Then the process was continued as mentioned before.

2.20.7. Cloning of *O-methyltransferase* (*Md*OMT) into expression vector (pRSETB)

*Nhe*I (forward primer) and *Kpn*I (reverse primer) restriction sites were present in the MdOMT and also present in MCS of pRSET B expression vector. The resulting fragment was digested with *Nhe*I and *Kpn*I and then ligated into the *Nhe*I / *Kpn*I linearized expression vector pRSET B. pRSET B was designed for expression of His-tag protein in *E. coli*, respectively. DNA insert was positioned in correct frame. This sequence includes an ATG translation initiation codon and permits the use of affinity chromatography for the purification of fusion protein. Digestion reaction was listed in table 2.34.

Table 2.34: Components for restriction digestion reaction

Component	**Volume (Insert)**	**Volume (Vector)**
0.2 µg purified DNA insert or vector	10 µl	5.5 µl
10 × reaction buffer Nhe1	2.0 µl	1.0 µl
Nhe1	1.0 µl	0.5 µl
Kpn1	4.0 µl	2.0 µl
Nuclease free water	3.0 µl	1.0 µl

Reaction was incubated at 37°C for 2 h. Following digestion, the gel-purification of the digested vector was performed. Both digestion products were purified using Gene elute PCR purification kit to exclude residual protein and salts which may inhibit the ligation reaction. The digested vector is subjected to dephosphorylation using shrimp alkaline phosphatase. Dephosphorylation of the 5` group of the vector ends prevent self-ligation of the vector during the ligation reaction (Table 2.35).

Table 2.35: Components for de-phosphorylation reaction

Component	**Volumn (Insert)**
pRSET B vector solution	3.0 µl
10 × reaction buffer	2.0 µl
Shrimph Alkaline phosphatise enzyme (1 U/1 µl)	1.0 µl
Nuclease free water	14.0 µl

The reaction was incubated in PCR at 37 °C with lead temperature 60 °C for 30 min. The reaction was terminated at 65 °C for 5 min. Which later used directly for ligation.

2.20.8. Ligation of DNA fragments

To promote the ligation reaction, the insert amount should be 2-6 fold more than the vector amount. The vector and insert are mixed together in PCR tubes and kept at 55 °C for 5 min, then chilled on ice. This step is done to avoid mispriming of the sticky ends. The tubes are centrifuged and then the buffer and the enzyme are added and the reaction is incubated by 4 °C overnight. A negative control reaction which contains all the components except the insert is done in parallel.

Table 2.36: Components for ligation reaction

Component	**Volume**
Digested vector 50 ng	1 µl
Digested insert 50 ng	6 µl
10x ligation buffer	1 µl
T4-DNA-Ligase (5U/ µl)	0.5 µl
Nuclease free water up to	10 µl

2.20.9. Transformation of DNA products into *E.coli*

Ligation reaction (5 µl) is used to transform 50 µl competent cells. Transformations occurred into *E. coli* DH5 α [F' φ80δlacZ9M15 end A1hsdR17(rk-mk+)supE44thi-1 λ-gyrA96 relA19(lacZYA-argFV169) deoR)] and *BL21(DE3)pLysS* [F- *ompT hsdS*B (rB-mB-) *galdcm* (DE3) pLysS (CamR)]. Chemically competent cells are prepared in the laboratory by calcium chloride method. Ligation product (5 µl) is added to DH5α competent cells (50 µl) and left for 25 min on ice, then transferred to a water bath at 40C for 45 s followed by immediate incubation on ice for 2 min. LB medium (250 µl) and bacterial suspension is shaken by 37 C for one and a half hours. The whole bacterial suspension is plated on LB-agar plates containing ampicillin. Transformation of plasmid into BL21(DE3) follows the same procedure except that the heat shock time is reduced to 20 s, and the selection medium contains chloarmphenicol, in addition to ampicillin. DH5 produces a high yield of plasmid while the BL21 strain is suited for expression of proteins.

2.20.10. Isolation of plasmid DNA by alkaline hydrolysis

A single colony of the transformed DH5 α was inoculated into 5 ml LB medium containing 20 µg/ml ampicillin and grown over night at 37C. On the following day, 4 ml cultures were centrifuged. Bacterial pellets were suspended in ice-cooled buffer I (300 µl) containing RNase A, then buffer II (300 µl) was added and the bacterial suspension was inverted cautiously 6 times and left on ice for 5 min. Lysis of the cell wall took place in addition to denaturation of large chromosomal DNA. RNA is destroyed by RNase I. Precipitation of proteins and denaturation of large chromosomal DNA were done by adding buffer III (300 µl), cautious inversion (6) and incubation on ice for 20 min. Centrifugation at 13.000 rpm for 10 min was done to exclude the denatured proteins and DNA. The supernatant containing the DNA solution (800 µl) was transferred to a new eppendorf tube. Residual contaminants and hydrolysed protein were extracted by vortexing with 800 µl chloroform followed by centrifugation at 13.000 rpm for 10 min. The aqueous layer was transferred to a new eppendorf tube. Isopropanol (0.7 volume) was added, vortexed and followed by centrifugation at 13000 rpm for 30 min to precipitate plasmid DNA. The pellets were washed with 70% ethanol (500 µl) followed by centrifugation at 13.000 rpm for 10 min. The supernatant is discarded and the plasmid pellets are dried by 37C and then dissolved in 30 µl water.

2.20.11. Heterologous expression of *MdOMT* in *Escherichia coli*

The PCR product for *Md*OMT coding sequence was double digested with *Nhe*1 and *Kpn*1 restriction enzymes and ligated into the pRSET B expression vector (Invitrogen). After verification by sequence analysis, *Md*OMT-pRSET B expression construct was heterologously expressed in *Escherichia coli* BL21 (DE3)-RIL cells (Stratagene) as N-terminal His_6-tagged proteins. Recombinant *Md*OMT protein was isolated using Ni-NTA agarose (Qiagen, India)-based affinity chromatography. Bacterial cell wall was disrupted by sonication for 5 min at duty cycle 40% and output control of 1.5. Ni-NTA slurry (200 µl) was added to 3 ml of the cleared lysate. All procedures were carried out at 4C. After shaking at 4°C for 1 h, the mixture was loaded into a column. Affinity purification started with 4 ml washing buffer (four times 1 ml each) (Table 2.21). The His6-tagged-fusion protein was eluted using 3.5 ml elution buffer. Imidazole,(used for elution) was removed from the eluate by gel filtration through a PD10 column equilibrated with 0.1 M Tris-HCl pH 7.5 buffer. SDS-PAGE was routinely performed to check the efficiency of affinity purification. Protein concentrations were determined by Bradford reagent (Bradford 1976) using bovine serum albumin as a standard.

2.20.12. SDS-PAGE gel electrophoresis

SDS-PAGE was used to confirm the successful expression of cloned cDNAs in heterologous systems. Proteins are loaded with SDS and become equally negatively charged. In addition, a thiol reagent disrupts their subunits. While migrating towards the anode, they are separated according to their molecular mass (Laemmli, 1970). The concentration of acrylamide and bisacrylamide in the separating gel was 12%, which allowed the highest resolution of proteins between 10 and 200 kDa. Protein samples to be analyzed were mixed with protein loading buffer in a 1:1 ratio and denatured at 95°C for 5 min. To estimate the molecular mass of the separated protein, a prestained 100 bp- -10 kDa protein marker was loaded in parallel with the samples. The running conditions were 25 mA in the stacking gel, 35 mA in the separating gel and 200 V supplied by a Standard Power Pack P25 (Biometra). To check for successful protein expression, the gel was incubated overnight at room temperature in Coomassie blue staining solution (II.1.4.1), followed by destaining solution until clear bands appeared.

2.20.13. *Md*OMT activity assay

The standard assay (total volume 200 µL) in 100 mM Tris-HCl buffer, pH 8.5, consists of 50 µM 3,5-dihydroxybiphenyl (substrate), 100 µM S-adenosyl-methionine (SAM), 25 µM ascorbic acid and 4 µg affinity purified recombinant *Md*OMT protein. The protein was added to start the reaction at 35˚ C for 30 min and then assay was terminated by acidification [by adding 30 µL of 10% (v/v) HCl]. Stopped assay mixture was then extraction twice with 200 µL of ethyl acetate. The combined extract was dried under vacum, and re-suspended into 100 µL of methanol prior to HPLC analyses. A range of compounds with related structure were tested as potential substrate for *Md*OMT at final concentrations of 50 µM (Table 3.8). For determination of pH optima, pH values from 6.5 to 11.5 were tested (100 mM potassium phosphate buffer for pH 6.5 and 100 mM Tris–HCl buffer for pH range 7.5 to 11.5). Other tested enzyme characteristics were, incubation temperatures ranging from 15°C to 55°C, incubation times ranging from 5 to 120 min, and recombinant *Md*OMT protein in the assay ranging from 0.1 - 10 µg. Enzyme stability was tested by keeping the protein at -80 ^{0}C for six months, with or without addition of glycerol (20%, v/v). For kinetic parameter determination, different concentrations of 3,5-dihydroxybiphenyl (1 - 100 µM) at a fixed concentration of SAM (100 µM) were used. To measure K_m value for SAM, its concentration varied from 1 to 100 µM keeping 3,5-dihydroxybiphenyl concentration fixed at 50 µM. Kinetic parameters were analyzed in triplicate. The kinetic parameters such as K_m and V_{max} were calculated by using the Hanes plot from Hyper 32 program (http://homepage.ntlworld.com/john.easterby/software.html).

2.20.14. Analysis of Enzymatic products

The reaction product of *Md*OMT assay was analyzed on a Phenomenex^{TM} (Torrance, USA) C_{18} column (RP-Hydro, 250 x 4.6 mm; 4 µm,) using a HPLC system (Shimadzu, Japan). HPLC conditions were used as described before (section **2.25.3)**. Enzymatic product was identified from their retention time and UV-spectra matching with those of standard compounds. The detection wavelengths were 254 nm for 3-hydroxy-5-methoxybiphenyl, 2-hydroxy-5-methoxybiphenyl and 3,5-dimethoxybiphenyl, 269 nm for aucuparin, and 310 nm for ferulic and sinapic acids. For GC-MS analysis, 2 mL assay volume was used. The reaction was terminated by adding 200 µL of 10 % (v/v) HCl and extracted twice ethyl acetate. Ethyl acetate fraction was dried under nitrogen. Trimethylsilyl derivatization (*N*-Methyl-*N*-(trimethylsilyl) trifluoroacetamide; MSTFA) of dried sample was performed as described before (section **2.23.3**). GC-MS analysis was carried out using a 7890A gas chromatograph coupled with an

Agilent 5975C mass detector (Agilent, USA). Derivatized sample (2 µL) was injected by automatic sampler (7683 B series, Agilent Technologies) with a split ratio of 1:5. Samples were separated on fused silica capillary column DB-5MS (5% phenyl methyl polysiloxane: 30 m x 0.25 mm i.d. x 0.25 µm, Agilent technologies). The temperature program was set as: Initial temperature of 80^0C for 1 min, followed by temperature increase to 220^0C at the ramp rate of 10°C/min, followed by temperature increase to 310°C at the ramp rate of 20°C /min and finally a 10 min hold at 320°C. Helium was used as carrier gas at a flow rate of 1 mL/min.

2.20.15. Quantitative Real-Time PCR analyses of *MdOMT*, *MdPAL* and *MdBIS* expression

Total RNA was isolated from 100 mg sample prepared from elicited cell cultures and *V. inaequalis* infected stem. 1 µg of RNA was used for reverse transcription at at 42°C to synthesize cDNA. Quantitative RT-PCR (qPCR) was performed on Thermo Fisher Scientific's QuantStudio 3.0 Real-Time PCR system. PowerUp ™ SYBR™ Green Master Mix from Thermo Fisher Scientific was used following the manufacturer's instructions. PCR program was set as: initial denaturation for 2 min at 95°C, then 45 cycles at 95°C for 15 s, 61°C for 30 sec and 72°C for 30 sec. Gene-specific amplification was evaluated by a melt-curve analysis. Six serial dilutions of cDNA from all samples were taken to determine amplification and correlation efficiencies. For relative quantification, the PCR efficiency was taken into account to transform cycle threshold values into numerical raw data. Primer details of qPCR expression analyses are given in Table 2.30b .Expression of the *MdOMT* gene was evaluated using the gene-specific primers 6 and 7. qPCR primer pairs for *Md*OMT were designed based on the sequence of *Md*OMT (Gene bank ID: MF740747). All samples were normalized using mRNA of the *MdActin* reference gene (forward primer 8 and reverse primer 9, derived from GDR sequence MDP0000921834), which served as an internal control sample for each line. Primer 10 (forward) and 11 (reverse), derived from the GDR sequence MDP0000191304, were used to analyze the expression of *MdPAL* (*phenylalanine ammonia-lyase*) gene. Forward primer 12 and reverse primer 13, derived from GDR sequence MDP0000287919 were used to analyze the expression level of the phytoalexin- specific biphenyl synthase isomer 3 gene (*BIS3*). In case of cell culture, scaling of *MdOMT*, *MdPAL* and *MdBIS3* expressions were performed by taking VIE treated samples (0h) as a calibrator. In case of *V. inaquelis* conidiospore-infected plants, then mRNA expression levels in mock inoculated stems were set to 1 for calculation of relative expression. Analyses were performed in biological and technical triplicates. Pfaffl (2001) method was used for the estimations of efficiency and relative quantifications.

2.20.16. Construction of Phylogenetic tree

Functional plant *O*-methyltransferase (OMT) sequences, which are related to *o*-methylation reactions in plant secondary metabolism, were used. The accession numbers and the OMT nomenclature are listed in Table 2.37. The phylogenetic tree was created following the neighbor-joining algorithm using MEGA 5.05 software (www.megasoftware.net) with 1,000 bootstrap support as it clearly defines the tree(Tamura et al. 2011). The evolutionary distances were computed using the Poisson correction method (Zuckerkandl and Pauling 1965; Sircar et al. 2015) and are in units of the number of amino acid substitutions per site. Missing data management and gap nullification was performed using the pair wise deletion method.

Table 2.37: Accession numbers of amino acid sequences used for phylogenetic reconstruction. MdOMT sequence is represented by its nucleotide accession number.

Plant Species	**OMT**	**Accession No.**
Arabidopsis thaliana	Caffeic acid O-methyltransferase (COMT)	AAB96879
Clarkia breweri	Isoeuginol-OMT	U86760
Fragaria x ananassa	Phenylpropanoid-OMT	AAF28353.1
Hordeum vulgare	Flavonoid-OMT	ABQ58825
Humulus lupulus	Xanthohumol-OMT	ABZ89567.1
Malus domestica	COMT	ABI54117.1
Malus domestica	Phenylpropene-OMT	AKN09016.1
Malus domestica	***Md*OMT**	**ASV64939**
Medicago sativa	Caffeic acid O-methyltransferase (COMT)	AAB46623
Medicago sativa	Isoflavone-OMT	AAB88294.1
Nicotiana tabacum	Catechol OMT	CAA50561.1
Ocimum basilicum	Caffeic acid O-methyltransferase (COMT)	AAD38189
Ocimum basilicum	Chavicol-OMT	AF435007
Ocimum basilicum	Euginol-OMT	AF435008
Oryza sativa	Caffeic acid O-methyltransferase	XP480185

	(COMT)	
Oryza sativa	Flavone-OMT	ABF72191.1
Pimpinella anisum	Isoeugenol-OMT	ACL13527.1
Pinus sylvestris	Pinosylvin-OMT1	AQX17825.1
Pisum sativum	Isoflavone 4'-OMT	O24305.1
Rosa chinensis	Orcinol-OMT	CAD29458.1
Rosa chinensis	Phloroglucinol-OMT	AB121046
Sorbus aucuparia	3,5-dihydroxybiphenyl-OMT	AHM25236.1
Sorbus aucuparia	Noraucuparin-OMT	AHM25237.1
Triticum aestivum	Caffeic acid O-methyltransferase (COMT)	ABP63535
Vitis vinifera	Resveratrol-OMT	FM178870
Vitis vinifera	Methoxypyrazines-OMT1	ADJ66850.1
Zea mays	Lignin-OMT	AAB03364
Pseudomonas aeruginosa	Bacterial-OMT	EQM82696.1

2.20.17. *Agrobacterium*-mediated transient expression and sub-cellular localization of *Md*OMT

In order to check sub-cellular localization of *Md*OMT, we performed localization studies using transiently expressed *Md*OMT protein in *Nicotiana benthamiana* leaves. Gateway cloning system (Invitrogen) was used as expression system. To make Gateway compatibility, PCR amplification involved either a stop codon (primer 14, forward primer *att*B1; primer 15, reverse primer *att*B2a) or no stop codon (primer 14, forward primer *att*B1; primer 16, reverse primer *att*B2b) to generate subsequent N- and C- terminal fusions with YFP, respectively. Primer details are provides in table 2.30b. The modified PCR products (*Md*OMT, with stop codon; *Md*OMT-DEL, without stop codon) were used to generate entry clone into pDONR/Zeo vector by using the Gateway BP reaction. From entry clones, target fragment was then transferred to the destination vectors by the Gateway LR reaction (Invitrogen). The *Md*OMT entry clone was used to transfer the coding sequence into the pEarly-Gate 104 (http://www.arabidopsis.org/abrc/catalog/vector1.html) destination vector leading to the N-terminal fusion of *Md*OMT with YFP (35S: YFP-*Md*OMT). Similarly, the coding sequence of the *Md*OMT-DEL entry clone was transferred to the pEarly-Gate 101 destination vector to allow for C-terminal fusion of MdOMT with YFP (35S: MdOMT-DEL-YFP).

Transient expression was performed using *Agrobacterium*-mediated transformation of *N. benthamiana* leaves following the protocol described before (Gaid et al. 2012). The binary Gateway expression vectors bearing the YFP-*Md*OMT and *Md*OMT-DEL-YFP constructs were transferred to the *A. tumefaciens* strain C58C1 by electroporation. Correct clones were identified by colony PCR using the *att*B1 and *att*B2a / *att*B2b primers. Positive clones were inoculated into 10 mL YMB medium supplemented with kanamycin (50 µg/mL) and rifampicin (100 µg/mL), grown overnight at 28°C, centrifuged at 5000 rpm to decant YMB medium, washed and re-suspended in activation medium to give OD_{600} = 1 (Bendahmane et al. 1999). A helper strain of *A. tumefaciens* carrying a p19 construct was used to increase the transformation efficiency and was grown under similar conditions until OD_{600} = 0.6. *A. tumefaciens* harboring either the YFP-*Md*OMT or the *Md*OMT-DEL-YFP constructs were gently mixed with the helper strain carrying the p19 construct in a 1:1 (v/v) ratio and the resulting bacterial suspension was infiltrated inside *N. benthamiana* leaves using a 10 mL syringe as reported previously (Sircar et al. 2015). After 48h of infiltration, leaves were analyzed for YFP expression by Zeiss 710 (Carl Zeiss, Germany) confocal laser scanning microscopy (CLSM). The argon laser 488 nm was used for excitation of both YFP and autofluorescence of chlorophyll. Fluorescence was detected using an emission bandwidth of 505–550 nm for YFP. Chlorophyll autofluorescence was observed with an emission bandwidth of 650–700 nm. When appropriate, a bright field image was taken using the transmitted light photomultiplier. The lambda mode was used to examine the spectral signature of fluorophore. The objective used was of C-Apochromat 40 x/1.2 water immersion type. For image processing, the Zeiss LSM Image Browser software was used and finally the combined images were generated by Photoshop 7.0.

2.20.18. Databases and software

A. MetaboAnalyst 3.0 (www.metaboanalyst.ca)

MetaboAnalyst (www.metaboanalyst.ca) is a web application based server designed to permit comprehensive metabolomic data analysis, visualization and interpretation of wide range of complex statistical metabolomics calculations.

B. The Genome Database for Rosaceae (GDR: http://www.rosaceae.org/)

This database provides centralized access to Rosaceae genomics and transcriptomics data to facilitate functional genomics. It is used to search apple genome and NCBI Malus EST for possible OMTs candidates.

C. Basic Local Alignment Search Tool (BLAST: http://blast.ncbi.nlm.nih.gov/Blast.cg)

It uses nucleotide or protein query to search nucleotide and protein databases available by website or any set of sequences supplied by the user.

D. Mega 5 (Molecular Evolutionary Genetic Analysis) was used to infer the phylogenetic tree (Tamura et al., 2011).

E. Primer Express 3.0 software (Thermofisher Scietific) was used to design primers for Quantitative Real Time expression analysis.

Chapter 3

Results

3.1. Callus induction from apple leaves

In the present study, callus induction was initiated by using various combinations of three growth regulators, 2,4-D, NAA and kinetin. The effect of growth regulators on in vitro callus induction and biomass accumulation is presented in (Table 3.1). The highest callus induction frequency (96 %) and biomass accumulation (13.8 g in 4 weeks) was observed in callus growing on LS medium supplemented with 2 µM 2,4-D, 1 µM NAA and 1 µM kinetin (Table 3.1). Callus induction and growth were observed in response to all levels of growth regulator treatment but the combination of 2,4-D, NAA and kinetin was found to be the most effective for biomass production. The optimum growth regulator combination selected for maintenance of callus was 2 µM 2,4-D, 1 µM NAA and 1 µM kinetin as shown in Figure 3.1. Callus developed in this optimum combination showed friable light yellow appearance. Minor callus formation (6%) was also observed in control medium. 2,4-D and NAA at higher and lower doses beyond the optimal concentration significantly reduced the callus formation frequency and resulted in marked reduction in the biomass (Table 3.1).

Figure 3.1: Friable callus induced from the leaves of apple (*Malus domestica* cv. 'Florina')

Table 3.1 The influence of different concentrations of growth regulators on callus induction in apple cultivar 'Florina' after four weeks of culture. Data represent mean value ± standard deviation (n = 3).

Treatment			**Callus Response**	
2, 4 D (µM)	**NAA (µM)**	**Kinetin (µM)**	**Callus induction (%)**	**Callus fresh weight (g)**
0	0	0	6	2.5 ± 0.2
0.5	0	0	16	4.2 ± 0.4
0.5	0.5	0.5	42	9.0 ± 0.4
0.5	1.0	1.0	48	9.2 ± 0.4
1.0	0.5	0.5	64	9.2 ± 0.5
1.0	1.0	1.0	69	9.8 ± 0.6
1.5	0.5	0.5	62	9.6 ± 0.8
1.5	1.0	1.0	74	10.8 ± 0.4
2.0	0.5	0	84	12.0 ± 0.7
2.0	1.0	0.5	88	12.2± 0.6
2.0	**1.0**	**1.0**	**96**	**13.8 ± 0.5**
0.0	1.0	1.0	58	9.1 ± 0.4
0.0	0.5	1.0	34	7.6 ± 0.4
2.5	0.5	0.5	65	9.6 ± 0.4
2.5	1.0	1.0	76	10.1 ± 0.5
2.5	1.0	0	72	9.6 ± 0.6

3.2. Establishment of cell suspension culture

Growth of cell suspension culture in liquid LS-medium showed best result with 2 µM 2,4-D and 1 µM NAA as shown in Figure 3.2. Addition of kinetin in cell suspension culture showed cell clumping, thereby kinetin was removed. Although there are a few studies on callus induction in apple, no previous report on detailed characterization of callus induction in terms of frequency and biomass are available.

Figure 3.2: Cell suspension culture of apple cv. 'Florina' developed from the friable callus

3.3. Antioxidant and anticancer activity of bioactive phenolic metabolites isolated from the yeast-extract treated cell culture of apple.

3.3.1. Elicitation of bioactive metabolites

Time course analyses of yeast extract treated cell culture showed significant enhancement in the accumulation of total phenolics and total flavonoids as compared to control cultures (Figure 3.3). Total phenolics content reached maximum at 48 hpe (842 µg gallic acid equivalent/DW). Total flavonoid also attained peak at 48 hpe (395 µg quercetin equivalent/DW). After 48 hpe, there was slight decline in the content of both total phenolic and flavonoids. HPLC analyses of soluble phenolics from elicited cell culture showed enhanced accumulation of phenolic acids and flavonoids. Predominant phenolics in soluble fraction were protocatechuic acid, catechin, chlorogenic acid, vanillic acid, 4-coumaric acid, ferulic acid, benzoic acid and rutin (Figure 3.4). Amount of phenolics, increased in response to elicitor-treatment. Time-course analyses revealed that chlorogenic acid, 4-coumaric acid, ferulic acid, benzoic acid and rutin contents were uplifted by elicitor treatment ((Figure 3.5). No significant enhancement in the amount of protocatechuic acid, catechin, and vanillic acid was observed upon elicitor treatment. Content of chlorogenic acid (112 µg/g DW), 4-coumaric acid (122 µg/g DW) ferulic acid (212 µg/g DW) and benzoic acid (244 µg/g DW) reached peak at 48 hpe. Rutin content (348 µg/g DW) attained maxima at 72 hpe. The content of protocatechuic acid, catechin and vanillic acid remained nearly unchanged over the time course studied. Non-elicited control cultures showed no change in phenolic acid content over the same time-course studied. Phenolic acids and flavonoids are ubiquitous compounds in plants, which are known to possess several biological properties such as antioxidant, anti-proliferative, anti-cancer activities

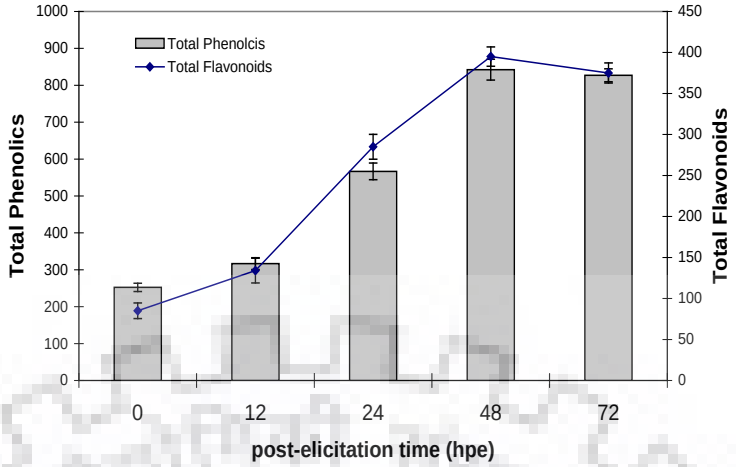

Figure 3.3: Time-course analyses of total phenolics and flavonoid accumulation in yeast-extract-treated cell culture of apple cultivar 'Florina'. Total phenolic was represented as microgram gallic acid equivalent/ dry mass; total flavonoid was represented as microgram quercetin equivalent/ dry mass. (Mean ± SD, n =3).

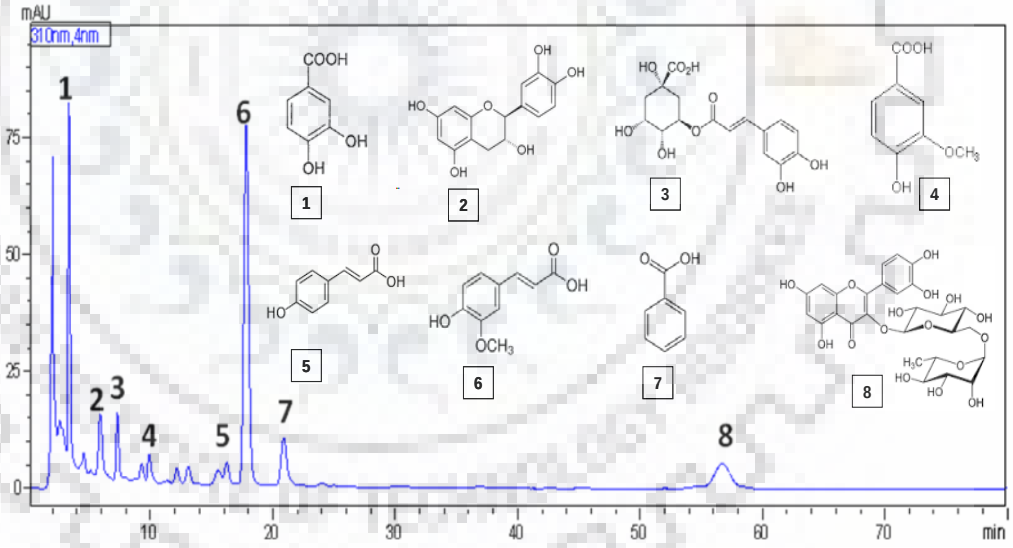

Figure 3.4: HPLC-chromatogram showing phenolics metabolite from yeast-extract-treated (48 h post elicitation) cell culture of apple cultivar 'Florina'. Chromatogram was monitored at 310 nm. Key to peak identity: 1: protocatechuic acid; 2: catechin; 3: chlorogenic acid; 4: vanillic acid; 5: 4-coumaric acid, 6: ferulic acid; 7: benzoic acid; 8: rutin.

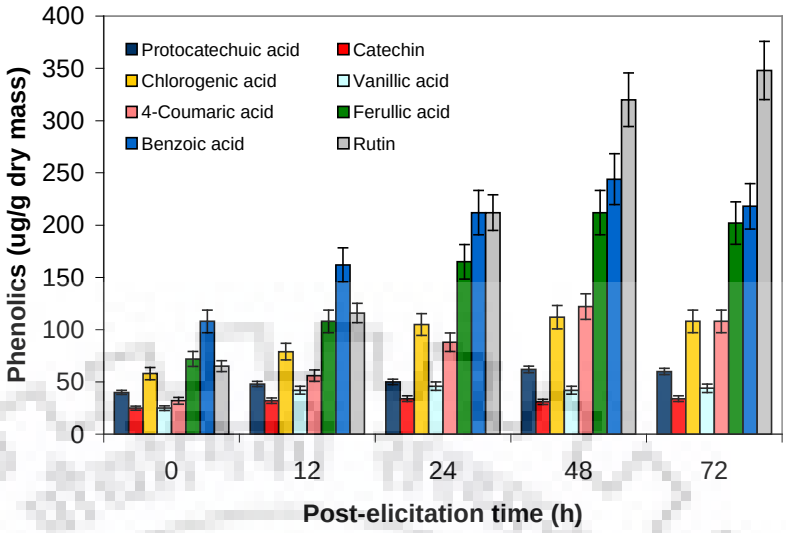

Figure 3.5: Time-course analyses phenolic metabolites upon yeast extract treatment in cell suspension culture of apple. All results are the mean ± SD, n =3.

3.3.2 Phenylalanine ammonia-lyase (PAL)

The activity of phenylalanine ammonia-lyase (PAL), the first enzyme of phenylpropanoid pathway rapidly increased after yeast-extract treatment. PAL activity attained peak at 12 hpe (14 pkat/mg protein). Thereafter, a slow decrease in PAL activity was noticed up to 48 h (Figure 3.6). Beyond, 48h, PAL activity decreased rapidly, reaching near to zero at 72 hpe. Enhanced PAL activity precedes phenolic accumulation suggesting PAL-mediated biosynthesis of phenolics upon elicitor treatment.

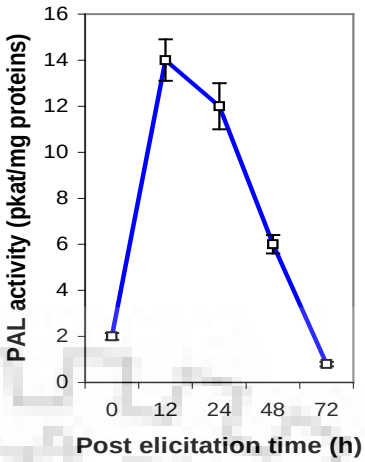

Figure 3.6 Time-course analyses of PAL activity in yeast extract-treated cell cultures of apple. All results are the mean ± SD, n =3.

3.3.3. Antioxidant activities

The results of the FRAP and DPPH assays from apple callus extracts is presented in (Table 3.2). Elicited cell culture showed high antioxidant activities as revealed from FRAP and DPPH assays. Highest FRAP activity was observed at 72 hpe (22.2 ug AAE/mg DW). Maximum DPPH activity was observed at 72 hpe (IC_{50} = 45.3 ug/ml). There was a strong positive correlation between total phenolic as well as flavonoid contents and the antioxidant activity assessed by both the methods, which is in agreement with several previous studies.

Table 3.2: Quantitative estimation of antioxidant activities of yeast-extract treated cell culture of apple at various post elicitation time points.

Elicited extract	**FRAP value µg AAE/mg extract**	**DPPH assay IC_{50} µg/mL**
0h	15.2 ± 1.2	80.6 ± 3.0
12h	18.6 ± 1.6	72 ± 4.0
24h	20.2 ± 1.9	58.3 ± 4.5
48h	19.4 ± 1.3	50.6 ± 3.0
72h	22.2 ± 1.8	45.3 ± 4.1

3.3.4. Cytotoxic effect of metabolites from elicited cell culture

The effect of apple callus extract on the growth of human cervical cancer cell line (HeLa cells) and human breast cancer cell line (MCF-7 cells) in vitro is summarized in (Table 3.3). The results showed that both breast and cervical cancer cell growth was inhibited by elicited extract. The anti-proliferative activity was expressed as IC_{50} values. The lower IC_{50} values represent higher cell growth inhibitory activities. In both the tested cell lines, elicited extract (48 hpe) had almost two-fold lower IC_{50} values as compared to the untreated control cultures (Table 3.3). 5-FU was used as positive control (MCF-7 IC_{50} = <0.65; HeLa IC_{50} = 5.2 ± 0.4). Moreover, when the extract was tested in non-cancer cell lines like CHO cells, it was found to have IC_{50} values above 200 µg/ml concentrations, indicative of poor response as anti-proliferative functions. When MCF-7 and HeLa cells were treated with elicited extract at a concentration equivalent to IC50 values, clear apoptosis was observed after 24 h of incubation. AO/EB dual staining served the purpose of measuring apoptosis. Since AO permeated all cells, the nuclei appeared green in vehicle treated MCF-7 and HeLa cells (Figure. 3.7 control cells). EB is taken up by the cells only when the cytoplasmic membrane integrity is lost and served as the marker for late apoptosis (Figure 3.7). Further research is needed to delineate the specific metabolites or metabolite combinations (synergistic effect) that are responsible for the cytotoxic effects as shown by elicited extract and analyzing the underlying mechanism of actions.

Table 3.3: IC_{50} Values for the inhibition of cellular proliferation by the cell culture extracts

Cell Line	**IC_{50} value (µg/ml) [a]**	
	Control extract (0 hpe)	Elicited extract (48 hpe)
HeLa	75.0 ± 5.5 [b]	38.0 ± 3.0 [b]
MCF-7	62.0 ± 4.8 [b]	31.0 ± 3.4 [b]
CHO	> 200	> 200

a = 50% Growth inhibition as determined by MTT assay (24 h exposure with cell culture extract)

b = Experiments were conducted in triplicate, and data expressed as mean value ± SD of three independent experiments

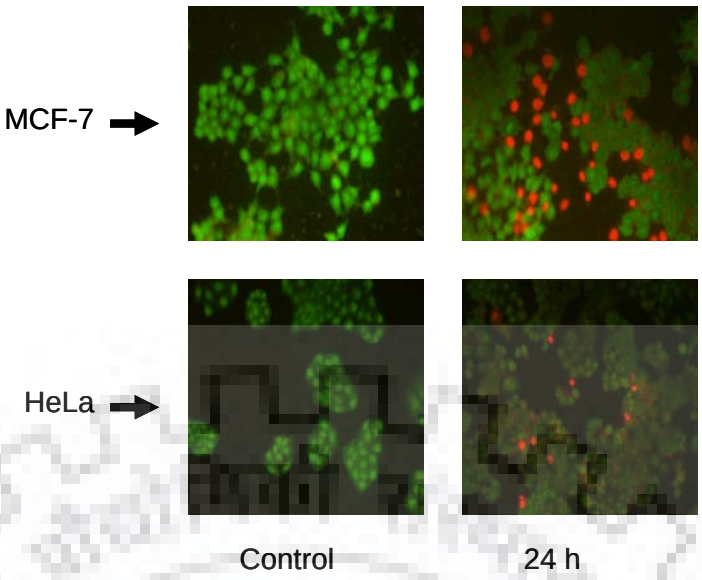

Figure 3.7: Apoptosis assay by elicited extracts from apple cell culture on MCF-7 and HeLa cells. The cells were incubated for 24 h with IC_{50} value equivalent of extract and 5-FU (positive control; 55 µM). Nuclear staining was visualized under 200 x objectives. Red cells indicate late apoptotic stage.

3.4. Chemical synthesis of aucuparin, noraucuparin and eriobofuran

Since aucuparin, noraucuparin and eriobofuran are not available commercially, they were synthesized following the published protocols. The starter substrate for the synthesis of both aucuparin and noraucuparin were 3,4,5-trimethoxybiphenyl, which was synthesized as described by (Hüttner et al., 2010). Newly synthesized aucuparin, noraucuparin and eriobofuran were derivative with MSTFA and subjected to GC-MS analyses. Chemical identities were confirmed by comparing the mass spectrum with aucuparin, noraucuparin and eriobofuran (obtained from Prof. L. Beerhues, TU-BS, Germany as gift). Slilylated-derivative of aucuparin showed molecular ion peak of 302.10 (Figure 3.8 A), noraucuparin showed molecular ion peak of 360.20 (Figure 3.8 B), and eriobofuran showed a peak at 316.0 (Figure 3.8 C), which were the characteristic identity as per published record (Hüttner et al., 2010). Since mass-spectrum were in complete agreement with the standard aucuparin and noraucuparin, no further structural confirmation was performed. Aucuparin, noraucuparin and eriobofuran was dissolved in methanol (100%) at 50 mM final concentration and stored at – 20 ^{0}C till further use.

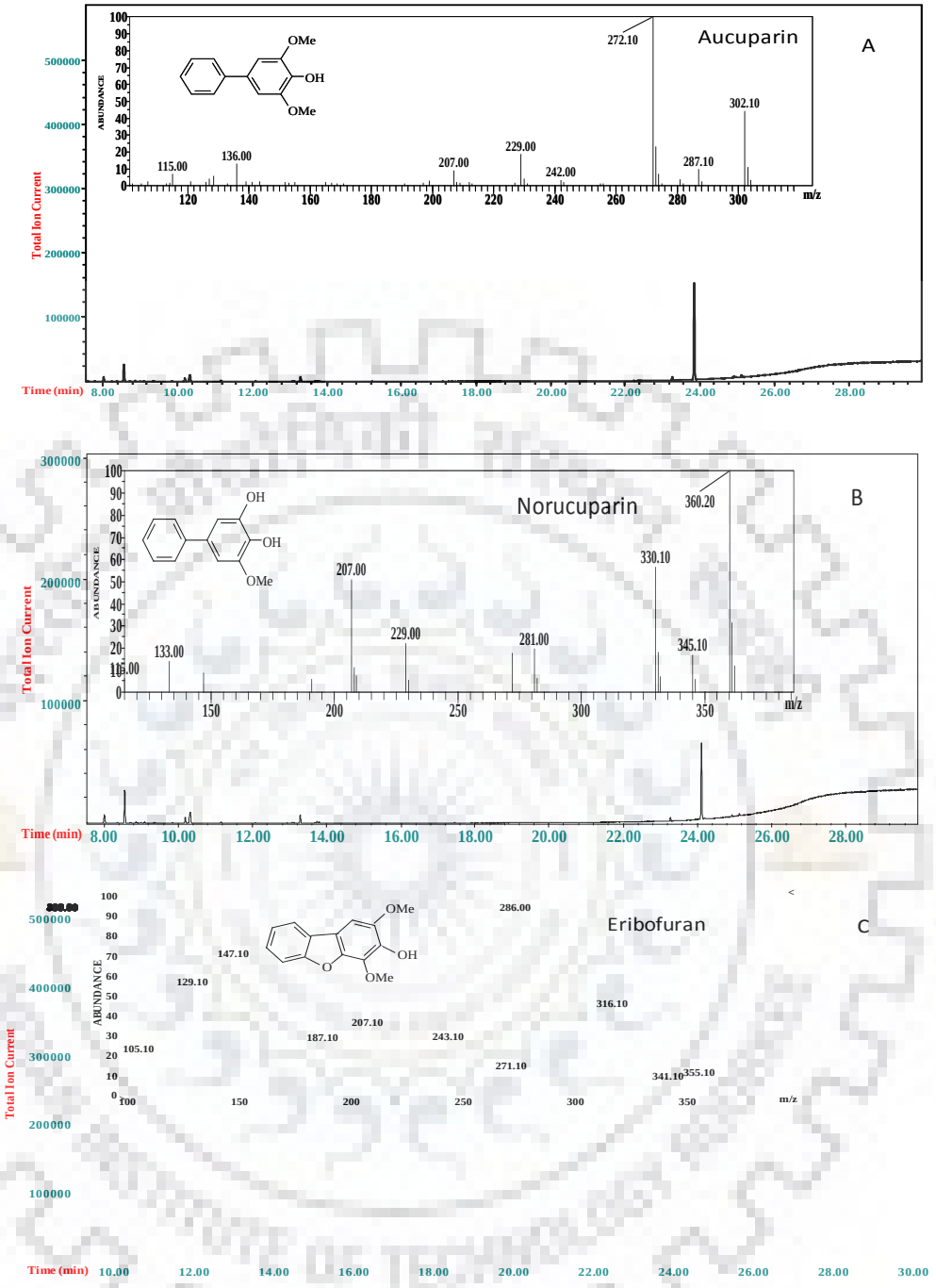

Figure 3.8: TIC and mass-spectrum (GC-MS) of chemically synthesized (A) aucuparin, (B) nor-aucuparin and (C) eriobofuran.

3.5. GC-MS based untargeted metabolomics of apple cell cultures treated with *Venturia inaequalis* elicitor

3.5.1. Comparative metabolomics of VIE-treated apple culture

To understand the metabolic changes in apple cell culture cv. 'Florina' treated with elicitor prepared from *V. inaequalis*, non-targeted GC-MS based metabolomics was performed. At different post elicitation time points (0-72h), elicited cells were extracted for isolation of metabolites and, after double derivatization, submitted to GC-MS metabolomics analyses. Dynamic changes in the metabolite levels post elicitation were compared with the non-treated control cells. One representative GC−MS chromatogram (total ion chromatogram) of apple cell culture (24 h post elicitation) was shown in Figure 3.9. A total of 36 low-molecular weight metabolites were detected (Table 3.4). Metabolites were characterized based on their retention time and specific fragmentation pattern. Detected metabolites were grouped under primary metabolites comprising of amino acids (7), sugars (4), sugar alcohols (3), organic acids (8), vitamin (1), Phenolics and biphenyl-dibenzofuran phytoalexin (13) (Figure 3.10). Out of 36 identified metabolites 22 metabolites were significantly up-regulated after elicitor treatment. The dominance of carbohydrates and phenolics were detected in the elicited cell cultures. When compared with the untreated control cultures, three new metabolites, noraucuparin, aucuparin and eriobofuran were detected from the elicited cell cultures. From metabolomics point of view, VIE-treatment appears to trigger a metabolic alteration, in both the primary and secondary metabolism. Metabolite feature areas were normalized using the area of internal standard.

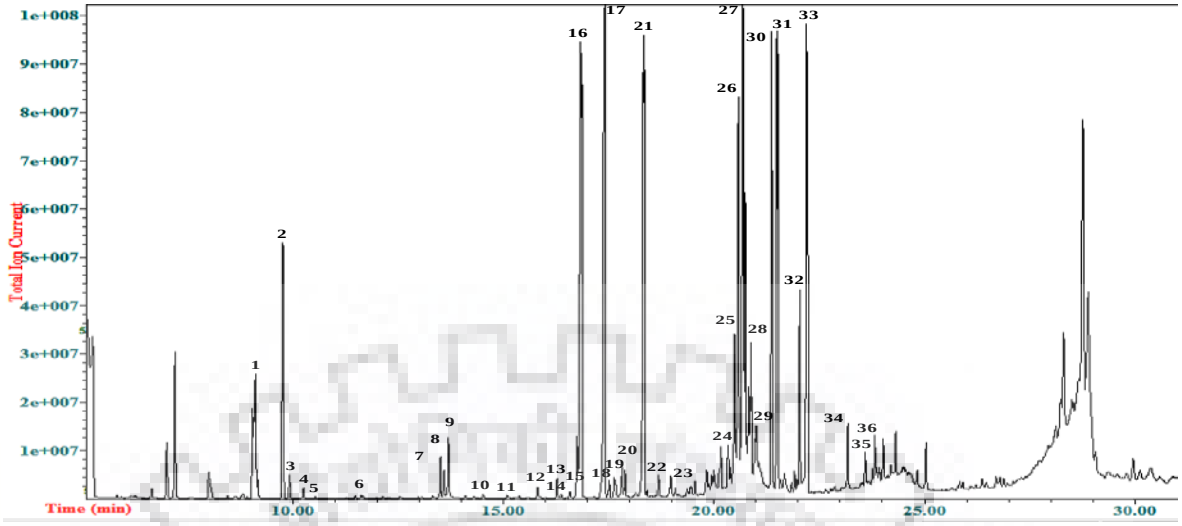

Figure 3.9: Typical GC-MS chromatograms (TIC): of VIE-treated (24h post elicitation) cell cultures of apple cv. 'Florina'

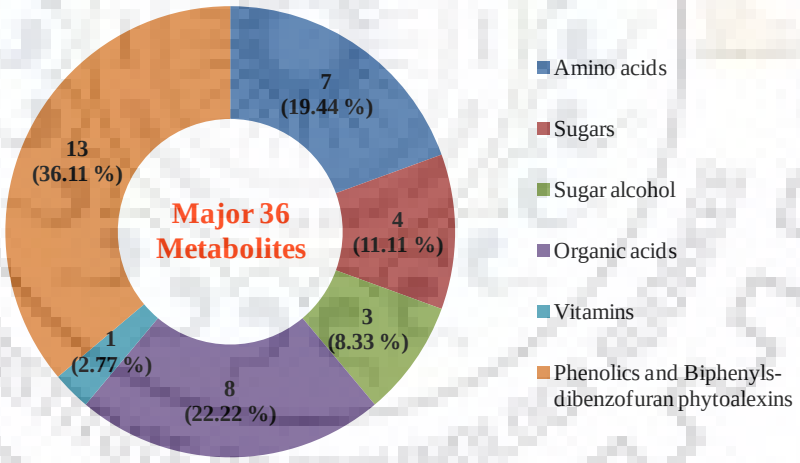

Figure 3.10: Metabolites grouped under specific class.

Table 3.4: List of 36 identified metabolites from VIE-treated cell cultures of apple cv. 'Florina'. The peak area of the quantification ion was used for comparative quantification. Variable importance in the projection (VIP) values greater than one represented the most relevant metabolites for explaining the responses.

Sr. No.	Metabolite	Derivate	PubChem ID	Retention time (min)	Qualification Ions [*m/z*]	VIP values
1	Aspartic acid	3 TMS	529617	13.52	130, 174	1.0536
2	Ascorbic acid	4 TMS	54670067	18.26	449, 332	0.44282
3	Aucuparin	1 TMS	442503	24.08	302, 287	0.99378
4	Benzoic acid	1 TMS	10887905	13.6	179, 135	0.60694
5	Caffeic acid	3 TMS	689043	22.86	396, 381	0.97899
6	Catechin	5 TMS	73160	26.25	649, 634	0.39766
7	Chlorogenic acid	6 TMS	1794427	21.24	419, 345	1.9278
8	Citric acid	4 TMS	553132	16.53	363, 375	1.2436
9	p-Coumaric acid	2 TMS	637542	22.2	308, 293	0.54185
10	trans-Cinnamic acid	1 TMS	444539	17.81	220, 205	0.90259
11	Eribofuran	1 TMS	178939	25.19	316, 288	1.0038
12	Ferulic acid	2 TMS	445858	23.6	338, 323	0.68827
13	Fructose	5 TMS	20845408	19.61	217, 307	1.3311
14	Fumaric acid	2 TMS	5353016	14.85	245, 230	1.0177
15	Glucose	5 TMS	20836750	19.86	103, 205	1.0306
16	Glycolic acid	2 TMS	575	13.53	177, 147	0.65732
17	Glycine	2 TMS	530141	9.5	176, 204	0.74288
18	Malic acid	3 TMS	522155	16.69	245, 335	1.1536
19	Malonic acid	2 TMS	87656	15.51	233, 148	0.97383
20	Mannitol	6 TMS	6251	24.85	421, 319	1.0691
21	Mannose	5 TMS	18950	18.81	435, 393	1.0903
22	Myoinositol	6 TMS	520232	23.58	217, 318	0.50979
23	Noraucuparin	2 TMS	44605718	23.8	330, 313	1.5614
24	Phenylalanine	2 TMS	522502	16.05	192, 219	1.0959
25	Proline	2 TMS	522501	11.85	216, 143	1.3189
26	Protocatechuic acid	3 TMS	72	20.82	370, 355	1.1269
27	Pyruvic acid	1 TMS	1060	10.78	217, 147	1.1804
28	3-phosphoglyceric acid	4 TMS	5327006	14.58	292, 133	1.0419
29	Rutin	10 TMS	5280805	28.75	354, 309	1.1819
30	Salicylic acid	2 TMS	338	17.2	303, 233	0.80507
31	Serine	3 TMS	522136	12.75	305, 218	0.9945
32	D-Sorbitol	6 TMS	5780	19.48	217, 147	0.85141
33	Sucrose	8 TMS	632328	26.79	217, 362	1.0278
34	Succinic acid	2 TMS	520988	12.03	262, 172	0.56631
35	Tryptophan	3 TMS	21632772	20.29	291, 203	0.4357
36	Tyrosine	3 TMS	529998	19.09	280, 179	0.43692

3.4.1.1. Amino acids: A total of 7 amino acids were detected from both, control and VIE-treated cells (Figure 3.11 A-G). No significant changes in the level of glycine, serine and tyrosine (Figure 3.11 A-C) were observed in the elicited cells over the time-course studied. The content of tryptophan, phenylalanine, proline and aspartic acid were significantly up-regulated after elicitor-treatment (Figure 3.11 D-G). Aspartic acid showed highest accumulation at 36 h whereas tryptophan and proline showed peak at 24 h. Phenylalanine attained peak, comparatively rapidly.

3.4.1.2. Sugars: Sucrose, fructose, glucose, and mannose sugars (Figure 3.11 H-K) were detected from both the elicited and non-elicited apple cell cultures. Glucose and fructose is derived from sucrose after hydrolyses. Furthermore, fructose transforms into mannose. The sucrose content was down-regulated upon VIE-treatment, where as glucose, fructose and mannose contents were up-regulated. Fructose showed highest accumulation at 6 h whereas glucose showed highest accumulation at 12h. Mannose showed a steady increase in content with highest accumulation at 72h. This indicates that sucrose catabolism was higher in VIE-treated cell culture.

3.4.1.3. Sugar alcohols: Three sugar alcohols, manitol, sorbitol and myo-inositol, were identified in VIE-treated apple cell cultures (Figure 3.11 L-N). Both, manitol and sorbitol content up-regulated upon VIE-treatment with highest accumulation at 72 h. No significant change in myo-inositol content was observed over the time course studied.

3.4.1.4. Organic acids: Seven organic acids were detected from the VIE-treated apple cell cultures. Except for glycolic acid, the levels of all identified organic acids (3-phosphoglyceric acid, pyruvic acid, citric acid, succinic acid, fumaric acid, malic acid, malonic acid and) were up-regulated upon VIE-treatment (Figure 3.11 O-V). Glycolic acid content remained more or less constant throughout the time-course studied. We hypothesized that, high organic acid accumulation after VIE-treatment was probably due to higher turnover number of glycolysis and TCA cycle which generated more abundant intermediate.

3.4.1.5. Vitamin: Ascorbic acid (vitamin C) was the only vitamin identified from both the non-elicited and elicited cell cultutres (Figure 3.11 W). After VIE-treatemnt ascorbic acid level was first increased, reached peak at 24 h and decreased thereafter.

3.4.1.6. Phenolics and biphenyl-dibenzofuran phytoalexins

Metabolomics analyses showed that phenolics were the most abundant metabolites in apple cell cultures. Plant phenolics play crucial role in pathogen defense (Lattanzio et al., 2006; Bisht et al., 2016; Bera et al., 2017). In this study, a total of 10 phenolics, two biphenyls and one dibenzofuran phytoalexins were detected from the VIE-treated apple cell cultures. Phenolics detected in apple cell cultures were caffeic acid, protocatechuic acid, catechin, chlorogenic acid, benzoic acid, ferulic acid, 4-coumaric acid, *trans*-cinnamic acid, rutin, and salicylic acid (Figure 3.12 A-J). The biphenyl phytoalexins detected were noraucuparin and aucuparin (Figure 3.12 K-L) whereas detected as dibenzofuran phytoalexin was eriobofuran (Figure 3.12 M). All these phenolics showed differential accumulation upon VIE-treatment. The content of these phenolics were first up-regulated after VIE-treatment and thereafter declined to the basal level. In this study a rapid enhancement of benzoic acid was observed after VIE-treatment. It was know that benzoic acid serves as the precursor for biphenyl and dibenzofuran class of phytoalexins of apple and other members of Malinae. Upon scab-infection, benzoic acid forms benzoyl-CoA, which combines with malonyl-CoA to produce 3,5-dihydroxybiphenyl, the precursor for all other biphenyl and dibenzofurans. Enhanced biosynthesis of benzoic acid in VIE-treated apple cells might attribute its higher resistance against scab fungus *V. inaequalis* and *E. amylovora* by fascilitating rapid formation of bipehnyl phytoalexins upon pathogen attack. Furthermore, a considerable up-regulation of salicylic acid (SA) biosynthesis was observed in VIE-treated apple cell (Figure 3.12 J). SA can induce local resistance in form of hypersensitive reaction or long distance systemic acquired resistance (SAR) by triggering the production of pathogenesis-related proteins (PR proteins). VIE-treatment to apple cell culture led to production of aucuparin, noraucuparin and eriobofuran, the marker phytoalexins of Malinae. It has been shown that biphenyl and dibenzofuran phytoalexin can efficiently inhibit the growth of *Venturia inaequalis* and *E. amylovora* (Chizzali et al., 2012). Interestingly, in our study, biphenyl and dibenzofuran phytoalexins were absent from the control cells and only formed after VIE-treatment. Notably, malusfuran **(**2,4-methoxy-3-hydroxy-9-*O*-b-D-glucosyloxydibenzofuran), a glucosylated dibenzofuran detected earlier from the elicited cell culture of apple cv. Liberty, has not been detected in our study. In contrary a non-conjugated dibenzofuran, eriobofuran has been detected from the VIE-treated cv. ‘Florina’ cell cultures.

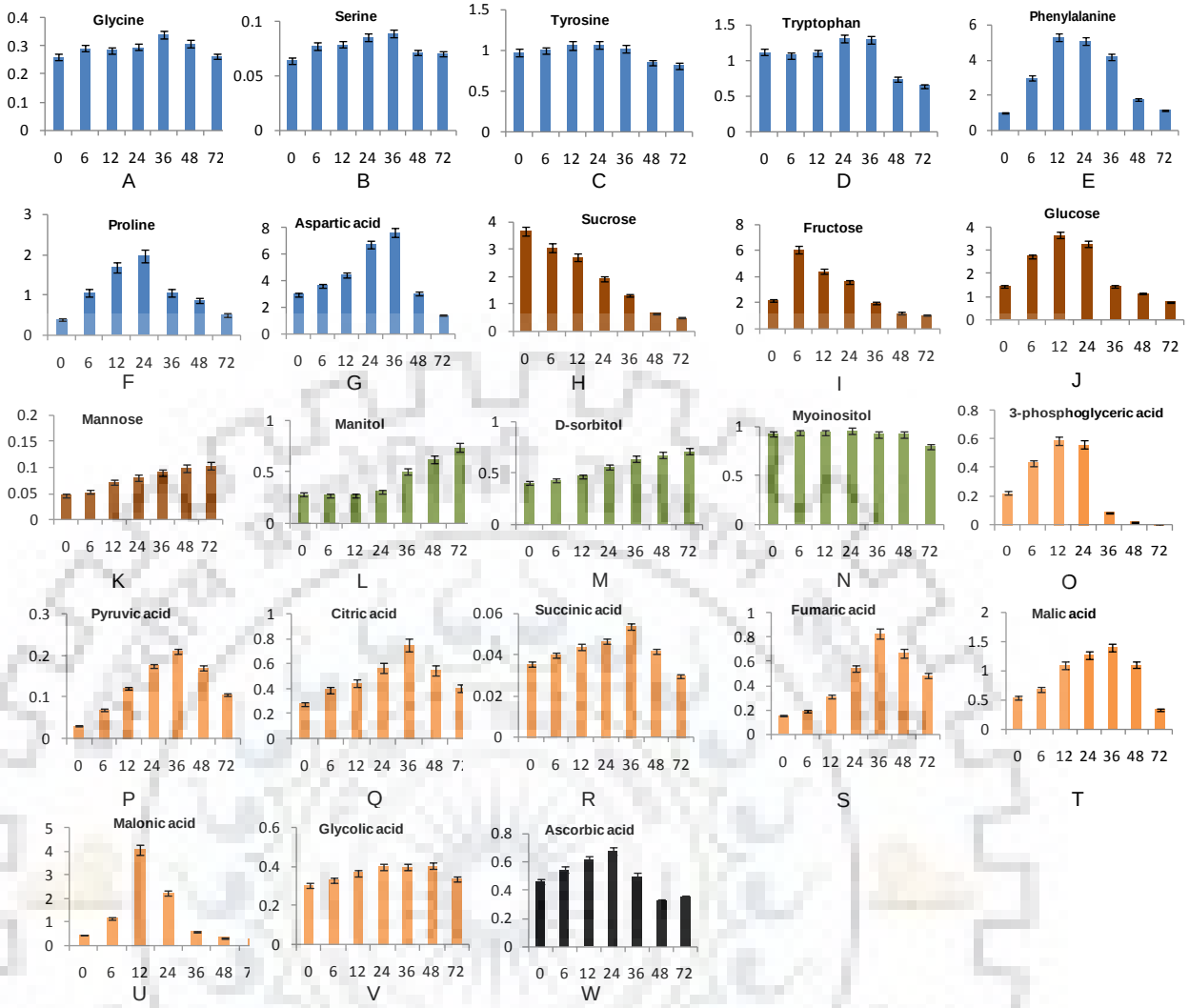

Figure 3.11: Differentially accumulating metabolites in the VIE-treated cell culture of apple cv. 'Florina'. Amino acids (A-G); Sugars (H-K); Sugar alcohols (L-N); Organic acids (O-V); Vitamin (W). Error bars represent standard deviations. The y-axis gives the normalized relative metabolite abundance in terms of the area of internal standard. The x-axis represents post-elicitation time points (h)

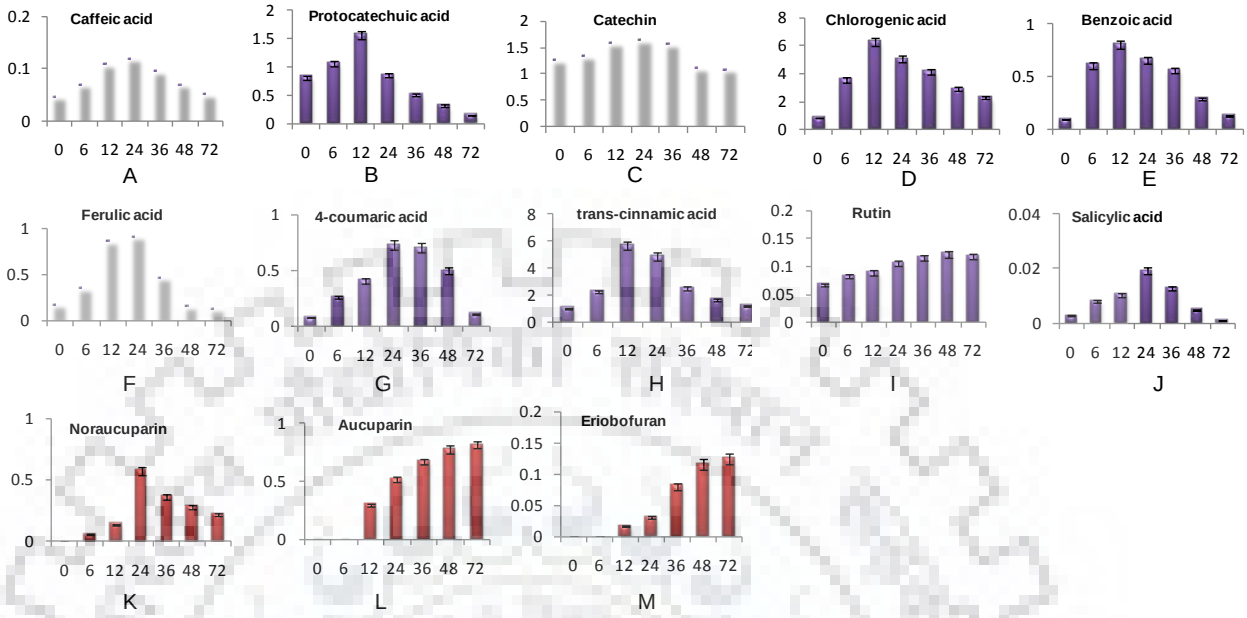

Figure 3.12: Differential accumulation of phenolics and biphenyl-dibenzofuran phytoalexins in the VIE-treated cell cultures of apple cv. 'Florina'. Error bars represent standard deviations. The y-axis gives the normalized relative metabolite abundance in terms of the area of internal standard. The x-axis represents post-elicitation time points (h).

3.5.2. Principal component analysis (PCA) reveals metabolic alterations in VIE-treated cell cultures

The metabolite variations between the VIE-treated samples at defined post-elicitation time points were analyzed by PCA. The PCA helps to reduce the dimensionality of complex data sets, which facilitate better visualization of the inherent patterns in the data. PCA analyses uses, linear orthogonal transformation of the original data variables to generate a new set of uncorrelated variables known as principal components (PCs) (Park et al., 2015). As shown in Figure 3.13A, the first and second PCs of the analyzed PCA score plot represented 38.4 % (PC1) and 24.7% (PC 2) of the total variance of the samples. The PC 1 determined the metabolomics profiles of control and VIE-treated cells. The Metabolomics profile at various time points in VIE-treated cells was separated by PC 2. Furthermore, a PCA loading plat (Figure 3.13 B) was constructed to show the abundant variable (metabolites) contributing the PCA results. Metabolites included in loading plot were differentially accumulating 36

metabolites as shown in table 3.4. Our results suggest that these metabolites are probably contributing to the different degree of defense responses against pathogen attack

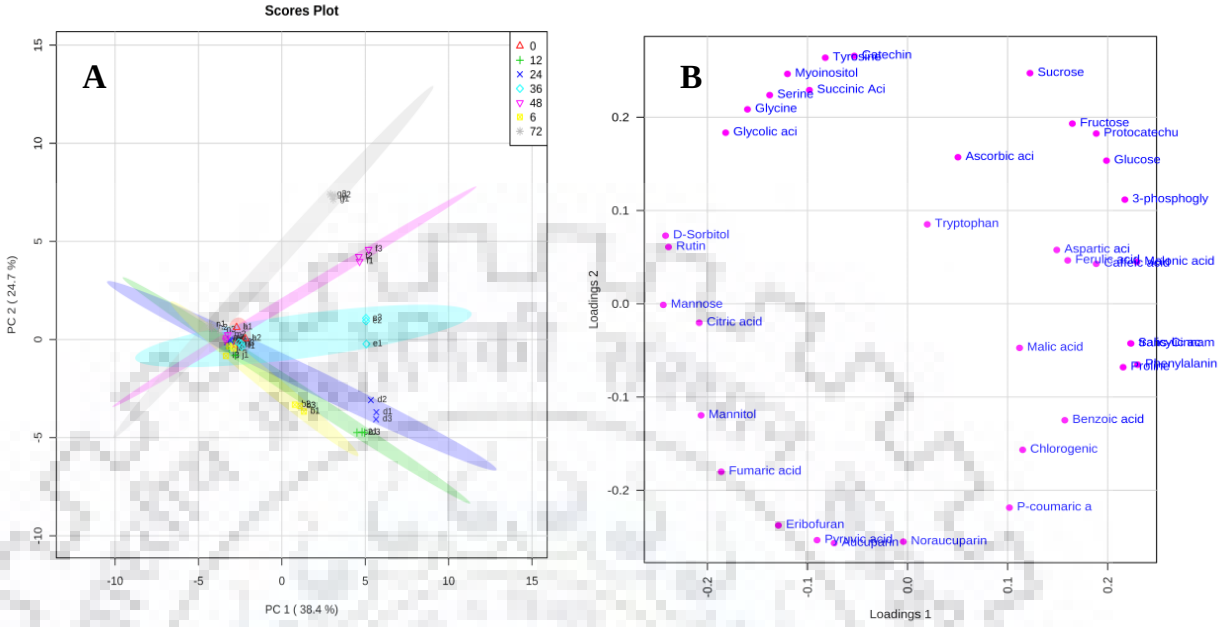

Figure 3.13: Scores plot (A) and loading plots (B) of principal components (PC1) and (PC2) of the PCA results obtained from 36 identified metabolites from the VIE-treated cell cultures of apple cv. 'Florina'.

3.5.3. Hierarchical clustering analysis of the metabolite profiles

In order to search for any probable discrepancies in the metabolite profiles of all the seven (0 - 72 h) sample groups, the 36 identified metabolites were organized and visualized by hierarchical clustering analysis (HCA) tool of Metaboanalyst 3.0 (Figure 3.14) (Shen et al., 2015). The hierarchical clustering offered excellent separation of the metabolite trend between the non-elicited (0h) and VIE-treated (6-72h). VIE-treated cells were the major source of variance in the result, which indicated that change in metabolite concentration by VIE-treatment.

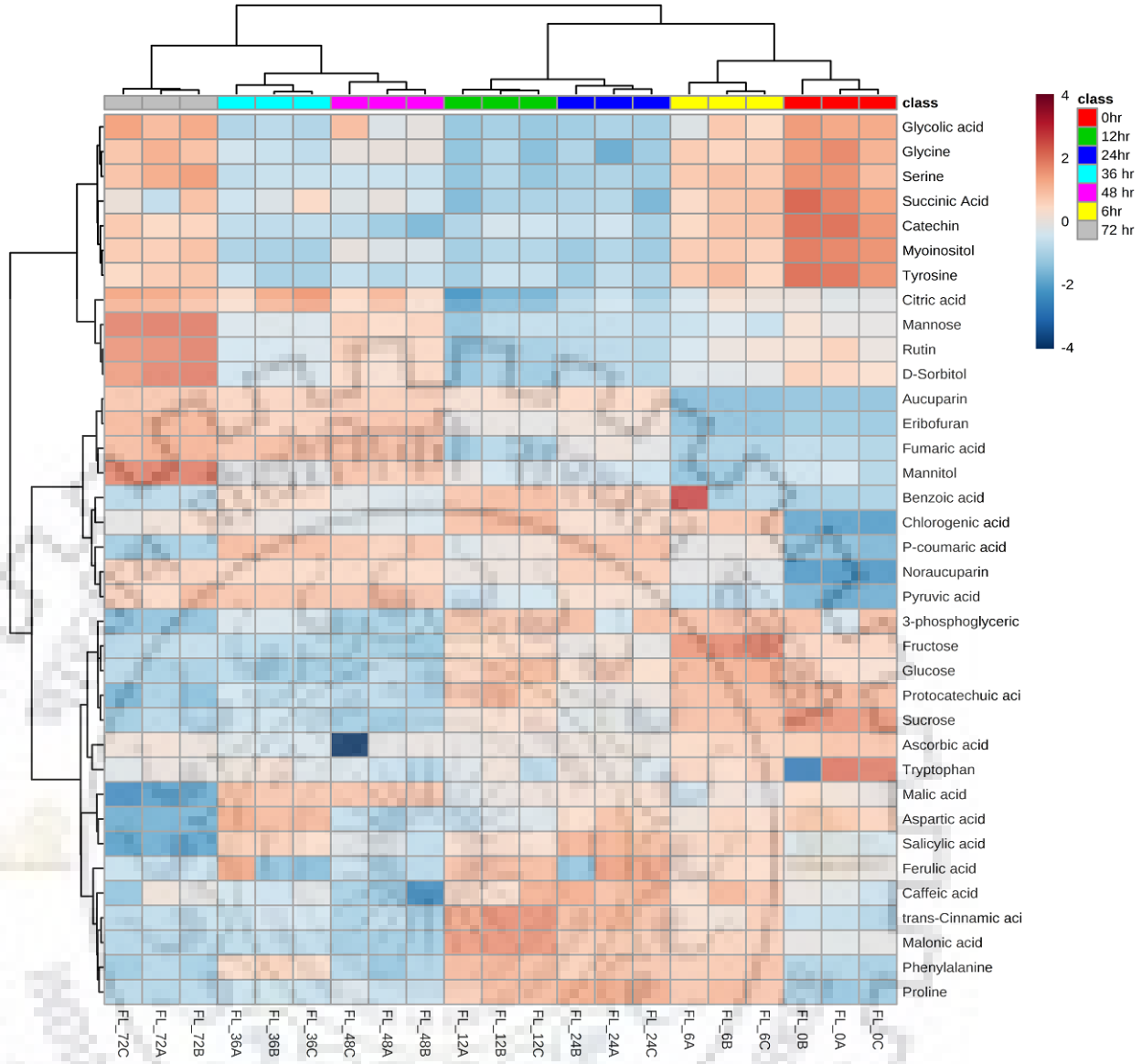

Figure 3.14: Hierarchical clustering analyses of 36 detected metabolites from VIE-treated cell culture of apple cv. 'Florina'. Similarity assessment for clustering was done on the basis of Euclidean distance coefficient and the average linkage method (metaboanalysts 3.0). Rows and columns represent individual metabolites and different samples, respectively.

3.5.4. Changes in metabolic pathways: metabolic pathway network

A simplified metabolic pathway network was reconstructed using key metabolic pathways, such as the shikimic acid pathway, the phenylpropanoid pathway, the glycolytic pathway, the pentose phosphate pathway, the biphenyl biosynthetic pathway, the flavonoids biosynthesis pathway, TCA cycle, and the amino acid biosynthetic pathway to show the regulated pattern diversity of each detected metabolites with respect to their proportional incorporation into key

metabolic pathways. As shown in Figure 3.15, sucrose as the precursor for glucose and fructose was higher in non-elicited cells than that of VIE-treated cells. However, sucrose hydrolysis product, the glucose and the fructose were higher in the VIE-treated cells, suggesting that more active sucrose catabolism occurred in the VIE-treated cells. The level of mannose, sorbitol and manitol were higher in VIE-treated cells suggesting that fructose is metabolized more towards these metabolites rather than re-entering into glycolytic pathway through fructose-6-phosphate. Metabolites of glycolyses pathway, especially pyruvic acid and 3-phosphoglyceric acid level were up-regulated in the VIE-treated cells whereas glycine and serine levels remained mostly unaltered among VIE-treated and un-treated cells. The level of identified TCA cycle metabolites such as citric, succinic, fumaric and malic acids were up-accumulated in leaves of VIE-treated cells suggesting higher turn-over number of TCA cycle. The metabolites derived from shikimate pathway showed an absolutely distinct accumulation pattern. The level of all the detected shikimate-derived metabolites such as caffeic acid, protocatechuic acid, catechin, chlorogenic acid, benzoic acid, ferulic acid, 4-coumaric acid, *trans*-cinnamic acid, rutin, and salicylic acid were higher in the VIE-treated cells. Aucuparin, noraucuparin and eriobofuran were only synthesized after VIE-treatment.

3.5.5. Expression analysis of phenylpropanoid biosynthetic genes in the VIE-treated apple cell cultures

Since the level of phenolics and biphenyl-dibenzofuran phytoalexins were significantly higher in the VIE-treated apple cells, we have examined the expression levels of four genes (*PAL*, *F3H*, *AOX* and *BIS3*) related to phenylpropanoid, flavonoids and biphenyl biosynthesis using qRT-PCR. The expression levels of *PAL, F3H, AOX* and *BIS3* are shown in Figure 3.16. The expression levels of all the four genes were up-regulated upon VIE-treatment demonstrating that phenylpropanoid and biphenyl biosynthesis was triggered by the VIE-treatment. These gene expression data were well correlated with the enhanced accumulation of phenylpropanoids such as cinnamic acid, flavonoids and biphenyls in the elicited cell cultures of apple.

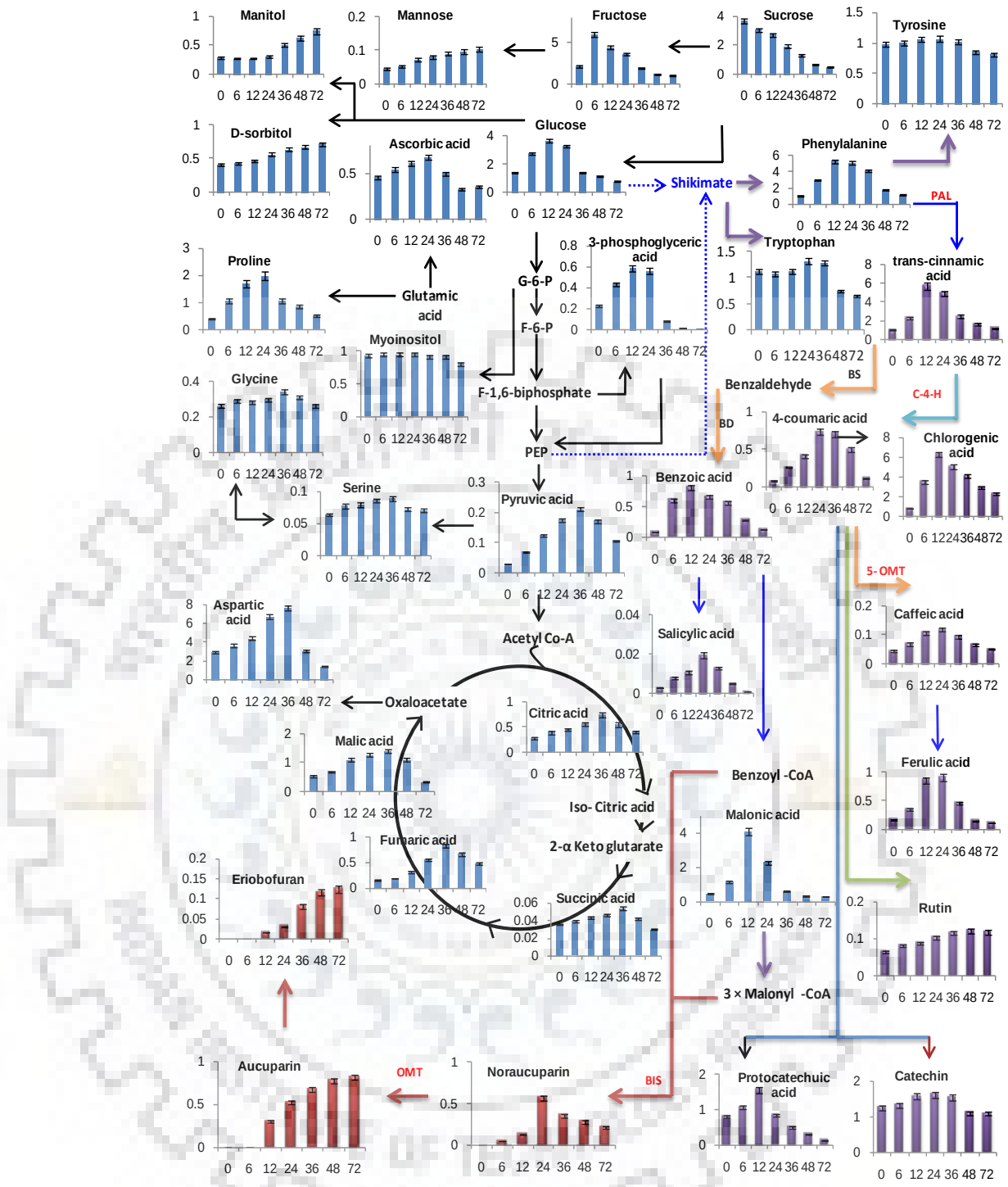

Figure 3.15: The proposed metabolic pathways network of VIE-treated apple cell culture cv. 'Florina'. Metabolic pathway network includes the sucrose hydrolyses, the glycolysis, the pentose phosphate pathway, the shikimate pathway, the phenylpropanoid and flavonoid pathway, the biphenyl phytoalexin pathway, the amino acid metabolism, and the TCA cycle. The bars represent the abundance of each metabolite in the control and VIE-treated apple cell culture.

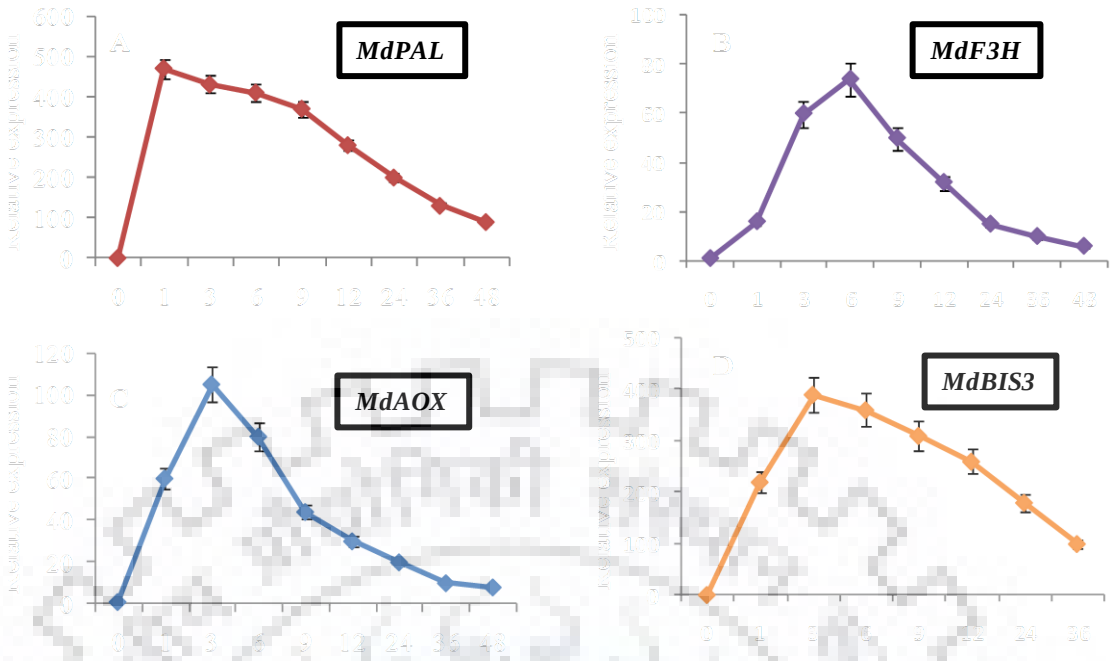

Figure 3.16: Changes in the *MDPAL, MdF3H MdAOX* and *MdBIS*$_3$ expression levels in *V. inaequalis* elicitor-treated cell cultures of apple cv. 'Florina'. The relative transcript levels were determined by real-time-PCR. Results are means ± SD (n = 3).

3.6. Salicylaldehyde synthase activity from *Venturia inaequalis* elicitor-treated cell cultures of apple

3.6.1. Effect of *Venturia inaequalis* elicitor (VIE)-treatment on salicylic acid (SA) accumulation

HPLC analyses showed an enhanced accumulation of total SA in the VIE-treated cell cultures compared to untreated control cells (Figure 3.17) Time-course analyses revealed that the total SA content was increased by VIE treatment and peaked at 24 h (4.5 ± 0.5 µg/g FW) and decreased after this until 48 h (1.5 ± 0.4 µg/g FW). Compared to untreated control cells, a maximum 5.6-fold increase in the total SA content was observed in elicitor-treated cells (Figure 3.18). A basal SA level was also detectable in the control cells.

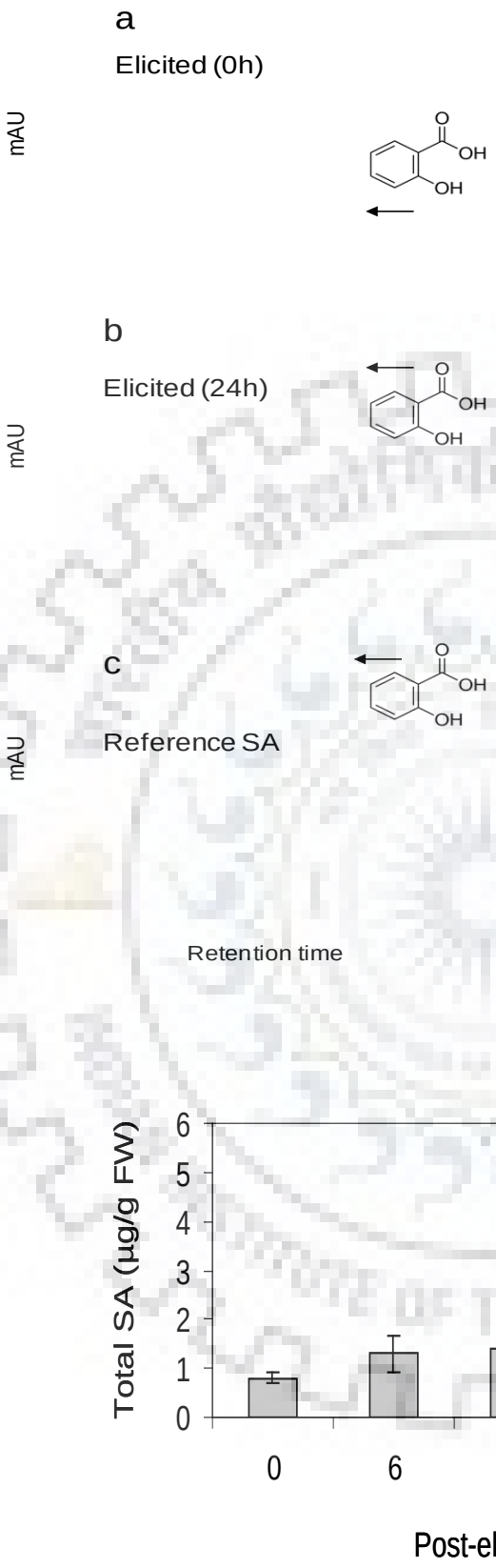

Figure 3.17: HPLC chromatogram showing accumulation of salicylic acid (SA) in the VIE-treated cell culture of apple. (a) Control cells (0 h); (b) salicylic acid accumulation after 24 h; (c) reference salicylic acid. The compounds were monitored at 227 nm.

Figure 3.18: Time-course accumulation of total salicylic acid in the elicitor-treated cell culture of *M. domestica*. Data are the mean of three biological repeats ± SD.

3.6.2. Effects of precursor feeding on the total SA accumulation

Precursor was added to the VIE-treated cell cultures after 6 h, since the marked increase in SAS activity starts at this time point. A higher accumulation of total SA was observed when VIE-treated cell suspension cultures were supplemented with *2*-coumaric acid (Figure 3.19). Compared to only VIE-treated cultures, the total SA content in 2-coumaric acid-fed cultures was higher by 1.8-fold. In 2-coumaric acid-fed cultures, minor accumulation of salicylaldehyde (0.74 ± 0.06 µg/g FW) and *2*-coumaric acid (0.9 ± 0.04 µg/g FW) was also observed. No adverse effect was visible in the cell cultures fed with only DMSO (50% v/v with water).

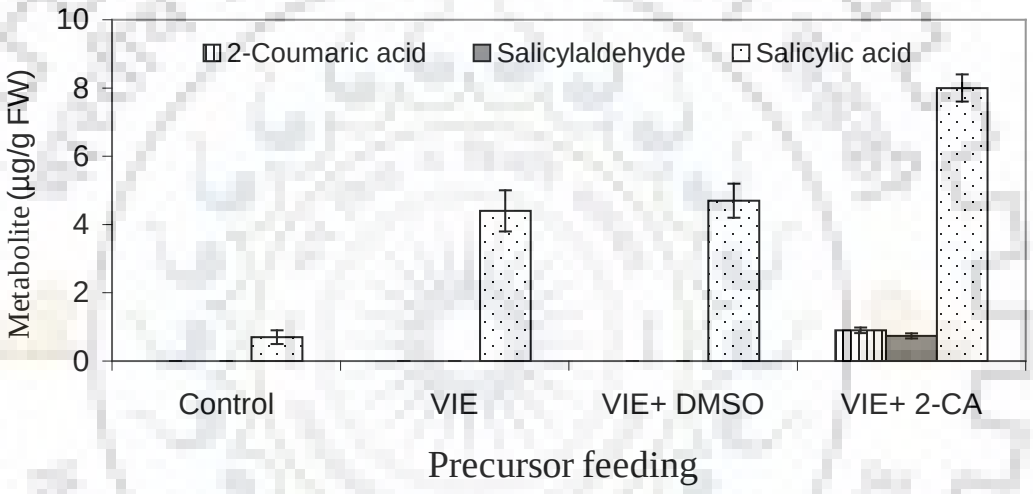

Figure 3.19: Effect of feeding 2-coumaric acid on the total salicylic acid accumulation in elicitor-treated *M. domestica* cell cultures. Data represent the average of triplicate measurements ± SD.

3.6.3. *In vitro* conversion of *2*-coumaric acid into salicylaldehyde by cell free extracts

Upon VIE-treatment, *M. domestica* cell cultures showed an enhanced accumulation of total SA. VIE-treated cell cultures were used to prepare cell-free extracts for the incubation with *2*-coumaric acid and cysteine to detect salicylaldehyde synthase (SAS) activity. Subsequent HPLC analysis revealed the formation of salicylaldehyde (Figure 3.20) suggesting in vitro conversion of *2*-coumaric acid to salicylaldehyde by the cell free extract. The identity of this enzymatic

product was confirmed by co-chromatography with an authentic standard of salicylaldehyde and UV spectrum matching. The results of GC-MS analysis showed that the mass spectrum of the SAS product agreed with that of the reference salicylaldehyde (Figure 3.21). In the GC-MS analyses of the SAS reaction, acetic acid was also detected (data not shown). In control assays containing heat-denatured partially purified protein, a slow but spontaneous conversion of *2*-coumaric acid to salicylaldehyde (3-4% of actual product formation) was observed in the presence of cysteine or DTT (Table 3.5). Assay containing heat-denatured protein without reducing agent showed very little change in the activity (1%) (Figure 3.22). The presence of reducing agent accelerated the non-enzymatic conversion of *2*-coumaric acid to salicylaldehyde.

3.6.4. Changes in SAS activity upon VIE treatment

VIE-treated cell cultures were harvested at defined time points (0-48 h) to prepare cell-free extracts that were used for the determination of PAL (Figure 3.23a) and SAS (Figure 3.23b**)** activities. There was basal SAS activity at 0 h. After the onset of elicitation, SAS activity rapidly increased and reached its peak at 12 h (21 ± 1.2 pkat/mg protein). At 48 h post-elicitation, SAS activity had nearly decreased to the basal level. No significant changes in SAS activity were observed in non-elicited control cells over the period studied. The maximum enzyme activity in treated cells (12 h post-elicitation) was almost 7-fold higher than that of the control cells. Values for spontaneous conversion were always substracted from the values obtained in the standard assay.

The rapid induction of PAL activity was also observed after the VIE treatment. Maximum PAL activity was detected at 9 h post-elicitation. The peak of PAL activity preceded the peak of SAS activity.

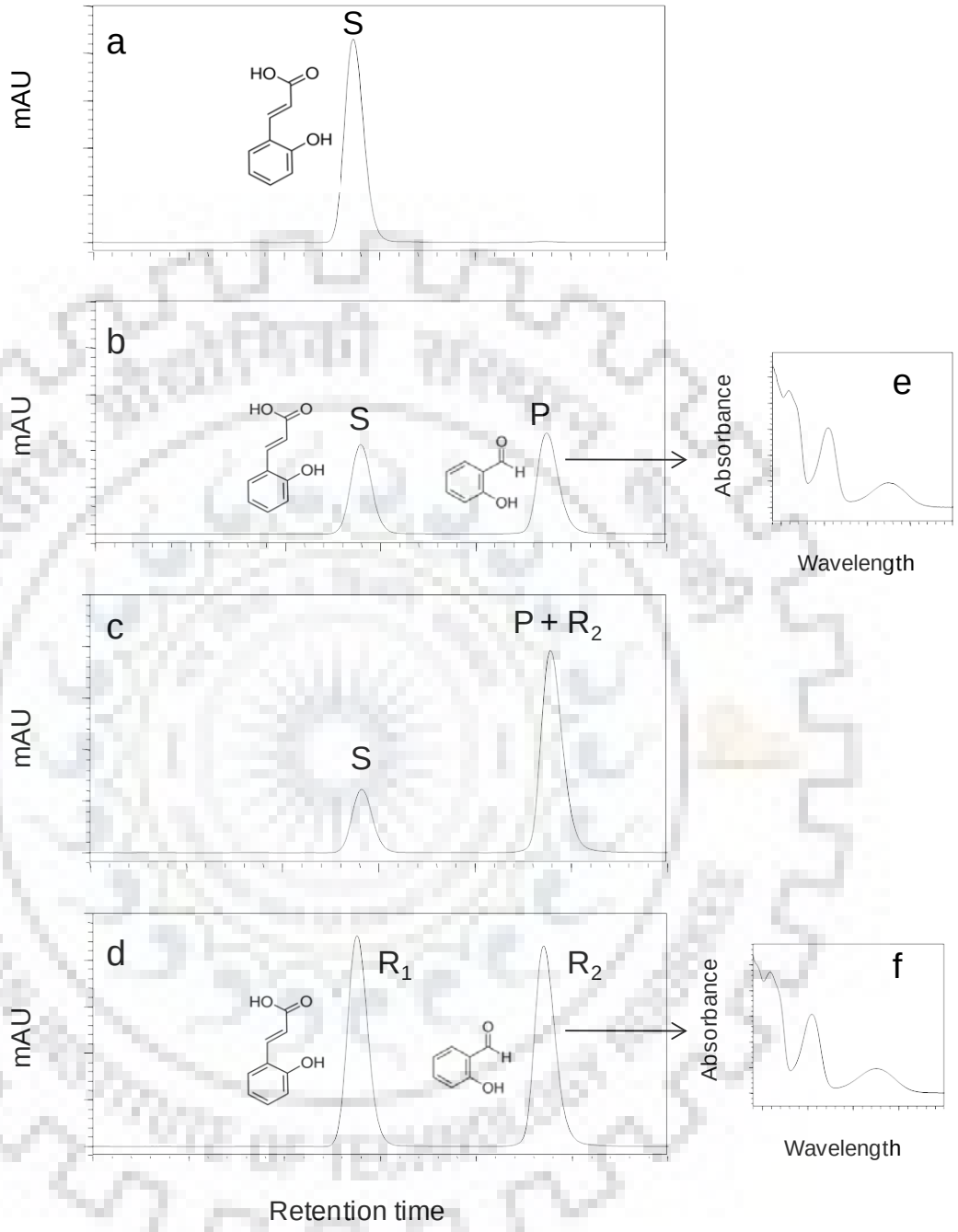

Figure 3.20: HPLC chromatograms showing salicylaldehyde synthase (SAS) activity from elicitor-treated cell culture of *M. domestica*: (a) control assay with boiled protein extract, (b) standard assay, (c) co-chromatography of standard assay and reference salicylaldehyde (product of SAS), (d) reference compounds (R1: 2-coumaric acid; R2: salicylaldehyde), (e) UV spectrum of SAS product, (f) UV spectrum of reference salicylaldehyde. Peak identity keys: S, substrate (2-coumaric acid); P, SAS product (salicylaldehyde); R, reference compound. The compounds were monitored at 256 nm.

Figure 3.21: GC-MS analyses of SAS assay. The product of SAS reaction and the standard salicylaldehyde were derivatized with MSTFA and subsequently analyzed by GC-MS: (a) control assay, (b) standard assay, (c) reference salicylaldehyde, (d) mass-spectrum of SAS product, (f) mass-spectrum of reference salicylaldehyde.

Table 3.5: Effect of various reducing agents on salicylaldehyde synthase (SAS) activity. The standard assay contained 2-coumaric acid (5 mM), reducing agent (1-20 mM) and 10 µg of partially purified protein. The results are the means of three independent experiments ± SD.

Reducing agent	**SAS relative activity (%)**	**Specific activity**
No reducing agent	2.5	2.4 ± 0.4
Cysteine (1 mM)	25.7	24.5 ± 1.3
Cysteine (5 mM)	65.3	62.2 ± 4.2
Cysteine (10 mM)	100	95.2 ± 3.0
Cysteine (20 mM)	90.7	86.4 ± 4.0
Dithiothreitol (10 mM)	73.5	70 ± 5.0
β-Mercaptoethanol (10 mM)	28.7	27.3 ± 3.0
Coenzyme A (10 mM)	10.6	10.2 ± 2.0
Coenzyme A (10 mM) + ATP (10 mM)	12.2	11.6 ± 3.0
Cysteine (10mM) with boiled protein	4.2	4.0 ± 0.9
Dithiothreitol (10 mM) with boiled protein	4.0	3.8 ± 0.6
No reducing agent with boiled protein	0.5	0.5 ± 0.05

Figure 3.22: Time-course analyses of enzymatic and non-enzymatic conversion of 2-coumaric acid to salicylaldehyde. E: enzyme (partially purified protein); BE: (boiled enzyme).

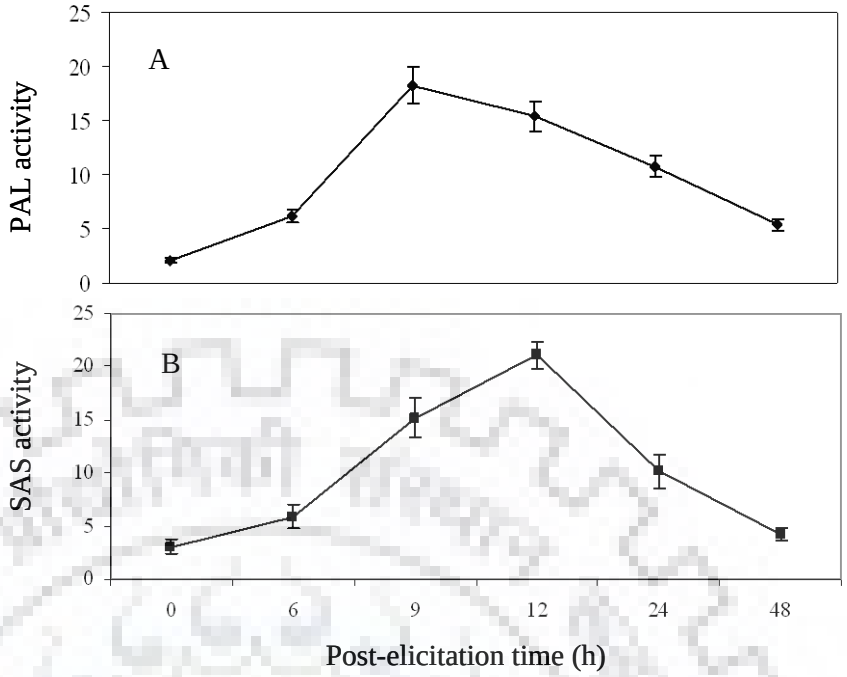

Figure 3.23: Time-course changes in the enzyme activities in elicitor-treated cell cultures of *M. domestica*: (a) phenylalanine ammonia-lyase (PAL); (b) salicylaldehyde synthase (SAS). Enzyme activity was expressed in pkat/mg protein. Data are the means ± SD of at least three independent experiments.

3.6.5 Characterization of SAS

Since the highest SAS activity was observed at 12 h post elicitation, we used 12 h post elicited cells to partially purify the SAS protein. Protein purification was conducted using ammonium sulfate and DEAE-Sepharose anion-exchange chromatography. The fraction with the highest SAS activity showed one prominent protein band in a Coomassie Blue-stained gel, at ~ 52 kDa (Figure 3.24, lane D). When compared with proteins in adjacent fractions (Figure 3.24, lane B and C), the increase in SAS activity correlated closely with the 52 kDa band. A 4.5-fold purification was achieved after DEAE-Sepharose purification. The apparent increase in specific activity during each purification step was listed in Table 3.6. This partially purified protein obtained after DEAE-Sepharose anion-exchange chromatography was used to characterize SAS. SAS activity was found to be strictly dependent on the presence of a reducing agent in the reaction buffer. The highest SAS activity was observed with 10 mM cysteine (Table 3.5). A linear increase in the activity was observed up to 10 mM cysteine, beyond which a slight decrease in activity was observed. A set of aromatic C_6-C_3 metabolites was tested as potential

substrates at saturating concentrations of 5 mM. Among the metabolites tested, the preferred substrate for SAS was *2*-coumaric acid (set as 100%), followed by 4-coumaric acid and *trans*-cinnamic acid (Table 3.7). No activity was detected with ferulic acid, caffeic acid or sinapic acid. The SAS activity was linear with time up to 30 min and with the protein concentration up to 50 µg per 200 µL in the standard assay. The SAS activity followed Michaelis-Menten kinetics. The apparent K_m values derived by the Hanes plots were *K*m = 0.35 ± 0.04 mM for *2*-coumaric acid and *K*m = 0.88 ± 0.14 mM for 4-coumaric acid. The pH optimum was 7.5 and the temperature optimum was 35 °C. A significant loss in SAS activity (up to 55%) was observed upon storage of the cell-free extract at -20 ºC for 24 h. At 4 ºC, the enzyme activity decreased to approximately 10% within 24 h.

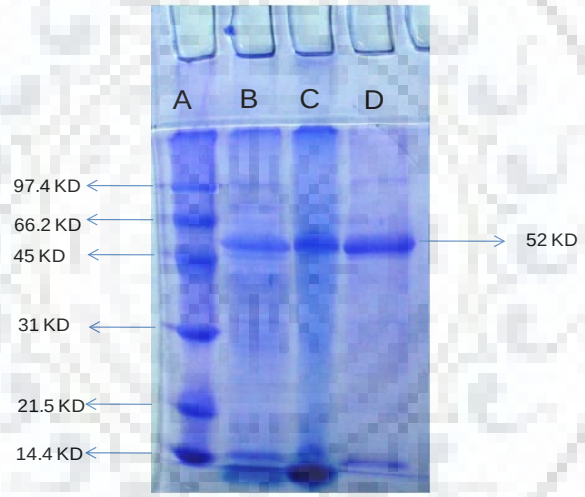

Figure 3.24: SDS–PAGE analysis of fractions obtained during the purification of SAS followed by Coomassie Blue staining of the gel: (A) molecular mass markers; (B) crude extract; (C) ammonium sulfate precipitation; (D) DEAE-Sepharose fractions (pooled) showing SAS activity.

Table 3.6: Partial purification of salicylaldehyde synthase (SAS) from elicitor-treated apple cell cultures.

Purification step	Total protein (mg)	Total activity (pkat)	Specific activity (pkat/mg protein)	Purification (-fold)	Yield (%)
Crude extract	112	2352	21	1	100
$(NH_4)_2SO_4$ precipitation	30.6	1235	40.35	1.9	20.4
DEAE-sepharose	10	952	95.2	4.5	34.5

Table 3.7: Substrate specificity studies of salicylaldehyde synthase (SAS) from VIE-treated cell cultures of *M. domestica*. The results are expressed as relative activity (%). The activity with *2*-coumaric acid (94.4 ± 3.7 pkat/mg protein) was set to 100%. Partially purified protein was used for the substrate specificity test.

S.No	Substrate	Product	Relative activity (%)	Specific activity (pkat/mg protein)
1	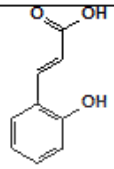 2-coumaric acid	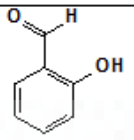 Salicylaldehyde	100	94.4 ± 3.7
2	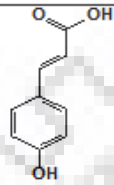 4-coumaric acid	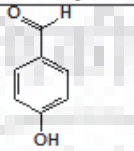 4-hydroxybenzaldehyde	77.6	74.0 ± 6.0
3	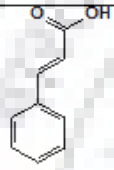 *trans*-cinnamic acid	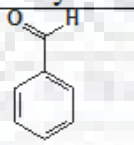 Benzaldehyde	32.0	30.3 ± 3.3
4	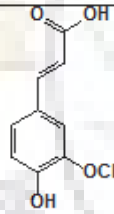 Ferulic acid	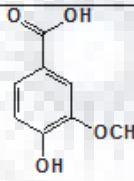 Vanillin	0	0
5	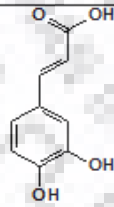 Caffeic acid	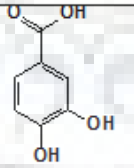 Protocatechuic aldehyde	0	0
6	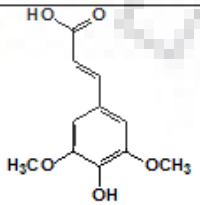 Sinapic acid	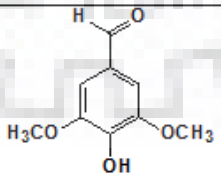 Syringalehyde	0	0

The results are the means of three independent experiments ± SD.

3.7. Molecular cloning and functional analyses of a biphenyl phytoalexin-specific *O*-methyltransferase (*Md*OMT) from apple cell suspension cultures

3.7.1 cDNA Cloning of a *O*-methyltransferase (*Md*OMT) from cell culture of *Malus domestica* cv. 'Florina'

The apple cultivar Golden Delicious sequence shares high degree of similarities with the 3,5-dihydroxybiphenyl *O*-methyltransferase from *Sorbus aucuparia* (accession no.: AHM25236.1) and other sequences targeting *O*-methylation of related substrates. *In silico* analyses of gleaned sequenced from GDR database (www.rosaceae.org; Table 2.32), identified two apple unigenes [MDP0000770800 and MDP0000745475] that shared high sequence similarity (97.3 and 96.4%, respectively) with *S. aucuparia* 3,5-dihydroxybiphenyl *O*-methyltransferase. Based on sequence similarity, MDP0000770800 unigene coding sequence was used to derive gene-specific primers for the amplification of the corresponding transcript from VIE-treated cell cultures of *Malus x domestica* cv. 'Florina'. After extension of 5'- and 3'- ends, the full-length cDNA was re-amplified using Phusion® High-Fidelity proof reading DNA polymerase. The resulting cDNA consisted of a coding sequence (cds) of 1113 bp a 5' untranslated region (UTR) of 200 bp, a 3' UTR (including poly A tail) of 242 bp. This coding sequence encoded a protein of 370 amino acids long with 41.09 kDa of predicted molecular mass and an isoelectric point of 6. The protein was named 3,5-dihydroxybipehnyl *O*-methyltransferase (*Md*OMT). Analyses of amino acid sequence alignment of *Md*OMT with other closely related published plant *O*-methyltransferase sequences revealed the presence of structural motifs (Figure 3.25) that are characteristic signature of plant OMTs (Joshi and Chiang, 1998; Khalil et al. 2015)

Figure 3.25: Alignment of selected amino acid sequences from plant OMTs including MdOMT and 3,5-dihydroxybiphenyl OMT from *S. aucuparia*. Coloured boxes highlights OMT signature motifs: dimer-forming amino acids (black), SAM-binding motif (blue), substrate-binding amino acids (red). Catalytic residues are marked with asterisk (*).

3.7.2 Functional Characterization of *Md*OMT

The *Md*OMT cds was cloned into the expression vector pRSET B and heterologously expressed in *E. coli* as N-terminal His_6-tagged recombinant protein. Recombinant *Md*OMT protein was purified using Ni-NTA affinity chromatography. During OMT assay, when 3, 5-dihydroxybiphenyl was incubated with recombinant MdOMT in presence of S-Adenosyl-L-methionine (SAM) and ascorbic acid, 3-hydroxy-5-methoxybiphenyl was formed as reaction product. Chemical identity of reaction product was confirmed by HPLC-DAD (Figure 3.26) and gas chromatography-mass spectrometry studies in comparison with an authentic reference compound (Figure 3.27). Mass-spectrum of MdOMT assay product agreed with the mass-spectrum of standard 3-hydroxy-5-methoxybiphenyl. In the standard assay, SAM served as methyl-group donor whereas ascorbic acid was added to protect reaction components (substrates and products) from oxidation. Among the substrates tested, the preferred substrate for MdOMT was 3,5-dihydroxybiphenyl, which was only once methylated by MdOMT to yeild 3-hydroxy-5-methoxybiphenyl (Table 3.8). No activity was detected with 2,5-dihydroxybiphenyl, 3-hydroxy-5-methoxybiphenyl, noraucuparin, 5-hydroxyferulic acid and caffeic acid. Enzyme activity was strictly dependent on presence of SAM. The pH and temperature optima were 8.5 and 35°C, respectively. MdOMT activity was linear with time up to 30 min and with increasing Md*OMT* protein in the standard assay up to 15 µg. The K_m values for 3,5-dihydroxybiphenyl and SAM were 13.09 ± 2.6 and 24.6 ± 2.8 µM, respectively. The kinetic properties of MdOMT were given in Table 3.9. No appreciable loss in *Md*OMT activity was observed upon storage of recombinant protein in glycerol (20% v/v) at -80°C for 6 months. At 4°C, enzyme activity decreased to about 20 - 25% within 24 h.

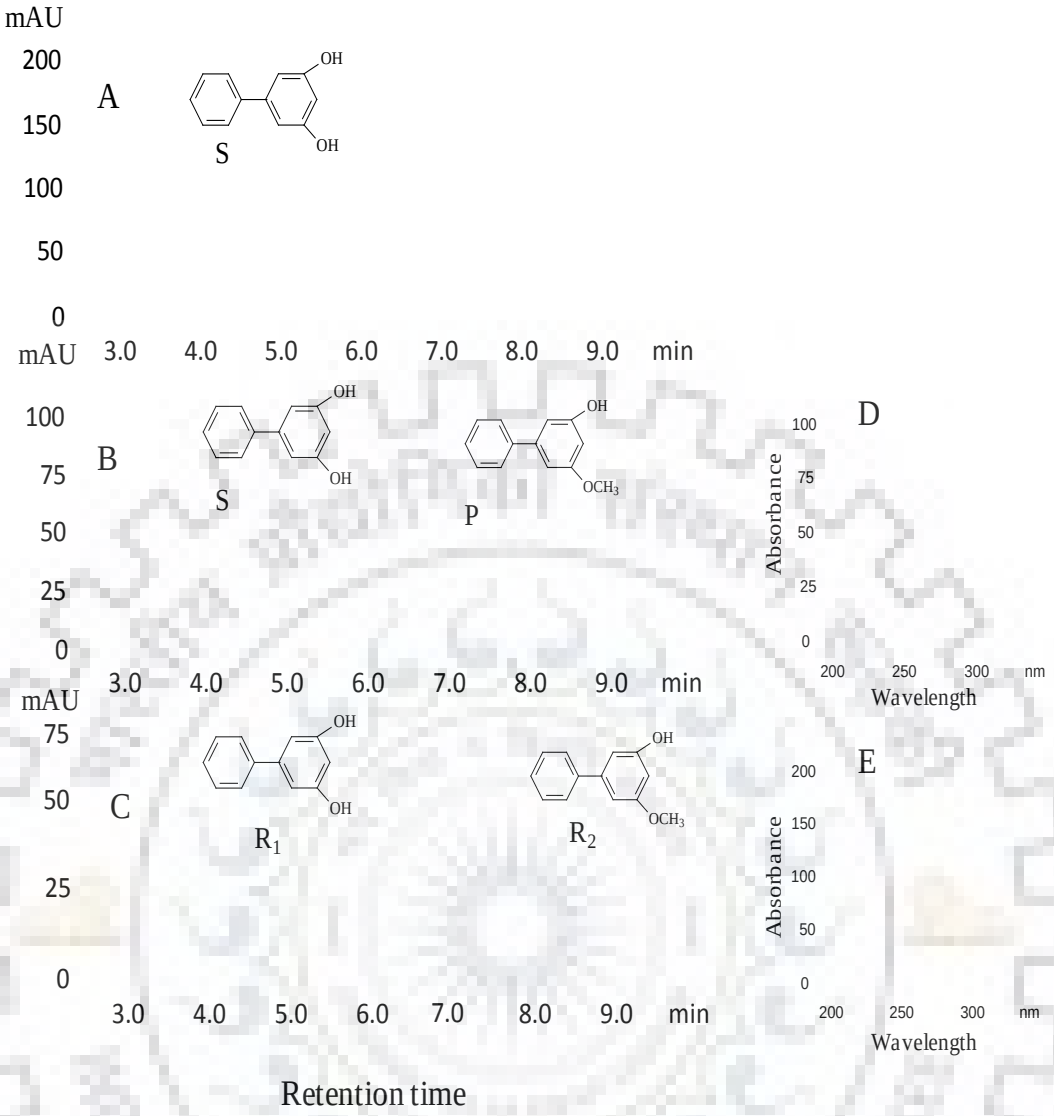

Figure 3.26: HPLC chromatograms showing in vitro conversion of 3,5-dihydroxybiphenyl to 3-hydroxy-5-methoxybiphenyl by recombinant MdOMT: (a) control assay with boiled protein, (b) standard assay, (c) reference compounds (R1: 3,5-dihydroxybiphenyl; R2: 3-hydroxy-5-methoxybiphenyl), (d) UV spectrum of MdOMT product, (e) UV spectrum of reference 3-hydroxy-5-methoxybiphenyl. Peak identity keys: S, substrate (3,5-dihydroxybiphenyl); P, MdOMT product (3-hydroxy-5-methoxybiphenyl); R, reference compound. The chromatograms were monitored at 254 nm.

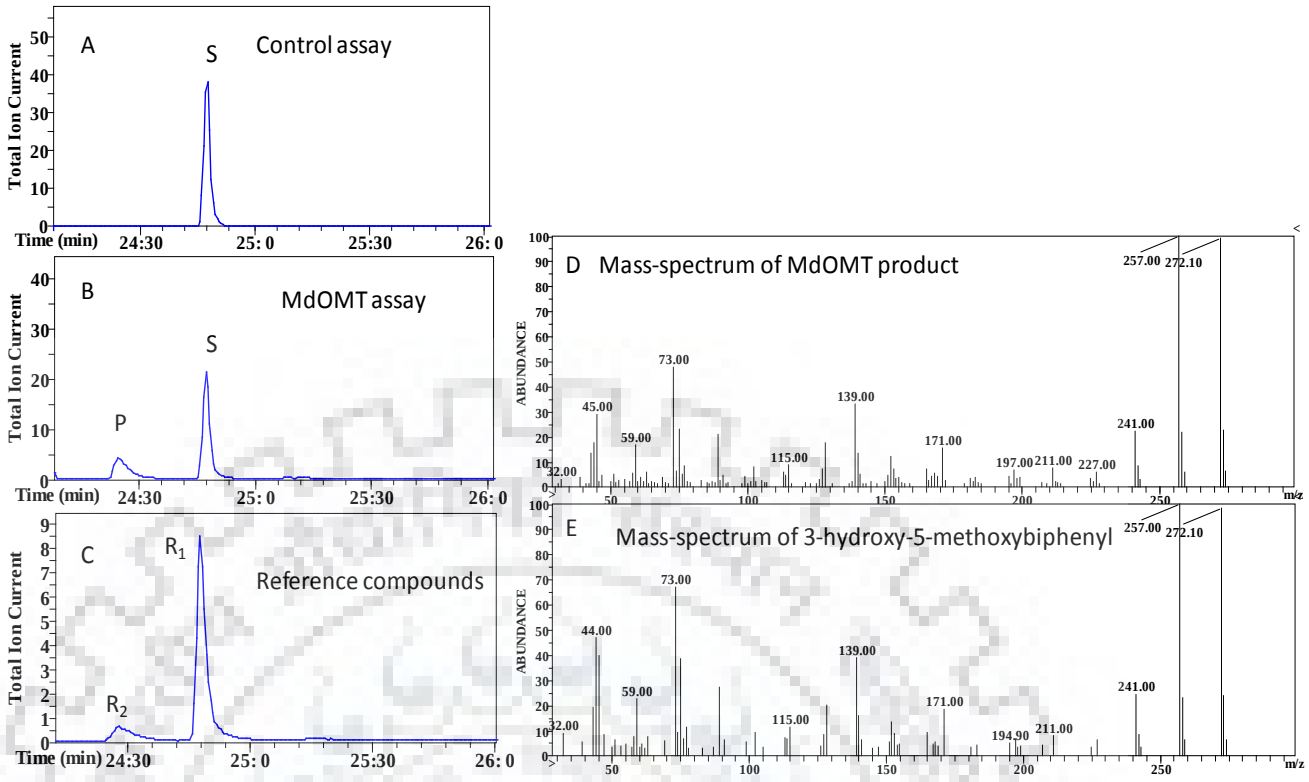

Figure 3.27: GC-MS analyses of *Md*OMT assay. The product of MdOMT assay and the standard 3-hydroxy-5-methoxybiphenyl were derivatized with MSTFA and subsequently analyzed by GC-MS: (a) control assay, (b) standard assay, (c) reference compounds (R1: 3,5-dihydroxybiphenyl; R2: 3-hydroxy-5-methoxybiphenyl), (d) mass-spectrum of MdOMT product P, (f) mass-spectrum of reference R2 3-hydroxy-5-methoxybiphenyl.

Table 3.8: Substrate specificity studies of recombinant MdOMT. Results are expressed as relative activity (%). The activity with 3,5-dihydroxybiphenyl (2.1 ± 0.1 nkat/mg protein) was set to 100%. The results are the means of three independent experiments ± SD.

S.No.	Substrate	Product	UV (λmax)	Relative Activity (%)	Specific activity (nkat/mg protein)
1	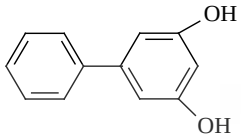 3,5-Dihydroxybiphenyl	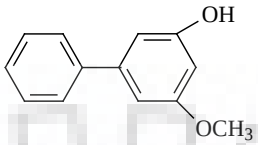 3-Hydroxy-5-methoxybiphenyl	254	100	2.1 ± 0.1
2	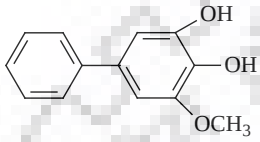 Noraucuparin	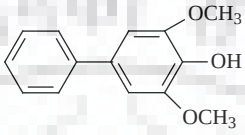 Aucuparin	269	0	0
3	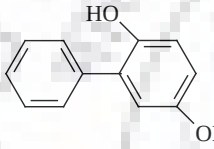 2,5-Dihydroxybiphenyl	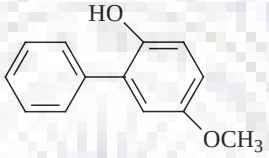 2-Hydroxy- 5-methoxybiphenyl	254	0	0
4	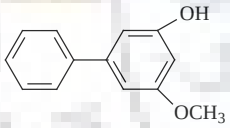 3-Hydroxy-5-methoxybiphenyl	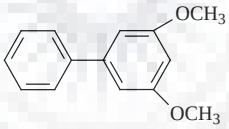 3,5-Dimethoxybiphenyl	254	0	0
5	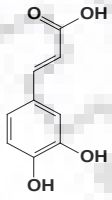 Caffeic acid	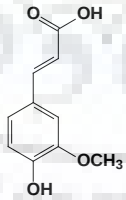 Ferulic acid	310	0	0
6	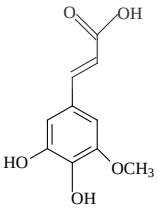 5-Hydroxyferulic acid	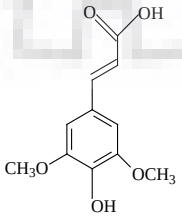 Sinapic acid	310	0	0

Table 3.9: Kinetic properties of recombinant MdOMT.

Substrate	K_m (µM)	V_{max} (nkat/mg protein)	K_{cat} (Min^{-1})	K_{cat}/K_m ($M^{-1}S^{-1}$)
3,5-Dihydroxybiphenyl	13.08 ± 2.68	2.89 ± 0.09	14.25 ± 0.46	18157.5

3.7.3. Phylogenetic reconstruction of MdOMT sequence

A neighbor-joining tree was constructed using a number of functionally characterized plant *O*-methyltransferases (OMTs) that contribute to various pathways of plant secondary metabolism (Figure 3.28). The accession numbers of these proteins are listed in table 2.27. The amino acids sequences were clustered into two groups, one with pinosylvin-OMT and other with resveratrol OMT. The majority of the included OMTs belong to either class 1 or class 2 of plant OMTs (Noel et al., 2003). The OMT sequence from the bacterium *Pseudomonas aeruginosa* was used to root the tree. The 3, 5-dihydroxybiphenyl OMT sequences from *Sorbus aucuparia* and apple which shared 94% identity grouped together. MdOMT was closest to a cluster that consisted of catechol OMT, phloroglucinol OMT and pinosylvin OMT.

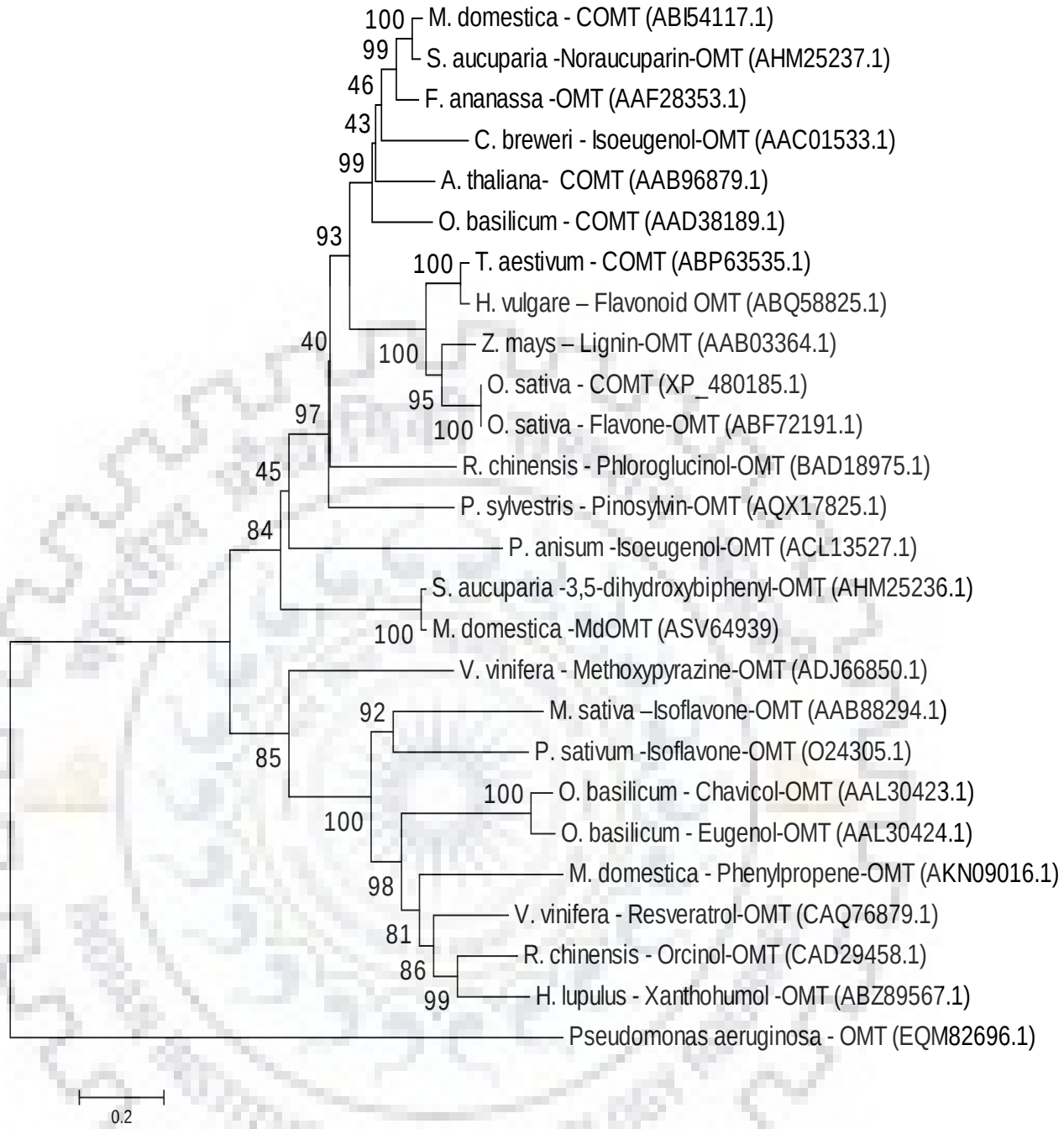

Figure 3.28: Neighbor-joining tree showing the phylogenetic relationships between MdOMT and other plant OMTs involved in secondary metabolism. Numbers at the branch points are bootstrap values arising from 1,000 replicates and Poisson correction. The scale bar = 0.2 amino acid substitutions per site. The accession numbers of the amino acid sequences included are listed in Supplemental Table S3. *Pseudomonas aeruginosa* OMT served to root the tree as out-group

3.7.4. Elicitor-induced accumulation of biphenyl and dibenzofuran phytoalexins

M. domestica cv. 'Florina' cell cultures responded to VIE-treatment with the accumulation of two biphenyl phytoalexins (noraucuparin and aucuparin) and one dibenzofuran phytoalexin (eriobofuran), as shown by HPLC analysis (Figure 3.29 A-E). The chemical identity of inducible phytoalexins was confirmed by matching retention time and UV-spectrum with those of authentic standards. The time-course accumulation patterns of these phytoalexins were shown in Figure 3.30. The accumulation of noraucuparin started 3 h after the elicitor-treatment, reached the peak at 24 h (10.8 ± 0.7 µg /g DW). After 24 h, the accumulation of noraucuparin started to decrease till 72 h. Aucuparin started to accumulate after 6h of elicitation and its value increased more or less continuously over the time course studied (12.8 ± 0.2 µg /g DW at 72h). Similar to aucuparin, dibenzofuran phytoalexin eriobofuran started to accumulate after 6 h and its value continuously increased over the time-course studied (11.4 ± 0.5 µg /g DW at 72h). Importantly, the product of *Md*OMT, 3-hydroxy-5-methoxybiphenyl, was undetectable from the VIE-treated apple cell cultures. Possibly 3-hydroxy-5-methoxybiphenyl was rapidly hydroxylated by the next enzyme biphenyl-4-hydroxylase (Sircar et al., 2015) and further metabolized into next detectable phytoalexin aucuparin and eriobofuran. When greenhouse-grown apple plants were infected with *V. inaequalis* conidia, noraucuparin, aucuparin and eriobofuran were detected in the intermodal region between two successive rows of leaves (Figure 3.31 A). Noraucuparin and aucuparin started to accumulate after 72h of conidial spray on leave, whereas eriobofuran started to accumulate after 96h (Figure 3.31 B). A more or less continuous increase in the level of all these three phytoalexins were observed over the time-course studied. Mock-inoculated plants lacked any phytoalexin accumulation. Interestingly, no biphenyl and dibenzofuran phytoalexins were detected in the leaves.

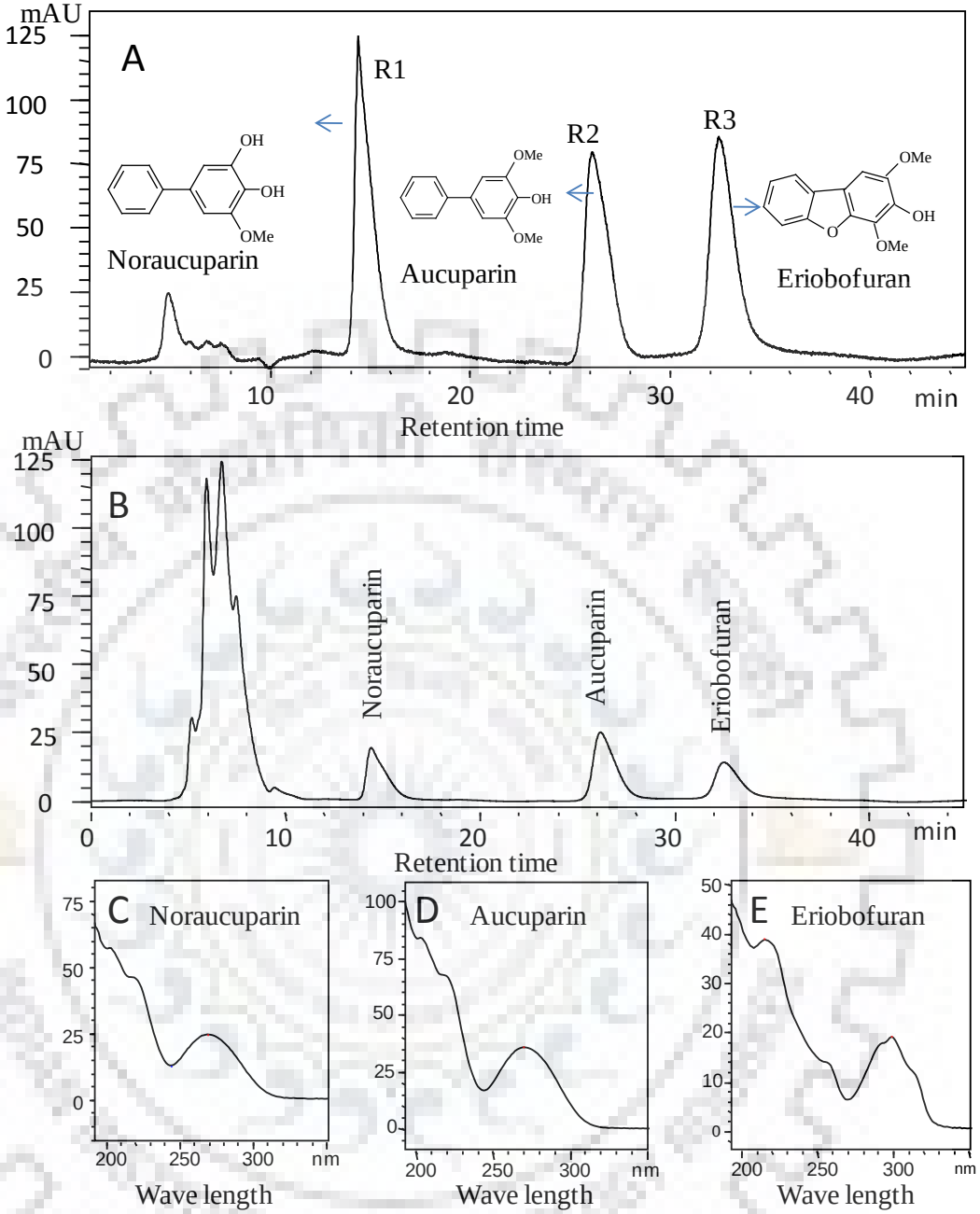

Figure 3.29: HPLC chromatogram showing accumulation of biphenyl (noraucuparin and aucuparin) and dibenzofuran (eriobofuran) phytoalexins in the VIE-treated cell culture of apple. (A) Reference compounds (R1: noraucuparin; R2: aucuparin; R3: eriobofuran); (B) phytoalexin accumulation after 48 h; (C-E) UV-spectra of noraucuparin (C); aucuparin (D); and eriobofuran (E). The chromatograms were monitored at 269 nm.

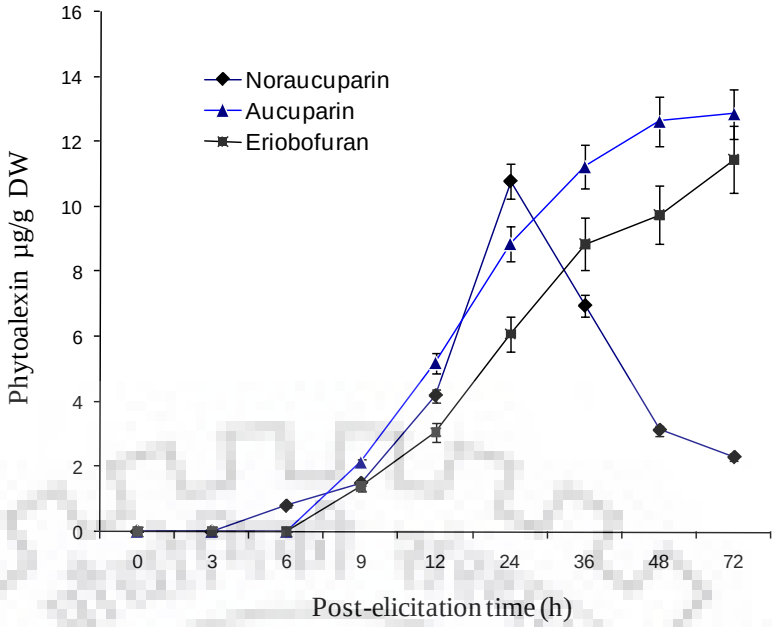

Figure 3.30: Time course accumulation of biphenyl and dibenzofuran phytoalexins in elicitor-treated cell cultures of *M. domestica*. Results are means ± SD (n = 3).

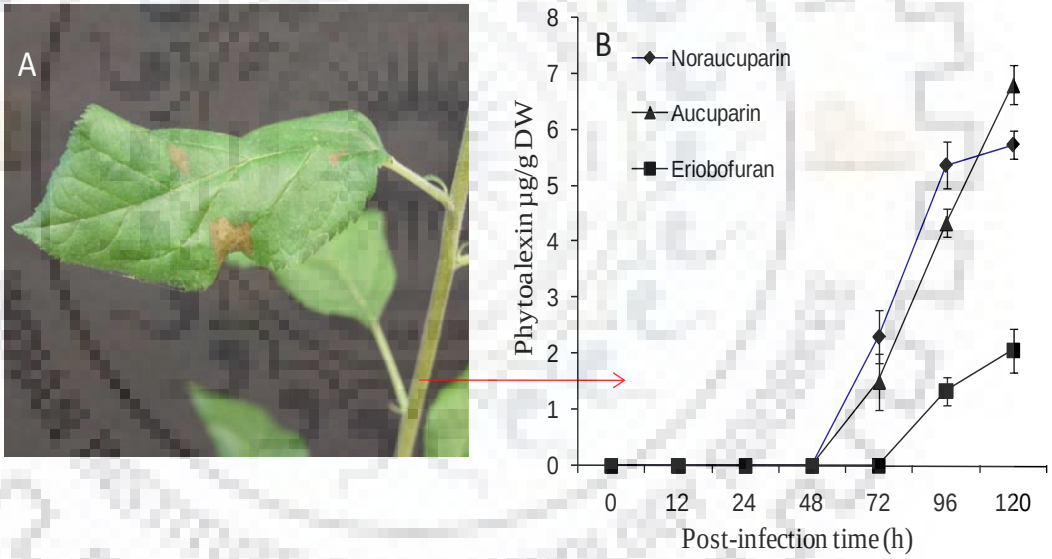

Figure 3.31: Time course accumulation of phytoalexins in the scab-infected shoots of apple. (A) Inter-nodal segment exhibiting phytoalexin accumulation after 5 days of inoculation; (B) time-course accumulation of phytoalexins from the scab infected apple shoots. Results are means ± (n = 3).

3.7.5. Expression of *MdOMT, MdPAL* and *MdBIS3*

After elicitor-treatment, transcript levels of *MdOMT, MdPAL* and *MdBIS3* in apple cell-cultures were analyzed by Real time-PCR over the time-course of 72h (Figure 3.32). In order to see the involvement of general phenylpropanoid and biphenyl biosynthesis pathway, *MdPAL* and *MdBIS3* were also selected for expression studies. Both *MdPAL* (Sircar et al. 2015) and *Md*BIS3 (Chizzali et al. 2012a) were known to be inducible. Actin mRNA served as control for equal template amounts. *Md*PAL transcripts were detectable as early as 0.5 h after the onset of elicitation. The mRNA level peaked at 1.5 h and decreased thereafter slowly. Similar expression pattern were observed for the BIS3 transcript level which, however, increased more slowly before reaching the maximum at 3 h. The expression of *Md*OMT mRNA followed alike the pattern of *Md*BIS3, however expression level was relatively less. Significantly faster increase was observed for the PAL mRNA level which already peaked after 1 - 2 h and returned rapidly to the basal *PAL* expression level that was present at the onset of elicitation. The expression of *MdOMT, MdPAL* and *MdBIS3* preceded the accumulation of noraucuparin, aucuparin and eriobofuran, suggesting involvement of these genes in biphenyl/dibenzofuran phytoalexin biosynthesis in apple.

Infection with the conidiospores of *V. inaquelis* did not show any visible symptoms on the leaves of greenhouse grown apple plants till 16 days after infection. In few leaves, a minor scab symptoms appeared 16 day post infection (Figure 3.33). This is possibly due to scab-resistance of 'Florina' cultivar used in this experiment. *MdOMT* expression in *V. inaquelis* -infected stems of cv. 'Florina' was measured in relation to that observed in mock-inoculated control stems (internodes) over the time-course of 72 h. The *Md*OMT transcript level in the internodal segment was approximately 880-fold higher in comparison to the mock-inoculated control shoots (Figure 3.34).

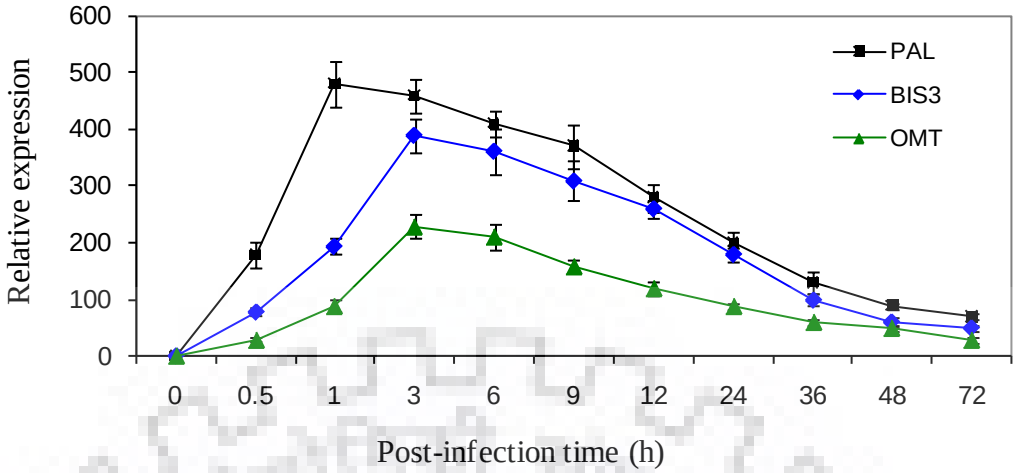

Figure 3.32: Changes in the *MdPAL*, *MdBIS3* and *MdOMT* expression levels in *V. inaequalis* elicitor-treated apple cell cultures. The relative transcript levels were determined by real-time-PCR. Results are means ± SD (n = 3).

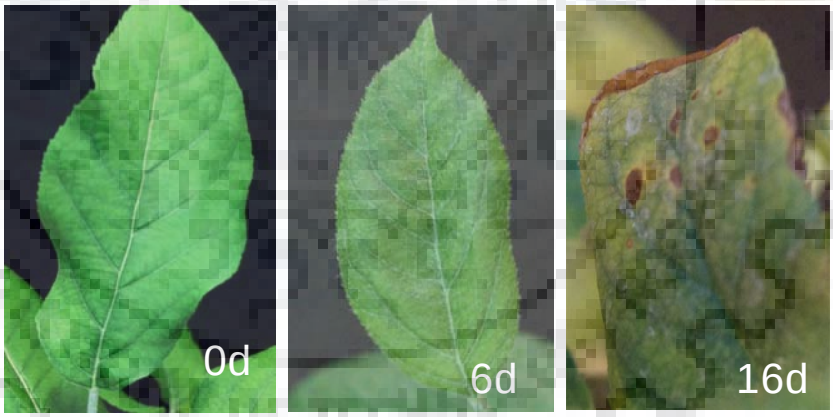

Figure 3.33: Progression of scab symptoms in *V. inaequalis* infected leaves of apple cv. 'Florina'.

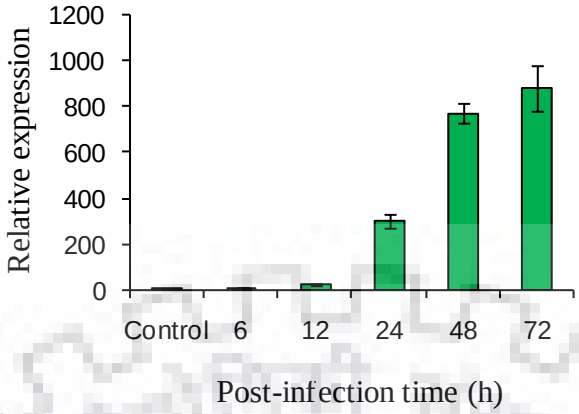

Figure 3.34: *Md*OMT expression levels in scab-infected plants of cv 'Florina'. Quantitative real-time PCR was used to determine *Md*OMT expression levels at various time points from internodal segment of scab-inoculated apple plants. Control mRNA was obtained at day zero from stem segments of mock-inoculated shoots. SD values are indicated (n = 3).

3.7.6. Subcellular localization of *Md*OMT reporter fusions

To ascertain the sub-cellular localization of *Md*OMT protein, constructs encoding fusion proteins of *Md*OMT with yellow fluorescent protein (YFP) were generated and transiently expressed in the *N. benthamiana* leaf epidermal cells. The *Md*OMT coding sequence was fused with YFP at either the N-terminus (YFP-*Md*OMT) or the C-terminus (*Md*OMT-DEL-YFP). In case of C-terminus fusion the stop codon being deleted from the *Md*OMT sequence. All constructs were driven under the control of the 35S promoter derived from Cauliflower mosaic virus. The products of the constructs were localized by confocal laser scanning microscopy. For both YFP-*Md*OMT and *Md*OMT-DEL-YFP, fluorescence was present throughout the cytoplasm suggesting cytoplasmic localization (Figure 3.35). The lambda mode was used to detect the spectral signatures of YFP, and chlorophyll, with peaks at, 525, and 680 nm, respectively

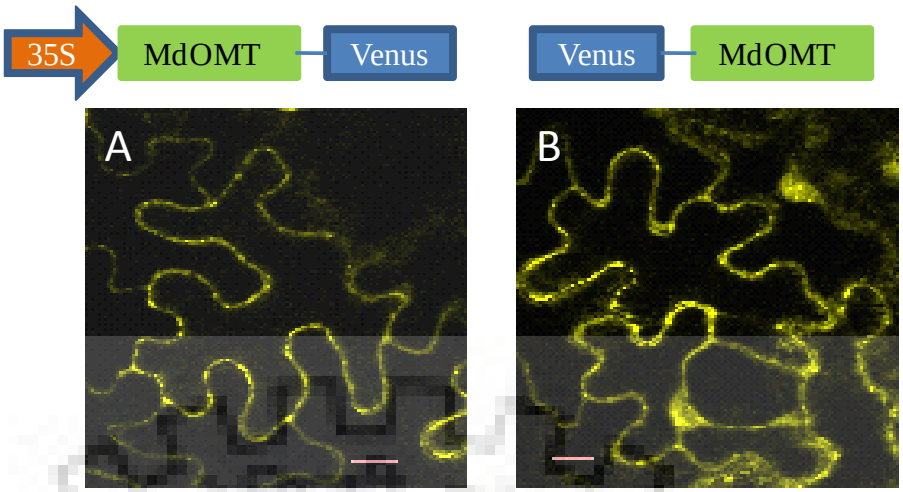

Figure 3.35: Sub-cellular localization of *Md*OMT reporter fusions in *N. benthamiana* leaf epidermis cells exhibiting cytoplasmic localization. (A) Transient expression of the *Md*OMT-Venus construct; (B) Transient expression of the Venus-*Md*OMT construct. In both cases fluorescence was observed in the cytoplasm. Bars =10 µm.

Chapter 4

Discussion

4. General Discussion

As described in the Introduction section, apple is one of the most important fruit crop growing mainly in the temperate region of the world with global production of approximately 84.6 million tonnes per year. In orchards, apple trees are mostly propagated by clonal propagation of single tree, thereby bringing genetic uniformity within the population, which adversely affect plant's pathogen resistance potential (Gessler and Patocchi, 2007). The most serious apple disease is apple scab, caused by the ascomyceteous fungus *Venturia inaequalis* (Jha et al., 2009). Most of the commercial apple cultivars, generally growing in humid region are susceptible to scab disease, which results into severe loss in apple production. The current practice of apple scab management uses huge amount of fungicides spay, which causes toxic effect to human health and environment. Furthermore, the use of multiple fungicide spray alone is not sufficient to completely control scab disease. Thereby, breeding of scab-resistant apple plant is considered as the most feasible and economical approach to manage the scab disease and its adverse impacts. Apart of existing scab resistant genes (*Rvi1*-*Rvi17*), there is an urgent need for searching new scab-resistance gene in apple to provide durable resistance. Interestingly, scab-resistant apple cultivars also have evolved diverse endogenous mechanisms to cope-up with the scab-fungus infection including production of specialized class of phytoalexins, biphenyl and dibenzofurans (Kokubun and Harborne, 1994) and several phenolics (Veberic et al., 2008; Mikulic-Petkovsek et al., 2009). However, systematic understanding the disease resistance mechanism in apples and identifying the defense-responsive metabolite(s) underlying scab-resistance are elusive and offers and area of considerable research interest. Based on the objectives and results, discussion section is sub-divided into following four sections.

4.1. Antioxidant and anticancer activity of bioactive phenolic metabolites isolated from the yeast-extract treated cell culture of apple.

The first aim of this doctoral thesis work was to develop cell suspension culture of scab resistant apple cultivar cv. 'Florina' and to investigate the antioxidant and anticancer activity of bioactive phenolic metabolites isolated from the yeast-extract elicitor-treated cell culture of apple. Plant cell suspension cultures offer excellent alternative for large scale production of biologically active secondary metabolites (Sarfaraj Hussain et al., 2012). Moreover, plant cell culture could potentially produce novel secondary metabolites possessing biological activities which cannot be produced by chemical synthesis (Siahsar et al., 2011). This approach provides several advantages such as little or no seasonal variation, high yield of metabolites and less production time. In this study, growth of cell suspension culture in liquid LS-medium showed best result with 2 µM 2,4-D and 1 µM NAA. Addition of kinetin in cell suspension culture showed cell clumping, thereby kinetin was removed. Although there are a few studies on callus induction in apple (Hrazdina et al., 1997; Kumar et al., 2016), no previous report on detailed characterization of callus induction in terms of frequency and biomass are available. (Hrazdina et al., 1997) reported that callus induction in McIntosh and Liberty cultivar requires 2, 4-D, indole-3-butyric acid and kinetin in MS medium. The differential response of different cultivars of the same species towards callus induction may be due to their selective physiological and biochemical response potential towards growth regulators. Callus induction and growth usually depends on the plant genotype, nature of explant, in vitro growth conditions and optimal concentration of growth regulators (Mathur and Shekhawat, 2013).

Yeast-extract-treatment caused enhancement of phenolics acid biosynthesis in the cell culture of 'Florina'. Phenolic acids and flavonoids are ubiquitous compounds in plants, which are known to possess several biological properties such as antioxidant, anti-proliferative, anti-cancer activities (Kumar et al., 2016). Phenolic acids, especially benzoic and cinnamic acid derivatives possess various biological activities such as antioxidant, anticancer activities (Sanchez-Maldonado et al., 2011). Phenolic acids also protects against oxidative stress arising from the damaging effect of reactive oxygen species (Khanizadeh et al., 2008). Elicitation of plant cell culture is an excellent strategy for enhanced accumulation of bioactive secondary metabolites in relatively short time (Sarfaraj Hussain et al., 2012). Among biotic elicitors, yeast extract is well known for triggering phenolic acid biosynthesis (Cai et al., 2014). Presence of chlorogenic acid, catechin, epicatechin, rutin, floridzin, Quercetin-3-rhamnoside, Avicularin was previously reported in the leaves of different apple cultivars (Petkovsek et al., 2010**;**

Liaudanskas et al., 2014). Other studies on the composition and content of phenolic compounds in apple leaves were conducted in relation to scab infections in the apple tree. However, biosynthetic potential of apple cultivar 'Florina' has never been tested in terms of bioactive phenolic metabolites. Yeast-extract elicitor used in our study represented effective elicitor for phenolics biosynthesis in the cell culture of 'Florina' cultivar of apple. Elicited apple cell culture might be an excellent production platform for high value phenolics such as catechin, rutin, chlorogenic acid etc. The advantages of using yeast extract elicitor, is low price and easy preparation procedure.

In this study, enhanced PAL activity precedes phenolic accumulation suggesting PAL-mediated biosynthesis of phenolics upon elicitor treatment. Being the first enzyme of phenylpropanoid biosynthesis, PAL activity is up-regulated by elicitor treatment, which in turn accelerates phenolics biosynthesis. This is in agreement with the previous finding, where yeast extract elicitor triggered enlistment in PAL activity in *Hypericum calycinum* cell culture directing towards enhanced xanthone biosynthesis (Gaid et al., 2012).

Furthermore as shown in the result section, the growth of both breast and cervical cancer cells were inhibited by elicited extract. The anti-proliferative activity was expressed as IC_{50} values. The enhanced accumulation of phenolics, especially rutin, could be a probable reason for higher cytotoxicity by elicited cells. Further, our results clearly demonstrated that the phenolic metabolites from elicited cell culture of apple cultivar 'Florina' had wide *in vitro* cytotoxicity, i.e., active against both cervical and breast cancer cell lines. Previously, anticancer activities from dried fruit extracts of Red Delicious, Fuji, Golden Delicious, and Granny smith apple cultivars against MDA-MB-468 human breast cancer cell line was reported (Thompson et al., 2009). This differential activity could be attributed to the activation of cell specific targets by different bioactive metabolites present in the extracts as tested (Sak, 2014; Tiwary et al., 2015). When MCF-7 and HeLa cells were treated with elicited extract at a concentration equivalent to IC50 values, clear apoptosis was observed after 24 h of incubation. AO/EB dual staining served the purpose of measuring apoptosis. Since AO permeated all cells, the nuclei appeared green in vehicle treated MCF-7 and HeLa cells. EB is taken up by the cells only when the cytoplasmic membrane integrity is lost and served as the marker for late apoptosis (Figure 3.7). Further research is needed to delineate the specific metabolites or metabolite combinations (synergistic effect) that are responsible for the cytotoxic effects as shown by elicited extract and analyzing the underlying mechanism of actions.

4.2. GC-MS based untargeted metabolomics of apple cell cultures treated with *Venturia inaequalis* elicitor

The second aim of this doctoral thesis work was to perform comparative metabolomics of Venturia inaequalis elicitor (VIE)-treated cell cultures of apple cv. 'Florina', to identify the scab-induced differentially accumulating metabolites, which could serve as metabolite marker for scab resistance. In this study, the effect of VIE-treatment on the metabolite profile of apple cv. 'Florina' cell suspension culture using GC-MS based metabolomics combined with multivariate data analysis such as principal component analysis (PCA) and partial least square–discriminant analysis (PLS-DA) were analyzed. Furthermore, to reveal the integrative biochemical networks of the apple cell culture in response to VIE-treatment, the metabolomic data were integrated with the expression data of selected secondary metabolite biosynthetic genes, which provided a more generalized view of the metabolite and molecular changes elicited by scab elicitor. As elicitors can mimic the pathogenesis related symptoms by triggering similar biochemical reactions as induced by original pathogen infection, elicitor-induced lant cell suspension culture offers a promising alternative system to study conventional pathogen interaction at biochemical and molecular levels (Bektas and Eulgem, 2014; Fan et al., 2009).

In this study, a rapid break down of sucrose was observed in the VIE-treated cell culture. This indicates that sucrose catabolism was higher in VIE-treated cell culture. Likewise, high glucose and fructose levels were probably due to rapid break-down of sucrose upon elicitation. Conversion of fructose to mannose was up-regulated in VIE-treated cells, resulting into higher mannose accumulation. Concerning organic acid accumulation, it was hypothesized that, high organic acid accumulation after VIE-treatment was probably due to higher turnover number of glycolysis and TCA cycle which generated more abundant intermediate. High organic acid concentration facilitates better ion absorption and thereby known to be associated with higher disease resistance (Hudina and Štampar, 2000). After VIE-treatemnt ascorbic acid level found to be up-regulated. Ascorbic acid is known to be associated with the enhanced defense responses in many plant species (Pastori et al., 2003; Jain, 2015) . High ascorbic acid might attribure greater tolerance to scab infection in resistant apple cultivar 'Florina'. As shown in result section, VIE-treatment leads to the up-regulation of phenolcis. The content of these phenolics were first up-regulated after VIE-treatment and thereafter declined to the basal level. Similar array of polyphenol compositions were previously detected in the leaves of Florina apple (Picinelli et al., 1995). However, in contrary to previous report, quercetin and avicularin

has not been detected from VIE-treated 'Florina' cell cultures. The phenolics acids and their derivatives are known to oxidize proteins, thereby inhibiting important enzyme functions of pathogen and restricting the disease progression. Phenolics also deposited along the cell wall and provide first line of defense against infection (Mikulic Petkovsek et al., 2008; Schwalb and Feucht, 1999).

Earlier it has been shown that differential accumulation of flavonols (catechins and proanthocyanidins) was key factors in providing scab resistance in apple cultivars (Treutter and Feucht, 1990; Picinelli et al., 1995 Mayr et al. 1997) have shown a positive association between procyanidins content and scab resistance in apple. In contrary, Sierotzki and Gessler (1993) have shown that there was no positive correlation between scab-resistance and basal level of flavonols in terms of scab susceptibility of apples. In our study, high basal level of catechin (flavonol) content was also observed in the 'Florina' cell culture. It was also reported that scab-resistant apple cultivars are particularly rich in the content of caffeic, chlorogenic, and ferulic acids and their concentration rapidly increases after scab-infection as compared to susceptible cultivars (Mikulic Petkovsˇek et al., 2003; Treutter, 2005). Furthermore, Liaudanskas et al., (2014) had shown that high phenolic content of scab-resistant apple is associated with higher nutritional quality and antioxidant properties. In this study a rapid enhancement of benzoic acid was observed after VIE-treatment. However, formation of benzoyl-CoA may take place using benoztae-CoA-ligase (Beuerle and Pichersky, 002; Ibdah and Pichersky, 2009), or using cinnamate-CoA-ligase route. It was know that benzoic acid serves as the precursor for biphenyl and dibenzofuran class of phytoalexins of apple and other members of Malinae (Hrazdina et al., 1997; Chizzali et al., 2012, 2016; Saini et al., 2017). Upon scab-infection, benzoic acid forms benzoyl-CoA, which combines with malonyl-CoA to produce 3,5-dihydroxybiphenyl, the precursor for all other biphenyl and dibenzofurans. Enhanced biosynthesis of benzoic acid in VIE-treated apple cells might attribute its higher resistance against scab fungus *V. inaequalis* and *E. amylovora* (Chizzali et al., 2012) by fascilitating rapid formation of bipehnyl phytoalexins upon pathogen attack. Likewise, high basal level of catechin is known to confers resistance against fungal infection (Amil-Ruiz et al., 2011). Earlier it has been shown that strawberry plant bearing high catechin content exhibit powerful resistance against *Botrytis cinerea* and *Alternaria alternata* (Hébert et al., 2002). Equally, high content of chlorogenic, caffeic and protocatechuic acids are also known to be associated with enhanced resistance towards fungal infection (Mikulic Petkovsek et al., 2008; Mandal, 2010). In our study, enhanced accumulation of chlorogenic, caffeic and protocatechuic acids in apple cell cultures probably attribute strong resistance against scab infection in apple cultivar cv. 'Florina'. *Trans*-

cinnamic acid serves as the precursor of many defense metabolites, such as phenylpropanoids, benzoic acid, lignans, and flavonoids (Gaid et al., 2012). Earlier it has been shown that aucuparin and nor-aucuparin phytoalexins biosynthesis in other members of Malinae such as in pear and *Sorbus aucuparia* are derived from benzoic acid. Benzoic acid in turn derived from benzaldehyde, and benzaldehyde is likely to be derived from *trans*-cinnamic acid through propyl-side-chain shortening, as demonstrated before in hairy roots of *Daucus carota* (Sircar and Mitra, 2008), *Vanilla planifolia* (Gallage et al., 2014; Podstolski et al., 2002). Upon VIE-treatment, up-regulation of *trans*-cinnamic acid biosynthesis in apple cell cultures thereby explains the reason underlying enhanced benzoic acid accumulation. It was worth speculating that after scab-infection, benzoic acid is further converted into biphenyl –dibenzofuran phytoalexins, which confers next level of resistance against scab-infection. Notably, peak of cinnamic acid accumulation precedes the peak of biphenyl and dibenzofuran phytoalexin accumulation in apple cell culture, suggesting a biogenic relationship. In this study, an enhanced biosynthesis of *p*-coumaric acid was observed in VIE-treated cell cultures. High level of *p*-coumaric acid is linked with synthesis of flavonoids. Accordingly, the peak of *p*-coumaric acid precedes the peak of catechin and rutin formation in VIE-treated apple cell cultures. Furthermore, a considerable up-regulation of salicylic acid (SA) biosynthesis was observed in VIE-treated apple cell. SA can induce local resistance in form of hypersensitive reaction or long distance systemic acquired resistance (SAR) by triggering the production of pathogenesis-related proteins (PR proteins) (Vasyukova and Ozeretskovskaya, 2007). Both HR and SAR reactions are linked with the biosynthesis of SA at the infection site or in the systemic parts of the plant. The crucial role of SA as signaling molecule in plant defense response is well established (Vlot et al., 2009). Nevertheless, in addition to pathogen-induced SA accumulation, a constitutive SA production is also detected in many plant species. Under stress conditions, apple plants are known to produce enhanced levels of salicylic acid (SA) (Wang et al., 2016). Furthermore, external SA application in apple plants showed enhanced resistance towards *Glomerella* leaf spot disease. Probably, enhancement of SA biosynthesis in our study is linked with higher scab-resistance in apple cv. 'Florina'. VIE-treatment to apple cell culture led to production of aucuparin, noraucuparin and eriobofuran, the marker phytoalexins of Malinae (Chizzali and Beerhues, 2012). It has been shown that biphenyl and dibenzofuran phytoalexin can efficiently inhibit the growth of *Venturia inaequalis* and *E. amylovora* (Chizzali et al., 2012). Interestingly, in our study, biphenyl and dibenzofuran phytoalexins were absent from the control cells and only formed after VIE-treatment. Notably, malusfuran (2,4-methoxy- 3-hydroxy-9-*O*-b-D-glucosyloxydibenzofuran), a glucosylated dibenzofuran detected earlier from

the elicited cell culture of apple cv. Liberty, has not been detected in this study, however, free dibenzofuran eriobofuran was detected. Glucosylated dibenzofurans are possibly broken down to give free dibenzofuran such as eriobofuran upon pathogen infection (Lattanzio et al., 2001).

Furthermore, the hierarchical clustering offered excellent separation of the metabolite trend between the non-elicited (0h) and VIE-treated (6-72h). VIE-treated cells were the major source of variance in the result, which indicated that change in metabolite concentration by VIE-treatment. When metabolic pathway network was considered, the significant different components in VIE-treated cells were, aspartic acid, pyruvic acid, 3-phosphoglyceric acid, citric acid, fumaric acid, succinic acid, Malic acid, aucuparin, noraucuparin, eriobofuran, benzoic acid, chlorogenic acid, protocatechuic acid, caffeic acid, *p*-coumaric acid, *trans*-cinnamic acid, catechin, glucose, mannose, sorbitol, and fumaric acid.

Gene expression data has shown that the expression levels of all the four genes studied were up-regulated upon VIE-treatment demonstrating that phenylpropanoid and biphenyl biosynthesis was triggered by the VIE-treatment. These gene expression data were well correlated with the enhanced accumulation of phenylpropanoids such as cinnamic acid, flavonoids and biphenyls in the elicited cell cultures of apple. Enhanced expression of *PAL* gene is known to be associated with increase in the phenylpropanoid biosynthesis (Gaid et al., 2012; Mukherjee et al., 2016). Likewise, high *F3H* expression is associated with higher accumulation of catechin. High *AOX* expression level in the VIE-treated cells is probably associated with the enhanced biosynthesis of phenylpropanoids. Previously, it was demonstrated that AOX expression is linked with high phenylpropanoid biosynthesis in many plant species (Arnholdt-Schmitt et al., 2006; Campos et al., 2016). High AOX expression level is known to be associated with the plant's ability to facilitate metabolic re-programming to cope up with the stressed conditions (Arnholdt-Schmitt et al., 2006; Costa et al., 2009; Costa and Arnholdt-Schmitt., 2017). Similar to PAL, a rapid up-regulation of BIS3 expression was observed. The expression of *MdPAL* and *MdBIS3* preceded the accumulation of noraucuparin, aucuparin and eriobofuran, suggesting involvement of these genes in biphenyl/dibenzofuran phytoalexin biosynthesis in apple. MdBIS3 is known to be the main BIS isoenzyme responsible for phytoalexin biosynthesis in apple shoots (Chizzali et al., 2012).

4.3. Salicylaldehyde synthase (SAS) activity from *Venturia inaequalis* elicitor-treated cell culture of apple

The third aim of this doctoral thesis work was to detect and characterize salicylaldehyde synthase (SAS) activity from the elicited cell culture of apple cv. 'Florina'. This study is the first report of a putative C_2-side chain cleavage enzyme activity from VIE-treated cell culture of apple that efficiently converts *2*-coumaric acid to salicylaldehyde *in vitro*, suggesting salicylaldehyde synthase (SAS) activity. The mechanism of the C_2 side chain cleavage was non-*β*-oxidative, which proceeds without the requirement of ATP and coenzyme A. This C_2-chain cleavage from phenylpropanoid backbone probably involves hydrolyase activity to eliminate the C_2-side chain from *2*-coumaric acid to yield salicylaldehyde with intermediate formation of 2-hydroxyphenyl-β-hydroxypropionic acid (Figure. 4.1), as suggested by (Podstolski et al., 2002). So far, such non-β oxidative C_2 chain cleavage activity has been poorly characterized in plants. Previous research indicated that SAS activity was observed during SA biosynthesis in tobacco mosaic virus (TMV)-infected *N. tabacum* (Malinowski et al., 2007). A similar mechanism of C_2-side chain shortening was previously shown to be mediated by 4-hydroxybenzaldehyde synthase (HBS) activity that catalyzes the formation of 4-hydroxybenzaldehyde from 4-coumaric acid in potato tubers (French et al., 1976), cell cultures of *Lithospermum erythrorhizon* (Yazaki et al., 1991) hairy roots of *Daucus carota* (Schnitzler et al., 1992; Sircar and Mitra, 2008) and *V. planifolia* cell cultures (Podstolski et al., 2002). However, except for the hairy roots of *Daucus carota*, the chain-cleavage enzyme was reported to be unstable. Similar to the SAS activity in tobacco (Malinowski et al., 2007) the SAS from apple cell culture was also found to be strictly dependent on the presence of a reducing agent. In both cases, 10 mM cysteine showed maximal SAS activity. In contrast, HBS activity in *D. carota* preferred dithiothreitol (DTT) as its reducing agent. In *V. planifolia*, HBS showed the highest activity in the presence of CoA (10 mM) and the lowest with cysteine (10 mM). The best substrate for the apple SAS was 2-coumaric acid, followed by 4-coumaric acid and *trans*-cinnamic acid. This strict substrate specificity of apple SAS distinguishes it from the tobacco SAS where no strict substrate specificity was observed (Malinowski et al., 2007). However, HBS activity from *V. planifolia* showed distinct substrate specificity with 4-coumaric acid as the preferred substrate (Podstolski et al., 2002). Similarly, to tobacco SAS and vanilla HBS, apple SAS did not show any activity with caffeic, ferulic and sinapic acids. Recently, a cDNA for the vanillin synthase gene (*VpVAN*) was cloned and functionally characterized from *V. planifolia* that participates in vanillin biosynthesis by converting ferulic acid to vanillin using a similar non-β-oxidative C_2-chain cleavage mechanism (Gallage et al., 2014) without the requirement for ATP and NAD. The best

substrate for VpVAN was ferulic acid. No activity was detected with 4-coumaric acid or caffeic acid. The apparent *K*m value for apple SAS (0.35 ± 0.04 mM) was less than that of tobacco SAS (0.625 mM) (Malinowski et al., 2007), which suggests better affinity towards *2*-coumaric acid compared to tobacco SAS. Notably, in comparison to other plant benzoate biosynthetic enzymes, the *K*m value determined for apple SAS is usually high (Gaid et al., 2009; Saini et al., 2017). This issue could be better addressed in the future through attempts to clone and purify recombinant SAS from apple. Our purification results indicate that the 52 kDa band obtained during the purification process correlate with the SAS activity. It might be possible that the SAS enzyme studied is the most abundant protein even in elicited crude extracts, thus giving a thick band (52 kDa) even after moderate 4.2-fold purification using the DEAE-Sepharose purification step. However, whether this 52 kDa protein does correspond to actual SAS activity could be better addressed in future studies using recombinant SAS protein.

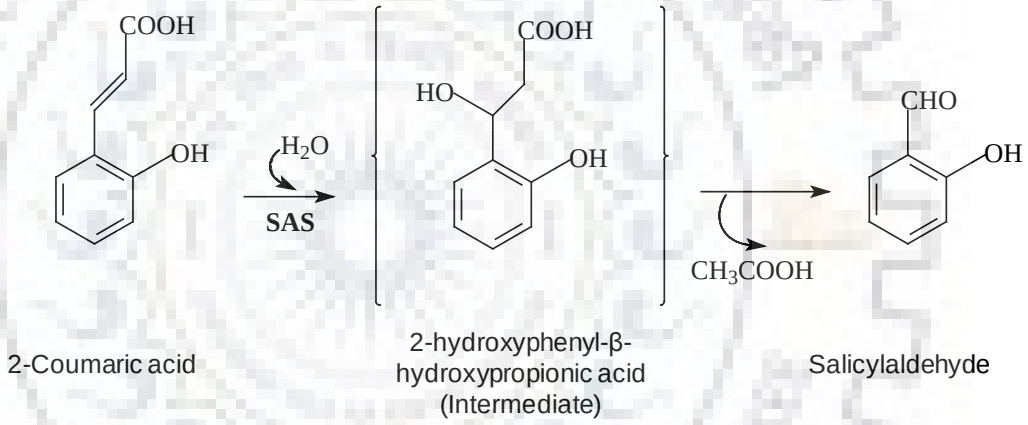

Figure 4.1: Salicylaldehyde synthase (SAS)-catalyzed formation of salicylaldehyde from 2-coumaric acid involving non-*β*-oxidative C_2-side chain cleavage.

Elicitor treatment induced a rapid increase in the PAL activity that precedes the peak of SAS activity. Since it is the first enzyme of the phenylpropanoid pathway, PAL activity needs to be increased to supply substrates for downstream metabolic pathways, as observed in many elicitor-treated plant biosynthetic pathways (Abd El-Mawla and Beerhues, 2002; Ogata et al., 2004). PAL and SAS activities were coordinately induced by elicitor treatment, suggesting that SA biosynthesis in apple cell culture could originate from phenylpropanoid pathways. A similar induction pattern for PAL was also reported for benzoic acid biosynthesis in *Hypericum androsaemum* and *Pyrus pyrifolia* cell cultures (Abd El-Mawla and Beerhues, 2002; Saini et al., 2017).

Interestingly, we observed a 1.8-fold increase in SA content when elicited cell cultures were fed with 2-coumaric acid with a minor accumulation of salicylaldehyde, which suggests that salicylaldehyde could be an intermediate in SA biosynthesis. The activity of a dehydrogenase is required to convert salicylaldehyde into SA, as reported before in studies of 4-hydroxybenzoic acid formation in *D. carota* (Schnitzler et al., 1992; Sircar and Mitra, 2008) and benzoic acid formation in apple (Saini et al., 2017). However, such dehydrogenase activity was not detected in our experiment, which questions whether salicylaldehyde participates in SA biosynthesis. Earlier experiments of (Yalpani et al., 1993) raise the possibility of 2-coumaric acid as a substrate for SA biosynthesis. However, experiments with *nahG* plants showed that the exogenous application of salicylaldehyde could enhance the SA content (Malinowski et al., 2007). It is possible that multiple pathways exist in a single plant for SA biosynthesis. In *Arabidopsis*, the existence of both isochorismate and phenylpropanoid pathway have been reported (Wildermuth et al., 2001). In apple, no ICS gene function contributing SA biosynthesis had been reported, suggesting the origin of SA, at least partially, from the phenylpropanoid pathway. The origin of 2-coumaric acid in apple remains elusive. One possibility is that the 2-hydroxylation of trans-cinnamic acid leads to the formation of 2-coumaric acid as reported in *Melilotus officinalis* (Gestetner and Conn, 1974).

4.4. Molecular cloning and functional analyses of a biphenyl phytoalexin-specific *O-methyltransferase* from apple cell suspension cultures

Members of the Rosaceae, sub-tribe Malinae, produce biphenyls and dibenzofurans phytoalexins upon pathogen infection. Aucuparin is the most abundant and commonly formed biphenyl phytoalexin in the Malinae (Chizzali and Beerhues, 2012). Till date, the biosynthesis of biphenyls and dibenzofuran, especially how dibenzofurans are formed is not well elucidated. In this study, we used cell cultures of apple cv. 'Florina', which provide an excellent model system to study phytoalexin biosynthesis due to less biosynthetic complexity (Gaid et al., 2012). Cell culture of apple cv. 'Florina' responded to *V. inaequalis* elicitor-treatment by producing two biphenyls (noraucuparin and aucuparin) and one dibenzofuran (eriobofuran) phytoalexins. Aucuparin was the most abundant phytoalexin detected in the apple cell cultures. In aucuparin the functional group substitution pattern consists of a hydroxyl group at 4-position which is flanked by two methoxy-groups at 3- and 5-positions. The 3- and 5-hydroxy groups of precursor 3,5-dihydroxybiphenyl originate from the reaction catalyzed by BIS (Chizzali et al., 2012a), the 4-hydroxy group is introduced by a CYP450 monoxygenase

biphenyl-4-hydroxylase (Sircar et al., 2015). The methoxy group at 3-position is introduced by a 3,5-dihydroxybiphenyl-*O*-methyltransferase, which here was named *Md*OMT. So far, 3,5-dihydroxybiphenyl-*O*-methyltransferase has not been cloned and functionally characterized from apple. However, in a recent study, a similar 3,5-dihydroxybiphenyl-*O*-methyltransferase (*Sa*OMT1; AHM25236.1) has been cloned and functionally characterized from elicitor-treated cell cultures of rowan (*S. aucuparia*; Khalil et al., 2015). At amino acid level, *Md*OMT shares 93% homology with *Sa*OMT1, 50.4% with *Sa*OMT2 (Noraucuparin OMT; AHM25237.1), 47.1% similarity with pinosylvin OMT (AQX17125.1) and 30.1% similarity with resveratrol OMT (CAQ76879.1).

*Md*OMT converts 3,5-dihydroxybiphenyl into 3-hydroxy-5-methoxybiphenyl (Figure 4.2), which was then taken up by B4H and converted into noraucuparin. Recently B4H enzyme has been characterized at biochemical level from *S. aucuparina* (Khalil et al., 2013) and a B4H cDNA has been cloned from Sorbus and Malus cv. Golden Delicious (Sircar et al., 2015). Noraucuparin is then converted into aucuparin by a noraucuparin-*O*-methyltransferase (Khalil et al., 2015).

*Md*OMT exhibits almost absolute specificity for 3, 5-dihydroxybiphenyl. However, the product of *Md*OMT (3-hydroxy-5-methoxybiphenyl) has not been detected at metabolite level from the elicited apple cell cultures. Possibly 3-hydroxy-5-methoxybiphenyl, the product of *Md*OMT, is rapidly hydroxylated by B4H to give noraucuaprin, the first detectable biphenyl phytoalexin from apple cell culture. The accumulation of aucuparin was preceded by the noraucuparin accumulation suggesting that noraucuparin is the precursor for aucuparin biosynthesis. Notably, unlike *S. aucuparia* cell culture (Khalil et al., 2015), noreriobofuran has not been detected from the apple cell cultures. Interestingly, 3,5-dihydroxybiphenyl, the preferred substrate for *Md*OMT, bears two hydroxyl groups at 3- and 5- positions for potential sequential methylations by OMT, however, only hydroxyl group at 5-positon undergoes regioselective methylation by *Md*OMT leading to the formation of 3-hydroxy-5-methoxybiphenyl. Similar selective methylation was exhibited before by *Sa*OMT1 and pinosylvin OMT (POMT). However, in contrast to POMT, which catalyzes methylation of a wide range of substrates (phenylpropanoids, stilbenes, flavonoids, coumarins; Chiron et al., 2000), *Md*OMT performs regioselective methyaltion of 3,5-dihydroxybiphenyl. *Md*OMT does not accept stilbene, such as pinosylvin, which have an additional double bond, and one-ring compounds. Nor does the enzyme convert cinnamic acid derivatives, such as caffeic acid and 5-hydroxycaffeic acid,

which are involved in lignin biosynthesis. In a phylogenetic tree, *Md*OMT is closest to isoeugenol OMT and pinosylvin OMTs, which catalyze formation of isoeugenol and stilbene (Chiron et al., 2000), respectively.

Figure 4.2: Proposed pathway of *MdOMT* catalyzed biphenyl and dibenzofuran biosynthesis in apple. Dashed arrow indicates non-established reactions in apple.

Gene expression analyses showed that *MdOMT* expression precedes the accumulation of noraucuparin and aucuparin suggesting its involvement in the biphenyl biosynthetic pathway. Expression profile of *MdOMT* and *biphenyl synthase gene 3* (*MdBIS3*) showed similar induction pattern, however *MdBIS3* expression level was higher than that of *MdOMT*. MdBIS3 is known to be the main BIS isoenzyme responsible for phytoalexin biosynthesis in

apple shoots (Chizzali et al., 2012a). Biphenyls and dibenzofurans are derived from benzoic acid, biosynthesis of which stem from the general phenylpropanoid pathway, initiated by PAL. Interestingly, the expression level of phenylalanine ammonia-lyase (*Md*PAL) precedes the expression of *Md*OMT and *Md*BIS. The fast increase in the *MdPAL* transcript level in *V.* inaequalis-treated apple cell cultures indicates rapid redirection of carbon flow from primary to secondary metabolism. A cDNAs encoding cinnamate: CoA ligase from *Hypericum calycinum* and *Petunia hybrida* were cloned and functionally characterized (Gaid et al., 2012; Klempien et al., 2012), which channels the metabolic flux from the general phenylpropanoid pathway to benzoyl-CoA biosynthesis and further to aucuparin biosynthesis. In apple cell cultures, aucuparin accumulation starts 9 h after the elicitor-treatment which is preceded by a fast increase in the PAL transcript level followed by OMT and BIS3 in a coordinated fashion. Peak of *MdOMT* expression (3 h) was slightly earlier than the peak expression reported for B4H 4-5 h; (Sircar et al., 2015). A similar gene expression pattern was observed for *SaOMT1* and *SaBIS3* before in rowan cell cultures (Khalil et al., 2015).

Starting from benzoyl-CoA, biphenyl aucuparin and noraucuparin biosynthesis is initiated by BIS (Chizzali et al., 2012a). In apples, upon fire blight or scab infection, biphenyl and dibenzofuran phytoalexins are accumulated in the transition zone in the stem, and not in the leaves (Hrazdina and Borejsza-Wysocki, 2003; Chizzali et al., 2012b; Sircar et al., 2015). In apple, *BIS* is represented by a gene family consisting of four differentially regulated subfamilies (Chizzali et al., 2012a). *BIS3* is expressed in stems upon fire blight infection. Infection of the greenhouse-grown apple shoots of scab-resistant cultivar 'Florina' with *V. inaequalis* conidia leads to formation of very minor scab symptoms after 16 days of infection. Unlike formation of a distinct transition zone in the fire-blight infected apple stems (Chizzali et al., 2012b; Sircar et al., 2015), no transition zone was observed in 'Florina' stems after scab-infection. Earlier, approx. 4000 fold induction in the *BIS*3 transcript level was observed in the transition zone of 'Holsteiner Cox' (Chizzali et al., 2012a). Relatively less expression was found for *MdOMT* in ''Florina'' from the internodal region of the infected shoot with approx. 880-fold enhancement compared to the mock inoculated plants. The enhancement of *Md*OMT transcript level was followed by the accumulation of noraucuparin, aucuparin and eriobofuran in the internodal region. No phytoalexin was observed in the infected leaves. However, how accumulation of biphenyl and dibenzofuran in the internodal stem region prevents scab infection and disease progression in the leaves and other aerial parts of apple shoot is not well understood and warrants future research.

The sub-cellular location properties of *Md*OMT may be affected by the metabolon formation through interaction with other enzymes of the biphenyl pathway which perhaps allows for an efficient transfer of biosynthetic intermediates between the pathway enzymes (Winkel, 2004; Jørgensen et al., 2005; Kaufholdt et al., 2015; 2016). In order to check whether *Md*OMT is localized into cytoplasm or form metabolon with other biphenyl pathway enzyme, sub-cellular localization studies were performed. *Md*OMT was localized to the cytoplasm upon transient expression of N- and C- terminal reporter gene construct in *N. benthamiana* leaf epidermis cells. Immunofluorescence localization studies of *Md*BIS3 (the main BIS isoenzyme responsible for phytoalexin biosynthesis in apple shoots) in the transition zone of apple showed that the enzyme is exclusively present at the plasmodesmata junctions between neighboring cortical parenchyma cells (Chizzali et al., 2012b). In contrast, B4H protein from apple was known to be localized into endoplasmic reticulum (Sircar et al., 2015), suggesting possible interaction between the three involved enzyme. Upon scab infection in green house-grown apple plants, *Md*OMT expression was observed in the internodal stem region with subsequent accumulation of aucuparin, noraucuparin and eriobofuran. How, scab infection in the leaves triggers phytoalexin biosynthesis in the internodal region and which role these phytoalexins are actually playing to prevent scab disease progression warrants future research.

Chapter 5

Summary, Conclusion and Future scopes

5.1. Summary:

5.1.1: Antioxidant and anticancer activity of bioactive phenolic metabolites isolated from the yeast-extract treated cell culture of apple.

- Apple cell suspension culture (cv. 'Florina') was developed and treated with yeast-extract elicitor to up-regulate the biosynthesis of bioactive phenolics.
- Methanolic extract from the elicited cell culture were analyzed by high performance liquid chromatography (HPLC) for the detection and quantification free phenolic acid and flavonoid. Predominant phenolics detected in the soluble fraction were protocatechuic acid, catechin, chlorogenic acid, vanillic acid, 4-coumaric acid, ferulic acid, benzoic acid and rutin. Out of these phenolics, the content of chlorogenic acid (112 µg/g DW), 4-coumaric acid (122 µg/g DW) ferulic acid (212 µg/g DW), benzoic acid (244 µg/g DW) and rutin (348 µg/g DW) were significantly enhanced upon elicitation.
- 1, 1-diphenyl-2-picrylhydrazyl (DPPH) and ferric reducing antioxidant power (FRAP) radical scavenging activity was significantly enhanced upon yeast extract treatment, and this was positively correlated with increased accumulation of phenolic metabolites.
- Anti-cancer effect of elicited cell culture extract was evaluated against human cervical (HeLa cells) and breast (MCF-7 cells) cancer cell lines using MTT assay. Elicited extract exhibited significant apoptosis mediated anti-cancer activity against both breast (IC_{50}: 31± 3.4 µg/ml) and cervical (IC_{50}: 38 ± 3.0 µg/ml) cancer cell lines. No growth inhibition was observed with control CHO cell line. These results indicated that yeast-extract treated cell culture of apple provides a promising system for sustainable production of natural antioxidants and anticancer therapeutics.

5.1.2. GC-MS based untargeted metabolomics of apple cell cultures treated with *Venturia inaequalis* elicitor

- In this study, the metabolomics analysis of scab resistant apple cv. 'Florina' cell cultures treated with elicitor preparation from *Venturia inaequalis* has been performed using gas chromatography-mass spectrometry (GC-MS). A total 36 differentially accumulating metabolites has been identified in the elicitor-treated cells. The score plots of principal component analysis (PCA) exhibited clear discrimination between untreated and elicitor-treated samples. The metabolomics analyses indicated elicitor-treatment could cause significant alternation in the metabolite levels, mainly on sugars, amino acids and phenolic metabolites. Furthermore, three new metabolites, aucuparin, noraucuparin and eriobofuran were detected only in elicitor-treated cells.

- Alteration in the metabolite level were correlated with the up-regulation in the transcript level of *phenylalanine ammonia-lyase (MdPAL)*, *flavones-3-hydroxylase (MdF3H)*, *Alternate oxidase (MdAOX)* and *biphenyl synthase isoform 3* (*MdBIS3*) gene.

- Kyoto Encyclopedia of Genes and Genomes (KEGG) pathway analysis of integration data demonstrated the possible biosynthetic relationship between carbohydrates, amino acids, organic acids and secondary metabolites biosynthesis. These results would facilitate further understanding of the mechanisms of scab-resistance in scab-tolerant apple cultivars. Taken together, these results suggest that scab-tolerant apple cultivar 'Florina' deploy a metabolic re-programming by synthesizing an array of differentially accumulating metabolites, especially phenolics and biphenyl-dibenzofuran phytoalexins upon elicitor-treatment.

- These differentially accumulating metabolites may serve as excellent targets for designing future metabolic engineering strategies to fortify defense potential of commercially important scab-susceptible apple cultivars.

5.1.3. Salicylaldehyde synthase (SAS) activity from *Venturia inaequalis* elicitor-treated cell culture of apple

- Salicylic acid (SA) is known to trigger a number of plant defense responses upon pathogen attack. It is well known that apple (*Malus domestica*) plants respond to pathogen invasion by synthesizing SA, but its biosynthesis is not well understood. This study reports salicylaldehyde synthase (SAS) activity from *Venturia inaequalis* elicitor (VIE)-treated cell

suspension cultures of apple (*Malus domestica* 'Florina'). SAS catalyzes non-oxidative C_2-side chain cleavage of *2*-coumaric acid to form salicylaldehyde (SALD) in the presence of a reducing agent such as cysteine.

- The side chain cleavage mechanism was found to be very similar to that of salicylaldehyde synthase activity from tobacco and 4-hydroxybenzaldehyde synthase activity from *Vanilla planifolia* and *Daucus carota*. A basal SAS activity was observed in the non-elicited cell cultures, and a 7-fold increase in SAS activity was observed upon elicitation.

- In parallel to SAS activity, the level of total SA accumulation increased by 5.6-fold after elicitation compared to the untreated control cells. Elicitor treatment further resulted in an 8.7-fold increase in the activity of the phenylalanine ammonia-lyase (PAL) enzyme that preceded the peak of SAS activity and total SA accumulation, suggesting the involvement of the phenylpropanoid pathway in SA metabolism.

- The preferred substrate for SAS was *2*-coumaric acid (*K*m = 0.35 mM), with cysteine being the preferred reducing agent. In addition, a 1.8-fold enhancement in the SA content and 0.7-fold enhancement in the SALD content was observed when elicited cell cultures were fed with 2-coumaric acid.

- These observations suggest the involvement of SAS in SALD biosynthesis.

5.1.4. Molecular cloning and functional analyses of a biphenyl phytoalexin-specific *O-methyltransferase* from apple cell suspension cultures

- Upon scab-infection, apple (*Malus* spp.) and other members of subtribe Malinae of Rosaceae family accumulate phytoalexins mainly dibenzofurans in addition to aucuparin as principal biphenyl.

- Aucuparin precursor, 3,5-dihydroxybiphenyl is benzoate-derived polyketide whose biosynthesis starts with sequential condensation of three malonyl-CoA and one benzoyl-CoA molecules *via* biphenyl synthase (BIS).

- Aucuparin biosynthesis involved 5´O-methylation reaction, followed by 4-hydroxylation and the final 3´ *O*-methylation reaction of 3,5-dihydroxybiphenyl. The formation of 3-hydroxy-5-methoxybiphenyl from 3,5-dihydroxybiphenyl is catalyzed by a 3,5-dihydroxybiphenyl *O*-methyltransferase (OMT).

- A sequence encodes OMT was cloned from elicitor-treated cell suspension cultures of *Malus domestica* (*cv.* 'Florina'; *Md*OMT). The coding sequence was functionally expressed in *E. coli*. *Md*OMT catalyzed regiospecific *O*-methylation of 3,5-dihydroxybiphenyl at 5´-position. The enzyme showed absolute substrate preference for the 3,5-dihydroxybiphenyl.

- Apple cell cultures treated with elicitor prepared from *Venturia inaequalis* (scab-fungus) exhibited transient increases in the *Md*OMT, *Md*BIS3, and phenylalanine ammonia-lyase (*Md*PAL) transcript levels preceding phytoalexin accumulation. Although *Md*OMT product was not detected in the cell cultures the level of noraucuparin, aucuparin and eriobofuran were significantly uplifted upon elicitor-treatment.

- *Md*OMT fused with N- and C- terminal yellow fluorescent protein showed cytoplasmic localization in the epidermis of *Nicotiana benthamiana* leaves.

- Functional *Md*OMT coding sequence was also isolated from scab-infected apple plants of cv. 'Florina'. When greenhouse-grown plants of cv 'Florina' were infected with the scab fungus, increased *Md*OMT transcript levels was observed in the internodal region with

accumulation of aucuparin, noraucuparin and eriobofuran phytoalexins. No phytoalexins were detected in the leaves.

5.2. Conclusions:

In conclusion, the cell suspension culture of apple cv. 'Florina' provides excellent platform for the enhanced biosynthesis of health-protective bioactive phenolics. This elicitation approach offers a starting point to improve the production of natural antioxidants and bioactive secondary metabolites for industrial purposes using apple cell culture in future.

Application of GC-MS based metabolomics in combination with PCA on the cell suspension culture of apple cv. 'Florina' undoubtedly revealed an altered metabolite profiles of VIE-treated cells as compared to the untreated control cells during a time course of 0–72 h. Glucose level was found to be up-regulated at 0–12 h in the VIE-treated cells compared to the control cells, but thereafter depletion of glucose occurred at 12–72 h in VIE-treated cells. In contrary, Sucrose level was down-regulated in VIE-treated cells from 0-72 h. The levels of some amino acids, organic acids and TCA cycle intermediates in the VIE-treated cells showed two maxima at 24 h and 36 h. A rapid up-regulation of a number of phenolics occurred after VIE-treatment with biosynthesis of three new phytoalexins, the aucuparin, noraucuparin and the eriobofuran. Overall the metabolic response probably exhibited an immediate biochemical response of VIE-treatment which mimics scab fungus infection.

SAS activity was detected from the elicitor-treated cell cultures of apple, which could be used as a model system to understand plant SA biosynthesis. Whether SAS-catalyzed salicylaldehyde participates in SA biosynthesis or acts as an airborne volatile signal to combat pathogen attack merits additional study. The cloning and functional characterization of SAS from *M. domestica* cell cultures is likely to help decipher its role in SA biosynthesis in apple.

MdOMT is a soluble *O*-methyltransferase, which is involved in biphenyl biosynthesis in apple initiated by BIS. The enzyme selectively add methyl-group to 5-position of 3,5-dihydroxybiphenyl to from 3-hydroxy-5-methoxybiphenyl. Upon scab infection in green house-grown apple plants, *Md*OMT expression was observed in the internodal stem region with subsequent accumulation of aucuparin, noraucuparin and eriobofuran. How, scab infection in the leaves triggers phytoalexin biosynthesis in the internodal region and which role these

phytoalexins are actually playing to prevent scab disease progression need to be investigated in detail. Transgenic approaches aiming at introduction of such phytoalexin producing gene into a susceptible apple cultivars may results into development of new scab-tolerant cultivars. Transformation protocols in apple are well established (Vanblaere et al., 2011; Würdig et al., 2015).

5.3. Future scopes

- In this work, yeast extract-treated apple cell culture showed enhanced phenolics biosynthesis with which exhibited significant anticancer properties. However, which particular metabolite or metabolite combinations is actually responsible for anticancer and antioxidant activities and their underlying detail mechanisms of action need to be investigated further.

- How scab elicitor infection triggers enhanced phenolic and phytoalexin biosynthesis need to be investigated in details. Differential accumulation of metabolites accumulated upon scab fungus infection to field grown apple plants needs to be investigated in future.

- How scab-induced differentially accumulating metabolites inhibit / kill scab fungus growth and what is the underlying mechanism of actions, need to be investigated in future with isolated pure metabolites.

- Till date, there is no report available on molecular details of salicylaldehyde synthase (SAS) enzyme from any plant system. The *VpVAN* from *Vanilla planifolia* (Gallage et al., 2014) is the only gene known so far, encoding a C_2-chain shortening enzyme involved in vanillin biosynthesis. In this context SAS from *apple cell culture* is a promising candidate for future cDNA cloning and functional expression. Since apple genome database is available (GDR: Genome Database of Rosaceae) a sequence homology based cloning could be a quicker approach to clone SAS cDNA from elicited apple cell cultures using sequence information from *VpVAN* or from *HBS* from *V. planifolia* (Havkin-Frenkel et al., 2003). Future cloning and functional analyses of SAS cDNA will provide new insight on role of SAS in salicylic acid biosynthesis and regulation.

- Likewise cloning and functional analyses of second *O*-methyltransferase converting noraucuparin to aucuparin needs to be investigated in future to complete the biphenyl biosynthetic pathway at molecular level. Taking the advantage of apple genome database, cloning and functional analyses of noraucuparin o-methyltransferase (*MdOMT2*) (from apple cell culture is an area of considerable research interest. A set of putative genes has already been identified in this work (Table 2.32 under material & method section), which need to be functionally validated using cloning and functional analyses.

References

Abd El-Mawla, A.M.A., Beerhues, L., 2002. Benzoic acid biosynthesis in cell cultures of *Hypericum androsaemum*. Planta 214, 727-733.

Agrois, G.N., 2005. Plant Pathology, 5 th edn. San Diego, California, USA: Academic Press Ltd.

Aliferis, K.A., Faubert, D., Jabaji, S., 2014. A metabolic profiling strategy for the dissection of plant defense against fungal pathogens. PLoS ONE 9(11), e111930. https://doi.org/10.1371/journal.pone.0111930

Amil-Ruiz, F., Blanco-Portales, R., Muñoz-Blanco, J., Caballero, J. L., 2011. The strawberry plant defense mechanism: A molecular review. Plant Cell Physiol. 52, 1873–1903. doi:10.1093/pcp/pcr136.

Aprea, E., Gika, H., Carlin, S., Theodoridis, G., Vrhovsek, U., Mattivi, F. 2011. Metabolite profiling on apple volatile content based on solid phase microextraction and gas-chromatography time of flight mass spectrometry. J. Chromatogr. A. 1218, 4517–4524. doi: 10.1016/j.chroma.2011.05.019

Arnholdt-Schmitt B., Jose. H.C., Fernandes de Melo, D., 2006. AOX-a functional marker for efficient cell reprogramming under stress. Trends in Plant Science 11(6), 281–287.

Arnholdt-Schmitt, B., Hansen, L.D, Nogales, A., 2016. Calorespirometry, oxygen isotope analysis and functional-marker-assisted selection ('CalOxy-FMAS') for genotype screening: A novel concept and tool kit for predicting stable plant growth performance and functional marker identification. Briefings in Functional Genomics. 13, 541-548.

Bao, K., Fan, A., Dai, Y., Zhang, L., Zhang, W., Cheng, M., Yao, X., 2009. Selective demethylation and debenzylation of aryl ethers by magnesium iodide under solvent-free conditions and its application to the total synthesis of natural products. Org. Biomol. Chem. 7, 5084. doi:10.1039/b916969e.

Bektas, Y., Eulgem, T., 2014. Synthetic plant defense elicitors. Front Plant Sci. 5, 804.

Bendahmane, A., Kanyuka, K., Baulcombe, D.C., 1999. The Rx gene from potato controls

separate virus resistance and cell death responses. Plant Cell 11, 781–792.

Benzie, I.F.F., Strain, J.J., 1996. The ferric reducing ability of plasma (FRAP) as a measure of 'antioxidant power': the FRAP assay. Analytical Biochemistry 239, 70-76.

Benzie, I.F.F., Choi, S.W., 2014. Antioxidants in food: content, measurement, significance, action, cautions, caveats, and research needs. Advances in food and nutrition research 71, 1-53.

Bera, P., Mukherjee, C., Mitra, A., 2017. Enzymatic production and emission of floral scent volatiles in Jasminum sambac. Plant Science: An International Journal of Experimental Plant Biology 256, 25–38.

Bessadat, N., Benichou, S., Kihal, M., Henni, D. E., 2014. Aggressiveness and morphological variability of small spore Alternaria species isolated from Algeria. Journal of Experimental Biology and Agricultural Sciences 2(2S)

Beuerle, T., Pichersky, E., 2002. Purification and characterization of benzoate:coenzyme A ligase from *Clarkia breweri*. Arch. Biochem. Biophys. 400, 258–264.

Bisht, S., Kant, R., Kumar, V., 2013. α-d-Glucosidase inhibitory activity of polysaccharide isolated from Acacia tortilis gum exudate. International Journal of Biological Macromolecules 59, 214–220.

Borejsza-Wysocki, W., Lester, C., Attygalle, A., Hrazdina, G., 1999. Elicited cell suspension cultures of apple (*Malus×domestica)* cv. Liberty produce biphenyl phytoalexins. Phytochemistry 50, 231–235. doi:10.1016/S0031-9422(98)00509-3.

Bourgaud, F., Gravot, A., Milesi, S., Gontier, E., 2001. Production of plant secondary metabolites: a historical perspective. Plant Sci 161, 839-851.

Boyer, J., Liu, R.H., 2004. Apple phytochemicals and their health benefits. Nutrition Journal 3, 5-12.

Bradford, M., 1976. A rapid and sensitive method for the quantification of microgram quantities of protein utilizing the principle of protein– dye binding. Anal. Biochem. 72, 248-254.

Bulajic, A., Filajdic, N., Babovic, M., Sutton, T.B., 1996. First report of *Alternaria mali* on apples in Yugoslavia. Plant Disease 80.

Bus, V.G.M., Rikkerink, E.H.A., Caffier, V., Durel, C.E., Plummer, K.M., 2011. Revision of the nomenclature of the differential host-pathogen interactions of *Venturia inaequalis* and Malus . Annu Rev Plant Physiol PlantMol Biol 49, 391–413.

Cai, Z., Kastell, A., Smetanska, I., 2014. Chitosan or yeast extract enhance the accumulation of eight phenolic acids in cell suspension cultures of *Malus* × *domestica* Borkh. The Journal of Horticultural Sci and Biotechnol 89, 93-99.

Campbell, C.S., Evans, R.C., Morgan, D.R., Dickinson, T.A., Arsenault, M.P. 2007. Phylogeny of subtribe Pyrinae (formerly the Maloideae, Rosaceae): Limited resolution of a complex evolutionary history. Plant Systematic Evolution 266, 119-145.

Campos, M.D., Campos, C., Cardoso, H.G., Simon, P.W., Oliveira, M., Nogales, A., Arnholdt-Schmitt, B. 2016. Isolation and characterization of plastid terminal oxidase gene from carrot and its relation to carotenoid accumulation. Plant Gene 5, 13–21.

Catinot, J., Buchala, A., Abou-Mansour, E., Métraux, J.P., 2008. Salicylic acid production in response to biotic and abiotic stress depends on isochorismate in *Nicotiana benthamiana*. FEBS Lett. 582, 473-478.

Chagne, D., Dayatilake, D., Diack R., Oliver, M., Ireland, H., Watson A, Gardiner S.E., Johnston, J.W., Schaffer, R. J., Tustin, S., 2014. Genetic and environmental control of fruit maturation, dry matter and firmness in apple (*Malus* × *domestica* Borkh.)

Chatterjee, D., Kudlinzki, D., Linhard, V., Saxena, K., Schieborr, U., . Gande, S. L., Wurm, J. P., Wöhnert, J., Abele, R., Rogov, V., Dötsch, V., Osiewacz, H. D., Sreeramulu, S., Schwalbe H., 2015. Structure and biophysical characterization of the *S*-Adenosylmethionine-dependent *O*-methyltransferase PaMTH1, a putative enzyme accumulating during senescence of *Podospora anserine*. J Biol Chem. 290(26), 16415–16430. doi: 10.1074/jbc.M115.660829

Chizzali, C., Beerhues, L., 2012. Phytoalexins of the Pyrinae: Biphenyls and dibenzofurans. Beilstein J. Org. Chem. 8, 613–620.

Chizzali, C., Gaid, M.M., Belkheir, A.K., Hansch, R., Richter, K., Flachowsky, H., Peil, A., Hanke, M.V., Liu, B., Beerhues, L,. 2012a. Differential expression of biphenyl synthase gene family members in fire-blight infected apple 'Holsteiner Cox'. Plant Physiol. 158, 864–875.

Chizzali, C., Khalil, M.N.A., Beuerle, T., Schuehly, W., Richter, K., Flachowsky, H., Peil, A., Hanke, M.-V., Liu, B., Beerhues, L., 2012b. Formation of biphenyl and dibenzofuran phytoalexins in the transition zones of fire blight-infected stems of *Malus domestica* cv. "Holsteiner Cox" and *Pyrus communis* cv. "Conference." Phytochemistry 77, 179–185. doi:10.1016/j.phytochem.2012.01.023.

Chizzali, C., Liu, B., Richter, K., Flachowsky, H., Peil, A., Hanke, M.-V., Beerhues, L., 2014. Biphenyls and Dibenzofurans - Fire Blight-induced phytoalexins of Pear. Acta Horticulturae (1056), 181–185.

Chizzali, C., Swiddan, A. K., Abdelaziz, S., Gaid, M., Richter, K., Fischer, T. C., Beerhues, L., 2016. Expression of Biphenyl Synthase Genes and Formation of Phytoalexin Compounds in Three Fire Blight-Infected *Pyrus communis* Cultivars. PLOS ONE, 11(7), e0158713. doi:10.1371/journal.pone.0158713.

Chiron, H., Drouet, A., Claudot, A.C., Eckerskorn, C., Trost, M., Heller, W., Ernst, D., Sandermann, H., Jr. 2000. Molecular cloning and functional expression of a stress-induced multifunctional O-methyltransferase with pinosylvin methyltransferase activity from Scots pine (*Pinus sylvestris L.*). Plant Mol Biol. 44(6), 733-45

Cornille, A., Gladieux, P., Smulders, M. J. M., Roldán-Ruiz, I., Laurens, F., Le Cam, B., Nersesyan, A., Clavel, J., Olonova, M., Feugey, L., Gabrielyan, I., Zhang, X.G., Tenaillon, M.I., Giraud, T., 2012. New insight into the history of domesticated apple: Secondary contribution of the European wild apple to the genome of cultivated varieties. PLoS Genet. 8(5):e1002703. doi: 10.1371/journal.pgen.1002703.

Cornille, A., Giraud, T., Smulders, M.J.M., Roldán-Ruiz. I., Gladieux, P., 2014.The domestication and evolutionary ecology of apples. Trends in Genetics 30(2) , 57 – 65.

Cuthbertson, D., Andrews, P.K., Reganold, J.P., Davies, N.M., Lange, B. M. 2012. Utility of metabolomics toward assessing the metabolic basis of quality traits in apple fruit with an emphasis on antioxidants. J Agric Food Chem. 60(35), 8552–8560.

Delgado-Pelayo, Raul., Gallardo-Guerrero, L., Hornero-Méndez, D., 2014. Chlorophyll and carotenoid pigments in the peel and flesh of commercial apple fruit varieties. Food Research International. 65, 272-281.

Dianne, A.H., 2011. A Comprehensive reviews of apples and apple components and their

relationship to human health. Advances in Nutrition 2, 408-420.

Dzhangaliev, A.D., 2003. The wild apple tree of Kazakhstan. Hortic Rev John Wiley & Sons, Inc; pp. 63–303.

Eberhardt, M., Lee, C., Liu, R.H., 2000. Antioxidant activity of fresh apples. Nature 405, 903-904.

Eisenmann, Ehlers, M., Weinert, C. H., Tzvetkova, P., Silber, M., Rist, M. J., Luy, B., Muhle-Goll, C., 2016. Untargeted nmr spectroscopic analysis of the metabolic variety of new apple cultivars. metabolites. 6(3), 29.

El-Basyouni, S.Z., Chen, D., Ibrahim, R.K., Neish, A.C., Towers, G.H.N., 1964. The biosynthesis of hydroxybenzoic acids in higher plants. Phytochemistry 3, 485-492.

Evans, R.C., Campbell, C.S., 2002. The origin of the apple subfamily (Rosaceae: Maloideae) is clarified by DNA sequence data from duplicated GBSSI genes. Am. J. Bot. 89, 1478–1484.

Fan, Z., Shi, Z., Zhang, H., Liu, X., Bao, L., Ma, L., Zuo, X., Zheng, Q., Mi, N., 2009. Synthesis and biological activity evaluation of 1,2,3-thiadiazole derivatives as potential elicitors with highly systemic acquired resistance. J. Agric. Food Chem. 57, 4279–4286.

FAO (Food and Agriculture Organization of the United Nations)., 2016. FAOSTAT home page. http://faostat3.fao.org/browse/Q/QC/E

Fragnire, C., Serrano, M., Abou-Mansour, E., Métraux, J.P., L'Haridon, F., 2011. Salicylic acid and its location in response to biotic and abiotic stress. FEBS Lett. 585, 1847-1852.

Francini, A., Sebastiani, L., 2013. Phenolic Compounds in Apple (*Malus* x *domestica Borkh.*): Compounds Characterization and Stability during Postharvest and after Processing. *2*(3), 181-193. doi:10.3390/antiox2030181

French, C.J., Vance, C.P., Neil Towers, G.H., 1976. Conversion of p-coumaric acid to p-hydroxybenzoic acid by cell free extracts of potato tubers and *Polyporus hispidus*. Phytochemistry 15, 564-566.

Gaffney, T., Friedrich, L., Vernooij, B., Negrotto, D., Nye, G., Uknes, S., Ward, E., Kessmann, H., Ryals, J., 1993. Requirement of salicylic Acid for the induction of systemic acquired

resistance. Science 261, 754-756.

Gaid, M.M., Sircar, D., Beuerle, T., Mitra, A., Beerhues, L., 2009. Benzaldehyde dehydrogenase from chitosan-treated *Sorbus aucuparia* cell cultures. J. Plant Physiol. 166, 1343-1349.

Gaid, M.M., Sircar, D., Müller, A., Beuerle, T., Liu, B., Ernst, L., Hänsch, R., Beerhues, L., 2012. Cinnamate:CoA ligase initiates the biosynthesis of a benzoate-derived xanthone phytoalexin in *Hypericum calycinum* cell cultures. Plant Physiol 160, 1267-80.

Gallage, N.J., Hansen, E.H., Kannangara, R., Olsen, C.E., Motawia, M.S., Jørgensen, K., Holme, I., Hebelstrup, K., Grisoni, M., Møller, B.L., 2014. Vanillin formation from ferulic acid in *Vanilla planifolia* is catalysed by a single enzyme. Nat. Commun. 5, 1-14.

Galli, P., Broggini, G.A.L., Kellerhals, M., Gessler, C., Patocchi, A., 2010 High-resolution genetic map of the Rvi15 (Vr2) apple scab resistance locus. Mol Breeding 26, 561–572.

Gerhauser, C., 2008. Cancer chemo preventive potential of apples, apple juice, and apple components. Planta Medica 74, 1608-1624.

Gessler, C., Patocchi, A., 2007. Recombinant DNA technology in apple. Adv. Biochem. Eng. Biotechnol. 107, 113-32.

Gessler, C., Pertot, I., 2011. Vf scab resistance of Malus. Trees 26, 95–108.

Gestetner, B., Conn, E.E., 1974. The 2-hydroxylation of trans-cinnamic acid by chloroplasts from *Melilotus alba Desr*. Arch. Biochem. Biophys. 163, 617-24.

Giordano, D., Provenzano, S., Ferrandino, A., Vitali, M., Pagliarani, C., Roman, F., Cardinale, F., Castellarin, S. D., Schubert, A., 2016. Characterization of a multifunctional caffeoyl-CoA Omethyltransferase activated in grape berries upon drought stress, Plant Physiology and Biochemistry 101, 23-32.

Ginzberg, I., Fogelman, E., Rosenthal, L., Stern, R. A., 2014. Maintenance of high epidermal cell density and reduced calyx-end cracking in developing 'Pink Lady'apples treated with a combination of cytokinin 6-benzyladenine and gibberellins A4 + A7. Scientia Horticulturae 165, 324–330.

Gladieux, P., Zhang, X.G., Afoufa-Bastien, D., Sanhueza, R. V., Sbaghi, M., Cam, B.L., 2008. On the origin and spread of the scab disease of apple: out of Central Asia. PLoS ONE, 3,

e1455.

Gur, L., Reuveni, M., Cohen, Y., 2017 Occurrence and etiology of Alternaria leaf blotch and fruit spot of apple caused by *Alternaria alternata* f. sp. mali on cv. Pink lady in Israel Eur J Plant Pathol 147, 695–708.

Hammerschmidt, R., 1999. Phytoalexins: What have we learned after 60 years? Annual review of Phytopathol. 37, 285-306.

Harteveld, D. O. C., Akinsanmi, O. A., Drenth, A., 2013. Multiple Alternaria species groups are associated with leaf blotch and fruit spot diseases of apple in Australia. Plant Pathology 62, 289–297.

Harish, M.C., Dachinamoorthy, P., Balamurugan, S., Bala Murugan, S., Sathishkumar, R., 2013. Enhancement of α-tocopherol content through transgenic and cell suspension culture systems in tobacco. Acta Physiologiae Plantarum 35(4), 1121–1130.

Havkin-Frenkel, D., Podstolski, A., and Dixon, R.A., 2003. Vanillin biosynthetic pathway enzyme from *Vanilla planifolia*. US patent No.: 20030070188.

Hébert, C., Charles, M. T., Gauthier, L., Willemot, C., Khanizadeh, S., and Cousineau, J., 2002. Strawberry proanthocyanidins: Biochemical markers of *Botrytis cinerea* resistance and shelf-life predictability.ActaHortic. 659–662. doi:10.17660/ActaHortic.2002.567.143.

Hong, J., Yang, L., Zhang, D., Shi, J., 2016. Plant Metabolomics: An Indispensable System Biology Tool for Plant Science. Int. J. Mol. Sci. 17, 767.

Hrazdina, G., Borejsza-Wysocki, W., Lester, C., 1997. Phytoalexin production in an apple cultivar resistant to *Venturia inaequalis*. Phytopathology 87, 868-876.

Hrazdina, G., 2003. Response of scab-susceptible (McIntosh) and scab-resistant (Liberty) apple tissues to treatment with yeast extract and *Venturia inaequalis*. Phytochemistry 64, 485–492. doi:10.1016/S0031-9422(03)00150-X.

Hudina, M., Štampar, F., 2000. Sugars and organic acids contents of European *Pyrus comminus* L. and Asian *Pyrus serotina* Rehd. pear cultivars. Acta Aliment. 29, 217–230. doi:10.1556/AAlim.29.2000.3.2.

Huttner, C., Beuerle, T., Scharnhop, H., Ernst, L., Beerhues, L., 2010. Differential effect of elicitors on biphenyl and dibenzofuran formation in *Sorbus aucuparia* cell cultures. J.

Agric. Food Chem. 58, 11977–11984.

Ibdah, M., Pichersky, E., 2009. Arabidopsis Chy1 null mutants are deficient in benzoic acid-containing glucosinolates in the seeds. Plant Biol. 11, 574–581.

Ibrahim, R.K., De Luca, V., Khouri, H., Latchinian, L., Brisson, L., Charest, P.M., 1987 Enzymology and compartmentation of polymethylated flavonol glucosides in *Chrysosplenium americanum*. Phytochemistry 26, 1237–1245.

Ibrahim R. K., Bruneau, A., Bantignies, B., 1998. Plant O-methyltransferases: molecular analysis, common signature and classification. Plant Molecular Biology 36, 1–10.

Iqbal, M., Sharma, M., Ali, R.F., Yousuf, M., Hussain, A., 2013. In vitro antioxidant activity and spectrophotometric quantification of total phenolic and flavonoid contents of *Malus domestica*. World Journal of Pharmaceutical Research 3(1), 452-471.

Jain, M., 2015 Functional genomics of abiotic stress tolerance in plants: A CRISPR approach. Frontiers in Plant Science 6, 375.

Janick, J., 2005. The origin of fruits, fruit frowing and fruit breeding. Plant Breed. Rev. 25, 255–320. doi:10.1002/9780470650301.ch8.

Jarvis, A.P., Schaaf, O., Oldham, N.J., 2000. 3-hydroxy-3-phenylpropanoic acid is an intermediate in the biosynthesis of benzoic acid and salicylic acid but benzaldehyde is not. Planta 212, 119-126.

Jha, G., Thakur, K., Thakur, P., 2009. The venturia apple pathosystem: Pathogenicity mechanisms and plant defense responses. J. Biomed. Biotechnol. 28, 1-10.

Joshi, C.P., Chiang, V.L., 1998. Conserved sequence motifs in plant *S*-adenosyl-L-methionine-dependent methyltransferases. Plant Mol. Biol. 37, 663-674.

Jørgensen, K., Rasmussen, A.V., Morant, M., Nielsen, A.H., Bjarnholt, N., Zagrobelny, M., Bak, S., Møller, B.L., 2005. Metabolon formation and metabolic channeling in the biosynthesis of plant natural products. Curr Opin Plant Biol 8, 280–291.

Jung, K. H., 2007. Growth inhibition effect of pyroligneous acid on pathogenic fungus, *Alternaria mali*, the agent of blotch of apple. Biotechnology and Bioprocess Engineering 12, 318–322.

Kalkman, C., 2004. "Rosaceae". In Kubitzki K. Flowering plants—Dicotyledons: celastrales, oxalidales, rosales, cornales, ericales. The Families and Genera of Vascular Plants. 6(1), 343–386.

Kanwal, Q., Hussain, I., Latif Siddiqui, H., Javaid, A., 2010. Antifungal activity of flavonoids isolated from mango (*Mangifera indica L.*) leaves. Nat. Prod. Res. 24, 1907–14. doi:10.1080/14786419.2010.488628.

Kaufholdt, D., Baillie, C. K., Bikker, R., Burkart, V., Dudek, C.-A., von Pein, L., Hänsch, R., 2016. The molybdenum cofactor biosynthesis complex interacts with actin filaments via molybdenum insertase Cnx1 as anchor protein in *Arabidopsis thaliana*. Plant Science : An International Journal of Experimental Plant Biology 244, 8–18.

Kaufholdt, D., Baillie, C.-K., Wille, T., Lang, C., Hallier, S., Herschbach, C., Hänsch, R., 2015. Prospective Post-translational Regulation of Plant Sulfite Oxidase BT - Molecular Physiology and Ecophysiology of Sulfur. In L. J. De Kok, M. J. Hawkesford, H. Rennenberg, K. Saito, & E. Schnug (Eds.) 179–187.

Kellerhals, M., Szalatnay, D., Hunziker, K., Duffy, B., Nybom, H., Ahmadi-Afzadi, M., Höfer, M., Richter, K., Lateur, M., 2012. European pome fruit genetic resources evaluated for disease resistance. Trees 26:179–189.

Khalil, M.N.A., Beuerle, T., Müller, A., Ernst, L., Bhavanam, V.B.R., Liu, B., Beerhues, L., 2013. Biosynthesis of the biphenyl phytoalexin aucuparin in *Sorbus aucuparia* cell cultures treated with *Venturia inaequalis*. Phytochemistry 96, 101–9.

Khalil, M.N.A., Brandt, W., Beuerle, T., Reckwell, D., Groeneveld, J., Hänsch, R., Gaid, M.M., Liu, B., Beerhues, L., 2015. O-Methyltransferases involved in biphenyl and dibenzofuran biosynthesis. Plant J. 83, 263–76.

Khanizadeh, S., Tsao, R., Rekika, D., Yang, R., Charles, M.T., Rupasinghe, H.P.V., 2008. Polyphenol composition and total antioxidant capacity of selected apple genotypes for processing. Journal of Food Composition Analysis 21, 396-401.

Kim, J.K., Choi, S.R., Lee, J., Park, S.-Y., Song, S.Y., Na, J., Kim, S.W., Kim, S.-J., Nou, I.-S., Lee, Y.H., Park, S.U., Kim, H., 2013. Metabolic differentiation of diamondback moth (plutella xylostella (l.)) resistance in cabbage (*Brassica oleracea* L. ssp. capitata). J. Agric. Food Chem. 61, 11222–11230. doi:10.1021/jf403441t.

Klempien, A., Kaminaga, Y., Qualley, A., Nagegowda, D.A., Widhalm, J.R., Orlova, I., Shasany, A.K., Taguchi, G., Kish, C.M., Cooper, B.R., D'Auria, J.C., Rhodes, D., Pichersky, E., Dudareva, N., 2012. Contribution of CoA ligases to benzenoid biosynthesis in petunia flowers. Plant Cell 24, 2015–2030.

Kokubun, T., Harborne, J.B., 1994. A survey of phytoalexin induction in leaves of the rosaceae by copper ions. Zeitschrift fur Naturforsch. - Sect. C J. Biosci. 49, 628–634.

Kokubun, T., Harborne, J. B., 1995. Phytoalexin induction in the sapwood of plants of the Maloideae (Rosaceae): Biphenyls or dibenzofurans. Phytochemistry 40(6), 1649–1654.

Kollar, A., 1997. Aktuelle Forschung an dem bedeutendsten Erreger im Apfelbau, dem Apfelschorfpilz *Venturia inaequalis*. Nachrichtenblatt Deutscher Pflanzenschutzdienst 49, 131-136.

Kost, T.D., Gessler, C., Jänsch, M., Flachowsky, H., Patocchi, A., Broggini, G.A.L., 2015. Development of the first cisgenic apple with increased resistance to fire blight. PloS one. 10. e0143980.

Kota, P., Guo, D., Zubieta, C., Noel, J., Dixon, R.A. 2004. O-Methylation of benzaldehyde derivatives by “lignin specific” caffeic acid 3-O-methyltransferase. Phytochemistry 65, 837-846.

Kumar, N., Sharan, S., Chakraborty, A., Roy, P., 2004. Pterostilbene-isothiocyanate conjugate suppresses growth of prostate cancer cells irrespective of androgen receptor status. PLoS ONE 9(4), e933335.

Kumar, R.S., Joshi, C., Nailwal T.P., 2016. Callus induction and plant regeneration from leaf explants of apple (*Pyrus malus* L.) cv. Golden Delicious. Int J Curr Microbiol App Sci 5(2), 502-510.

Kumar, V., Nagar, S., 2014. Studies on *Tinospora cordifolia* monosugars and correlation analysis of uronic acids by spectrophotometric methods and GLC. Carbohydrate Polymers 99, 291–296.

Kumar, V., Jain, M., 2015. The CRISPR-Cas system for plant genome editing: advances and opportunities. Journal of Experimental Botany 66: 47-57.

Lam, K.C., Ibrahim, R.K., Behdad, B., Dayanandan, S. 2007. Structure, function, and

evolution of plant O-methyltransferases. Genome 50, 1001-1013.

Lancaster, J., 1992. Regulation of skin color in apples. Crit. Rev. Plant. Sci. 10, 487–502.

Lattanzio, V., Di Venere, D., Linsalata, V., Bertolini, P., Ippolito, A., Salerno, M., 2001. Low-temperature metabolism of apple phenolics and quiescence of *Phlyctaena vagabunda*. -J. Agr. Food Chem. 49, 5817-5821.

Lattanzio, V., Lattanzio, V. M., Cardinali, A., 2006. Role of phenolics in the resistance mechanisms of plants against fungal pathogens and insects. Phytochemistry: Advances in research, 661, 23–67.

Lavid, N., Wang, J., Shalit, M., Guterman, I., Bar, E., Beuerle, T., Menda, N., Shafir, S., Zamir, D., Adam, Z., Vainstein, A., Weiss, D., Pichersky, E., Lewinsohn, E., 2002. O-methyltransferases involved in the biosynthesis of volatile phenolic derivatives in rose petals. Plant Physiol. 129 (4), 1899-1907.

Lee, C.Y., Mattick, L.R., 1989 Composition and nutritive value of apple products, In: D. Downing. (ed.). Processed Apple Products. Van Nostrand Reinhold, New York. pp. 303-322.

Lee, K., Kim, Y., Kim, D., Lee, H., Lee, C., 2003. Major phenolics in apple and their contribution to the total antioxidant capacity. Journal of Agricultural and Food Chemistry 51, 6516-6520.

León, J., Yalpani, N., Raskin, llya, Lawton, M.A., 1993. Induction of benzoic acid 2-hydroxylase in virus-lnoculated tobacco. Plant Physiol. 103, 323-328.

Leontowicz, H., Gorinstein, S., Lojek, A., Leontowicz, M., Ciz, M., Soliva-Fortuny, R., Park, Y., Jung, S., Trakhtenberg, S., Martin-Belloso, O., 2002. Comparative content of some bioactive compounds in apples, peaches, and pears and their influence on lipids and antioxidant capacity in rats. Journal of Nutritional Biochemistry 13, 603-610.

Le Roux, P.M., Flachowsky, H., Jänsch, M., Kellerhals, M., Patocchi, A., & Hanke, M.V., 2014. Development of apple pre-breeding genotypes highly resistant to fire blight by early flowering. Acta Horticulturae. 1048, 55-64.

Liaudanskas, M., Viskelis, P., Raodonis, R., Kviklys, D., Uselis, N., Janulis, V., 2014. phenolic composition and antioxidant activity of *Malus domestica* leaves. Scientific World Journal

2o14, 1-10.

Linsmaier, E. M., Skoog, F., 1965. Organic growth factor requirements of tobacco tissue cultures. Physiol Plant 18,100-127.

Lisec, J., Schauer, N., Kopka, J., Willmitzer, L., Fernie, A. R., 2006. Gas chromatography mass spectrometry-based metabolite profiling in plants. Nature Protocols 1(1), 387–96.

Liu, B., Beuerle, T., Klundt, T., Beerhues, L., 2004. Biphenyl synthase from yeast-extract-treated cell cultures of *Sorbus aucuparia*. Planta 218(3), 492–496.

Liu, B., Raeth, T., Beuerle, T., Beerhues, L., 2007. Biphenyl synthase, a novel type III polyketide synthase. Planta 225, 1495–1503.

Lo, E. Y. Y., Donoghue, M. J., 2012. Expanded phylogenetic and dating analyses of the apples and their relatives (Pyreae, Rosaceae). Mol. Phylogenet. Evol. 63, 230–243. doi:10.1016/j.ympev.2011.10.005.

Machardy, B.W.E., 1996. Apple Scab: Biology , Epidemiology , And Management. American Phytopathological Society Press, St. Paul, MN.

Malnoy, M., Martens, S., Norelli, J.L., Barny, M.A., Sundin, G.W., Smits, T.H., Duffy, B., 2012. Fire blight: applied genomic insights of the pathogen and host. Annual Review of Phytopathology 50, 475-494.

Malinowski, J., Krzymowska, M., Godo, K., Hennig, J., Podstolski, A., 2007. A new catalytic activity from tobacco converting 2-coumaric acid to salicylic aldehyde. Physiol. Plant. 129, 461-471.

Mandal, S., 2010. Induction of phenolics, lignin and key defense enzymes in eggplant (*Solanum melongena* L.) roots in response to elicitors. African J. Biotechnol. 9, 8038–8047. doi:10.5897/AJB10.984.

Mathur, S., Shekhawat, G.S., 2013. Establishment and characterization of *Stevia rebaudiana* (Bertoni) cell suspension culture: an in vitro approach for production of stevioside. Acta Physiologiae Plantarum 35, 931-939.

Matsumoto, S., 2014. Apple Pollination Biology for Stable and Novel Fruit Production: Search System for Apple Cultivar Combination Showing Incompatibility, Semicompatibility, and Full-Compatibility Based on the S-RNase Allele Database," International Journal of

Agronomy 1-9. Article ID 138271, 2014. doi:10.1155/2014/138271

Mayr, U., Michalek, S., Treutter, D., Feucht, W., 1997. Phenolic compounds of apple and their relationship to scab resistance. J. Phytopathol. 145, 69-75.

Meuwly, P., Molders, W., Buchala, A., Metraux, J.P., 1995. Local and systemic biosynthesis of salicylic acid in infected cucumber plants. Plant Physiol. 109, 1107 -1114.

Mikulic Petkovsˇek, M., Usenik, V., Stampar, F., 2003. The role of chlorogenic acid in the resistance of apples to apple scab (*Venturia inaequalis* (Cooke) G. Wind. Aderh.). Research Reports Biotechnical Faculty University of Ljubljana 81, 233-242.

Mikulic Petkovsek, M., Stampar, F., Veberic, R., 2008. Increased phenolic content in apple leaves infected with the apple scab pathogen. Journal of Plant Pathology 90 (1), 49-55

Mikulic-Petkovsek, M., Stampar F., Veberic, R., 2009. Accumulation of phenolic compounds in apple in response to infection by the scab pathogen, *Venturia inaequalis*. Physiological and Molecular Plant Pathology. 74, 60-67. 10.1016/j.pmpp.2009.09.003.

Misra, A., Shukla, P.K., Kumar, B., Niranjan, A., Rawat, A.K.S., Srivastava, S., 2017. Simultaneous-hplc quantification of phenolic acids in traditionally used ayurvedic herb *Diplocyclos palmatus (L.)* Jeffry. Pharmacognosy Journal. 9, 483-487.

Morgan, D. R., Soltis, D. E., and Robertson, K. R. 1994. Systematic and evolutionary implications of RBCL sequence variation in Rosaceae. Am. J. Bot. 81, 890–903. doi:10.2307/2445770.

Mosmann, T., 1983. Rapid colorimetric assay for cellular growth and survival: application to proliferation and cytotoxicity assays. journal of immunological methods 65, 55-63.

Mukherjee, C., Samanta, T., and Mitra, A., 2016. Redirection of metabolite biosynthesis from hydroxybenzoates to volatile terpenoids in green hairy roots of *Daucus carota*. Planta, 243(2), 305–20.

Nieuwenhuizen, N.J., Green, S.A., Chen, X., Bailleul, E.J.D., Matich, A.J., Wang, M.Y.,Atkinson R.G., 2013. Functional genomics reveals that a compact terpene synthase gene family can account for terpene volatile production in apple. Plant Physiol. 161, 787–804. http://dx.doi.org/10.1104/pp.112.208249

Noel, J.P., Dixon, R.A., Pickersky, E., Zubieta, C., Ferrer, J.L., 2003. Structural, functional and

evolutionary basis for methylation of plant small molecules. Recent Adv. Phytochem. 37, 37–58.

Norelli, J.L., Jones, A.L., Aldwinckle, H.S., 2003. Fire blight management in the Twenty-first Century: Using new technologies that enhance host resistance in apple. Plant Disease 87, 756-765.

Nutan, M.M., Goel, T., Das, T., Malik, S., Suri, S., Rawat, A.K.S., Srivastava, S.K., 2013. Ellagic acid & gallic acid from Lagerstroemia speciosa L. inhibit HIV-1 infection through inhibition of HIV-1 protease & reverse transcriptase activity. The Indian journal of medical research 137 (3), 540-548.

Ogata, A., Tsuruga, A., Matsuno, M., Mizukami, H., 2004. Elicitor-induced rosmarinic acid biosynthesis in *Lithospermum erythrorhizon* cell suspension cultures: Activities of rosmarinic acid synthase and the final two cytochrome P450-catalyzed hydroxylations. Plant Biotechnol. 21, 393-396.

Oliveira, A.M.A.G., Raposo, M.M., Oliveira-Campos, A.M.F., Griffiths, J., Machado, A.E.H., 2003. Synthesis of psoralen analogues based on dibenzofuran. Helv. Chim. Acta 86, 2900–2906.

Oliveira, A. M.A.G, Oliveira-Campos, A.M.F., Raposo, M.M.M., Griffiths, J., Machado, A.E.H., 2004. Fries rearrangement of dibenzofuran-2-yl ethanoate under photochemical and Lewis-acid-catalysed conditions. Tetrahedron 60, 6145-6154

Paasela, T., Lim, K.J., Pietiainen, M., Teeti, T.F., 2017. The O-methyltransferase PMT2 mediates methylation of pinosylvin in Scots pine. New Phytol. 214(4), 1537-1550.

Park, Y. J., Thwe, A. A., Li, X., Kim, Y. J., Kim, J. K., Arasu, M. V., et al. (2015). Triterpene and flavonoid biosynthesis and metabolic profiling of hairy roots, adventitious roots, and seedling roots of *Astragalus membranaceus*. J. Agric. Food Chem. 63, 8862–9. doi:10.1021/acs.jafc.5b02525.

Parisi, L., Lespinasse, Y., Guillaumes, J., et al., 1993. A new race of *Venturia inaequalis* virulent to apples with resistance due to the *Vf* gene," Phytopathology 83, 533–537.

Pastori, G.M., Kiddle, G., Antoniw, J., Bernard, S., Veljovic-Jovanovic, S., Verrier, P.J., Noctor, G., Foyer, C.H., 2003. Leaf vitamin C contents modulate plant defense transcripts and regulate genes that control development through hormone signaling. Plant Cell 15,

939–51.

Pereira-Lorenzo, S., Ramos-Cabrer, A.M., D1áz-Hernández, M.B., 2007. Evaluation of genetic identity and variation of local apple cultivars (Malus x domestica) from Spain using microsatellite markers. Genet Resour Crop Ev. 54, 405-420.

Pfaffl, M.W., 2001. A new mathematical model for relative quantification in real-time RT-PCR. Nucleic Acids Research, 29(9), e45.

Picinelli, A., Dapena, E., Mangas, J.J., 1995. Polyphenolic pattern in apple tree leaves in relation to scab resistance. A preliminary study. J. Agr. Food Chem. 43, 2273-2278. .

Podstolski, A., Havkin-Frenkel, D., Malinowski, J., Blounta, J.W., Kourteva, G., Dixon, R.A., 2002. Unusual 4-hydroxybenzaldehyde synthase activity from tissue cultures of the vanilla orchid *Vanilla planifolia*. Phytochemistry 61, 611–620.

Potter D., Gao F., Bortiri P.E., Oh, S., Baggett S., 2002. Phylogenetic relationships in Rosaceae inferred from chloroplast matK and trnL-trnF nucleotide sequence data. Pl. Syst. Evol. 231, 77–89.

Potter, D., Eriksson, T., Evans, R.C., Oh, S., Smedmark, J.E.E., Morgan, D.R., Kerr, M., Robertson, K.R., Arsenault, M., Dickinson, T.A., Campbell, C.S., 2007. Phylogeny and classification of Rosaceae, Plant Systematics and Evolution 266, 5-43.

Rajeev Kumar, S., Kiruba, R., Balamurugan, S., Cardoso, H.G., Arnholdt-Schmitt, B., Zakwan, A., Sathishkumar, R., 2014. Carrot antifreeze protein enhances chilling tolerance in transgenic tomato. Acta Physiologiae Plantarum 36(1), 21–27.

Rana, S., Bhushan, S., 2016. Apple phenolics as nutraceuticals: assessment, analysis and application. Journal of Food Science and Technology 53, 1727-1738.

Reveal, J., 2012. Newly required infrafamilial names mandated by changes in the code of nomenclature for algae, fungi and plants. Phytoneuron 33, 1–32.

Ribnicky, D.M., Shulaev, V., Raskin, I., 1998. Intermediates of Salicylic Acid Biosynthesis in Tobacco Plant physiol. 118(2) , 565-572.

Roberts, J. W., 1924. Morphological characters of *Alternaria mali* Roberts. Journal of Agricultural Research, 27, 699–708.

Rotondo, F., Collina, M., Brunelli, A., Pryor, B. M., 2012. Comparison of Alternaria spp. collected in Italy from apple with A. mali and other AM-toxin producing strains. Phytopathology 102, 1130–1142.

Rowan, D.D., Hunt, M.B., Alspach, P.A., Whitworth, C.J., Oraguzie, N.C., 2009. Heritability and genetic and phenotypic correlations of apple (*Malus* × *domestica*) fruit volatiles in a genetically diverse breeding population. J Agric Food Chem. 57, 7944–7952.

Rupasinghe, H.P.V., Paliyath, G., Murr, D.P., 1998. Biosynthesis of α-farnesene and its relation to superficial scald development in 'Delicious' apples. J Am Soc Hortic Sci. 123, 882–886.

Saini, S.S., Teotia, D., Gaid, M., Thakur, A., Beerhues, L., Sircar, D., 2017. Benzaldehyde dehydrogenase-driven phytoalexin biosynthesis in elicitor-treated *Pyrus pyrifolia* cell cultures. J. Plant Physiol. 215, 154–162.

Sak, K., 2014. Cytotoxicity of dietary flavonoids on different human cancer types. Pharmacogn Rev 8, 122–146.

Sak, M., Dokupilov, I., Mihalik, D., Lakatosova, J., Gubisov, M., Kraic, J., 2014. Elicitation of phenolic compounds in cell culture of *Vitis vinifera* L by *Phaeomoniella chlamydospora*. Nova Biotechnologica et Chimica 13, 162-171.

Sanchez-Maldonado, A,F., Schieber, A., Ganzle, M.G., 2011. Structure–function relationships of the antibacterial activity of phenolic acids and their metabolism by lactic acid bacteria. Journal of Applied Microbiology 111, 1176-1184.

Sarfaraj-Hussain, Md., Fareed, S., Ansari, S., Rahman, M.A., Ahmad, I.Z., Saeed, M., 2012. Current approaches toward production of secondary plant metabolites. J. Pharm Bioallied Sci 4(1), 10-20.

Sarkate, A., Banerjee, S., Mir, J.I., Roy, P., Sircar, D., 2017. Antioxidant and cytotoxic activity of bioactive phenolic metabolites isolated from the yeast-extract treated cell culture of apple. Plant Cell, Tissue Organ Cult. 130, 641–649. DOI 10.1007/s11240-017-1253-0.

Schauer, N., Fernie, A. R., 2006. Plant metabolomics: towards biological function and mechanism. Trends Plant Sci. 11, 508–516.

Schmarr, H.G., Bernhardt, J., 2010. Profiling analysis of volatile compounds from fruits using

comprehensive two-dimensional gas chromatography and image processing techniques. J. Chromatogr, A. 1217, 565–574.

Schmidlin, L., Poutaraud, A., Claudel, P., Mestre, P., Prado, E., Santos-Rosa, M., Wiedemann-Merdinoglu, S., Karst, F., Merdinoglu, D., Hugueney, H., 2008. A stress-inducible resveratrol *o*-methyltransferase involved in the biosynthesis of pterostilbene in grapevine. Plant Physiol. 148(3), 1630–1639.

Schnitzler, J.P., Madlung, J., Rose, A., Ulrich Seitz, H., 1992. Biosynthesis of p-hydroxybenzoic acid in elicitor-treated carrot cell cultures. Planta 188, 594-600.

Schouten, H.J., Brinkhuis, J., Burgh, A.V., Schaart, J.G., Groenwold, R., Broggini, G.A.L., Gessler, C., 2014. Cloning and functional characterization of the Rvi15 (Vr2) genefor apple scab resistance. Tree Genetics & Genomes 10, 251–260.

Schwalb P., Feucht W., 1999. Changes in the concentration of phenolic substances in the bark during the annual development of the cherry tree (*Prunus avium* L.). Advances in Horticultural Science 13, 71-75.

Sciubba, F., di Cocco, M.E., Gianferri, R., Capuani, G., de Salvador, F.R., Fontanari, M., Gorietti, D., Delfini, M., 2015. Nuclear Magnetic Resonance-based metabolic comparative analysis of two apple varieties with different resistances to apple scab attacks. J. Agric. Food Chem. 63, 8339–8347. doi: 10.1021/acs.jafc.5b03311

Serrano, M., Wang, B., Aryal, B., Garcion, C., Abou-Mansour, E., Heck, S., Geisler, M., Mauch, F., Nawrath, C., Metraux, J.-P., 2013. Export of salicylic acid from the chloroplast requires the multidrug and toxin extrusion-like transporter EDS5. Plant Physiol. 162, 1815-1821.

Shen, J., Wang, Y., Chen, C., Ding, Z., Hu, J., Zheng, C., et al. 2015. Metabolite profiling of tea (*Camellia sinensis L.*) leaves in winter. *Sci. Hortic. (Amsterdam).* 192, 1–9. doi:10.1016/j.scienta.2015.05.022.

Shulaev, V., Cortes, D., Miller, G., Mittler, R., 2008. Metabolomics for plant stress response. Physiol Plant. 132(2), 199-208. doi: 10.1111/j.1399-3054.2007.01025.x.

Shuman, J. L., Cortes, D. F., Armenta, J. M., Pokrzywa, R. M., Mendes, P., Shulaev, V., 2011. Plant metabolomics by GCMS and differential analysis. In Plant Reverse Genetics: Methods and Protocols; Pereira, A., Ed.; Humana Press: Totowa, NJ, 229−246.

Siahsar, B., Rahimi, M., Tavassoli, A., Raissi, A.S., 2011. Application of biotechnology in production of medicinal plants. American-Eurasian J Agric & Environ Sci 11 (3), 439-444.

Sierotzki H., Gessler C., 1993. Flavan-3-ols content and the resistance of *Malus* x *domestica* to *Venturia inaequalis* (Cooke.) Wind. Physiological and Molecular Plant Pathology 42, 291-297.

Sil, B., Mukherjee, C., Jha, S., and Mitra, A., 2015. Metabolic shift from withasteroid formation to phenylpropanoid accumulation in cryptogein-cotransformed hairy roots of *Withania somnifera (L.)* Dunal. Protoplasma 252(4), 1097–1110.

Silverman, P., Seskar, M., Kanter, D., Schweizer, P., Metraux, J.P., Raskin, I., 1995. Salicylic acid in rice (biosynthesis, conjugation, and possible role). Plant Physiol. 108, 633-639.

Singleton, V.L., Orthofer, R., Lamuela-Raventos, R.M., 1999. Analysis of total phenol and other oxidation substrates and antioxidants by means of Folin-Ciocalteu reagent. Methods in Enzymology 299, 152-178.

Sircar, D., Mitra, A., 2008. Evidence for p-hydroxybenzoate formation involving enzymatic phenylpropanoid side-chain cleavage in hairy roots of *Daucus carota*. J. Plant Physiol. 165, 407–414.

Sircar, D., Mukherjee, C., Beuerle, T., Beerhues, L., Mitra, A., 2011. Characterization of p-hydroxybenzaldehyde dehydrogenase, the final enzyme of p-hydroxybenzoic acid biosynthesis in hairy roots of *Daucus carota*. Acta Physiol. Plant. 33, 2019–2024.

Sircar, D.. Gaid, M.M., Chizzali, C., Reckwell, D., Kaufholdt, D., Beuerle, T., Broggini, G.A.L., Flachowsky, H., Liu, B., Hänsch, R., Beerhues, L., 2015. Biphenyl 4-hydroxylases involved in aucuparin biosynthesis in rowan and apple are Cytochrome P450 736a proteins. Plant Physiology. 168, 428–442.

Smereka, K.J., MacHardy, W.E., Kausch, A.P., 1987. Cellular differentiation in Venturia inaequalis ascospores during germination and penetration of apple leaves. Canadian Journal of Botany 65, 2549–2561.

Soleimani, M. J., Esmailzadeh, M., 2007. First report of Alternaria mali causing apple leaf blotch disease in Iran. Australasian Plant Disease Notes 2, 57–58.

Strawn, M.A., Marr, S.K., Inoue, K., Inada, N., Zubieta, C., Wildermuth, M.C., 2007. Arabidopsis isochorismate synthase functional in pathogen-induced salicylate biosynthesis exhibits properties consistent with a role in diverse stress responses. J. Biol. Chem. 282, 5919–5933.

Takhtajan, A., 1997. Diversity and classification of flowering plants. Columbia University Press, New York.

Tamura, K., Peterson, D., Peterson, N., Stecher, G., Nei, M., Kumar, S., 2011. MEGA5: molecular evolutionary genetics analysis using maximum likelihood, evolutionary distance, and maximum parsimony methods. Mol Biol Evol 28:2731–2739

Thomson, S.V., 2000. Epidemiology of fire blight? In 'Fire Blight: The Disease and Its Causative Agent, *Erwinia amylovora*'. CABI, Wallingford 9–36.

Thomson, M.D., Stushnoff, C., McGinley, J.N., Thomson, H.J., 2009, In vitro measures used to predict anticancer activity of apple cultivars and their comparison to outcomes from a rat model of experimentally induced breast cancer. Nutr Cancer 61(4), 510-517.

Tiwary, B.K., Bihani, S., Kumar, A., Chakraborty, R., Ghosh, R., 2015. The *invitro* cytotoxic activity of ethno-pharmacological important plants of Darjeeling district of West Bengal against different human cancer cell lines. BMC Complementary and Alternative Medicine 15, 22.

Trapman, M., 2006. Resistance management in Vf resistant organic apple orchards. Bull OILB/SROP 29, 253–257.

Treutter, D., Feucht, W., 1990. The pattern of flavan-3-ols in relation to scab resistance of apple cultivars. Journal of Horticultural Science 65, 511-517.

Treutter D., 2005. Significance of flavanoids in plant resistance and enhancement of their biosynthesis. Plant Biology 7, 581-591.

Tsao, R., Yang, R., Young, J.C., Zhu, H., 2003. Polyphenolic profiles in eight apple cultivars using high-performance liquid chromatography (HPLC). J Agric Food Chem 51, 6347–6353.

Turkoglu, A., Duru, M.E., Mercan, N., Kivrak, I., Gezer, K., 2007. Antioxidant and antimicrobial activities of *Laetiporus sulphureus* (Bull.) Murrill. Food Chemistry 101,

267-273.

Vaclavic, L., Schreiber, A., Lacina, O., Cajka, T., Hajslova, J., 2012. Liquid chromatography-mass spectrometry-based metabolomics for authenticity assessment of fruit juices. Metabolomics. 8, 1-11.

Valadon, L.R.G., Rosemary, S. M., 1967. Carotenoids of certain compositae flowers. Phytochemistry 6, 983-988.

Vanblaere, T., Szankowski, I., Schaart, J., Schouten, H., Flachowsky, H., Broggini, G.A.L., Gessler, C., 2011. The development of a cisgenic apple plant. J Biotechnol 154, 304–311. doi:10. 1016/j.jbiotec.2011.05.013

Van der Zwet, T.B., Zoller, G., 1988. Controlling fire blight of aear and apple by accurate prediction of the blossom blight phase. Plant Dis. 72, 464-472. The American Phytopathological Society. DOI: 10.1094/PD-72-0464.

Van der Zwet, T.B., Beer, S.V., 1995. Fire Blight – Its nature, prevention and control; Practical guide to integrated disease management. U.S. Department of Agriculture, Information Bulletin No. 631, Washington DC

Vanzo, A., Jenko, M., Vrhovsek, U., Stopar, M. 2013. Metabolomic profiling and sensorial quality of 'Golden Delicious', 'Liberty', 'Santana', and 'Topaz' apples grown using organic and integrated production systems. J. Agric. Food Chem. 61, 6580–6587. doi: 10.1021/jf4011142

Vasco, C., Riihinen, K., Ruales, J., Kamal-Eldin, A., 2009. Phenolic compounds in Rosaceae fruits from Ecuador. J. Agric. Food Chem. 57, 1204–12. doi:10.1021/jf802656r.

Vasyukova, N.I., Ozeretskovskaya, O.L., 2007. Induced plant resistance and salicylic acid: A review. Appl. Biochem. Microbiol. 43, 367-373.

Velasco, R., Zharkikh, A., Affourtit, J., Dhingra, A., Cestaro, A., Kalyanaraman, A., Fontana, P., Bhatnagar, S.K., Troggio, M., Pruss, D., Salvi, S., Pindo, M., Baldi, P., Castelletti, S., Cavaiuolo, M., Coppola, G., Costa, F., Cova, V., Dal, Ri. A., Goremykin, V., Komjanc, M., Longhi, S., Magnago, P., Malacarne, G., Malnoy, M., Micheletti, D., Moretto, M., Perazzolli, M., Si-Ammour, A., Vezzulli, S., Zini, E., Eldredge. G., Fitzgerald, L.M., Gutin, N., Lanchbury, J., Macalma, T., Mitchell, J.T., Reid, J., Wardell, B., Kodira, C., Chen, Z., Desany, B., Niazi, F., Palmer, M., Koepke, T., Jiwan,

D., Schaeffer, S., Krishnan, V., Wu, C., Chu, V.T., King, S.T., Vick, J., Tao, Q., Mraz, A., Stormo, A., Stormo, K., Bogden, R., Ederle, D., Stella, A., Vecchietti, A., Kater, M.M., Masiero, S., Lasserre, P., Lespinasse, Y., Allan, A.C., Bus, V., Chagné, D., Crowhurst, R.N., Gleave, A.P., Lavezzo, E., Fawcett, J.A., Proost, S., Rouzé, P., Sterck, L., Toppo, S., Lazzari, B., Hellens, R.P., Durel, C.E., Gutin, A., Bumgarner, R.E., Gardiner, S.E., Skolnick, M., Egholm, M., Van de Peer. Y., Salamini, F., Viola, R., 2010. The genome of the domesticated apple (*Malus ×domestica* Borkh.). Nature Genetics 42, 833-839.

Veberic, R., Mikulic-Petkovsek, M., Stampar F., 2008. Increased phenolic content in apple leaves infected with the apple scab pathogen. Journal of Plant Pathology. 90, 49-55.

Villarino, M., Sandín-España, P., Melgarejo, P., De Cal, A., 2011. High chlorogenic and neochlorogenic acid levels in immature peaches reduce Monilinia laxainfection by interfering with fungal melanin biosynthesis. J. Agric. Food Chem. 59, 3205–3213. doi:10.1021/jf104251z.

Vinson, J., Su, X., Zubik, L., Bose, P., 2001. Phenol antioxidant quantity and quality in foods: fruits. Journal of Agricultural and Food Chemistry 49, 5315-5321.

Vlot, A.C., Dempsey, D.A., Klessig, D.F., 2009. Salicylic Acid, a multifaceted hormone to combat disease. Annu. Rev. Phytopathol. 47, 177–206.

Wang, H., Gao, X., Zhou, G.C., Cai, L., Yao, W.B., 2008. In vitro and in vivo antioxidant activity of aqueous extract from *Choerospondias axillaries* fruit. Food Chemistry 106, 888-895.

Wang, Q.J., Sun, H., Dong, Q.L., Sun, T.Y., Jin, Z.X., Hao, Y.J., Yao, Y.X., 2016. The enhancement of tolerance to salt and cold stresses by modifying the redox state and salicylic acid content via the cytosolic malate dehydrogenase gene in transgenic apple plants. Plant Biotechnol. J. 14, 1986–1997.

Way, R.D., Aldwinckle, H.S., Lamb, R.C., Rejman, A., Sansavini, S., et al. 1989. Apples (*Malus*). Acta Hortic. 290, 1–62.

Widhalm, J.R., Dudareva, N., 2015. A familiar ring to it: Biosynthesis of plant benzoic acids. Mol. Plant 8, 83–97.

Wildermuth, M.C., Dewdney, J., Wu, G., Ausubel, F.M., 2001. Isochorismate synthase is

required to synthesize salicylic acid for plant defence. Nature 414, 562–565.

Willits, M.G., Giovanni, M.T., Prata, R.T.N., Kramer, C.M., De Luca, V., Steffens, J.C., Graser, G., 2004. Bio-fermentation of modified flavonoids: an example of in vivo diversification of secondary metabolites. Phytochemistry 65, 31-41.

Winkel, B.S., 2004. Metabolic channeling in plants. Annu Rev Plant Biol 55, 85–107.

Wöhner, T., Klaus, R., Sundin, G.W., Zhao, Y., Stockwell, V.O., Sellmann, J., Flachowsky, H., Hanke, M.V.,Peil, A., 2017. Inoculation of Malus genotypes with a set of *Erwinia amylovora* strains indicate a gene-for-gene relationship between the effector gene eop1 and both Malus floribunda 821 and Malus 'Evereste'. Plant Pathology 10.1111/ppa.12784.

Wolfe, K., Wu, X., Liu, R.H., 2003. Antioxidant activity of apple peels. Journal of Agricultural and Food Chemistry 51, 609-614.

Würdig, J., Flachowsky, H., Saß, A., Peil, A., Hanke, M.V., 2015.

Yalpani, N., Leon, J., Lawton, M.A., Raskin, I., 1993. Pathway of salicylic acid biosynthesis in healthy and virus-inoculated tobacco. Plant Physiol. 103, 315–321.

Yang, L., Li, B., Zheng, X., Li, J., Yang, M., Dong, X., He, G., An, C., Deng, X.W., 2015. Corrigendum: Salicylic acid biosynthesis is enhanced and contributes to increased biotrophic pathogen resistance in Arabidopsis hybrids. Nat. Commun. 6, 8145.

Yazaki, K., Heide, L., Tabata, M., 1991. Formation of p-hydroxybenzoic acid from p-coumaric acid by cell free extract of *Lithospermum erythrorhizon* cell cultures. Phytochemistry 30, 2233–2236.

Yu, D., Liu, Y., Fan, B., Klessig, D.F., Chen, Z., 1997. Is the high basal level of salicylic acid important for disease resistance in potato? Plant Physiol. 115, 343–349.

Zhang, C.H., Mei, X.G., Liu, L., Yu, L.J., 2000. Enhanced paclitaxel production induced by the combination of elicitors in cell suspension cultures of *Taxus chinensis*. Biotechnol. Lett. 22, 1561–1564.

Zhang, H., Cha, S., Yeung, E.S., 2007. Colloidal graphite-assisted laser desorption/ionization MS and MSn of small molecules. 2. Direct profiling and MS imaging of small metabolites from fruits. Anal Chem. 79, 6575–6584. [PubMed: 17665874]

Zhang, Y., Shi, X., Li, B., Zhang, Q., Liang, W., Wang, C., 2016. Salicylic acid confers enhanced resistance to Glomerella leaf spot in apple. Plant Physiol. Biochem. 106, 64–72.

Zhao, J., Larock, R. C., 2006. Synthesis of Substituted Carbazoles, Indoles, and Dibenzofurans by Vinylic to Aryl Palladium Migration. J. Org. Chem. 71 (14), 5340–5348

Zhong, R., Morrison, W. H., Himmelsbach, D. S., Poole, F. L., Ye, Z. H., 2000. Essential role of caffeoyl coenzyme A O-methyltransfer ase in lignin biosynthesis in woody Poplar plants. Plant Physiol. 124(2), S563–578.

Zuckerkandl, E., Pauling, L., 1965. Evolutionary divergence and convergence in proteins, in Evolving Genes and Proteins, edited by Bryson V and Vogel HJ Academic Press, New York. 97-166.

Publications

A. Research papers

1. **Sarkate, A**., Banerjee, S., Mir, J.I., Roy, P., Sircar, D., **2017**. Antioxidant and cytotoxic activity ofbioactive phenolic metabolites isolated from the yeast-extract treated cell culture of apple. Plant Cell, Tissue Organ Culture 130: 641-649; DOI 10.1007/s11240-017-1253-0

2. **Sarkate, A**., Saini, S.S., Kumar, P., Sharma, A.K., Sircar, D., **2017**. Salicylaldehyde synthase activity from *Venturia inaequalis* elicitor-treated cell cultures of apple. Journal of Plant Physiology 221: 66-73. DOI: 10.1016/j.jplph.2017.12.002

B. Conference Paper/Poster

1. **Sarkate, A**., Gaid, M.M., Beerhues, L., Sircar, D., 2014. Phytochemical analyses and evaluation of antioxidant efficacy of in vitro callus extract of apple. International Conference on Molecular Signalling- Recent Trends in Biomedical and Translational Research (ICMS: RTBTR-2014), Department of Biotechnology, IIT Roorkee, Roorkee (India), December 2014, PP- 61. [Poster Presentation]

2. **Sarkate, A**. and Sircar, D., 2015. A novel o-methyltransferase involved in phytoalexin biosynthesis in apple. International Conference on Molecular Signalling: Recent Trends in Bioscience, North Eastern Hill University, Shilong (India) November 2015, PP-60. [Poster Presentation]

C. Manuscript Under Review

1. **Sarkate, A**., Saini, S.S., Sircar, D., 2017. GC-MS based untargeted metabolomics of apple cell cultures treated with *Venturia inaequalis* elicitors. Manuscript submitted to **Metabolomics** (Under Review).
2. **Sarkate, A.,** Saini, S.S., Gaid, M., Beerhues,L., Sircar, D., 2017. Molecular cloning and functional analyses of a biphenyl phytoalexin-specific *O-methyltransferase* from apple cell suspension cultures. Manuscript submitted to **Plant Molecular Biology** (Under Review).